Molecular studies on lead resistance in selected bacterial strains

Thesis submitted to Goa University

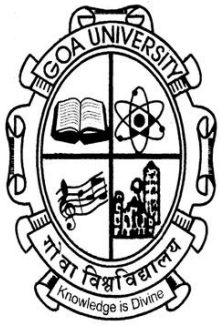

For the award of the degree of

DOCTOR OF PHILOSOPHY

In

MICROBIOLOGY

By

Jaya Sharma

Under the guidance of

Prof. Santosh Kumar Dubey

Department of Microbiology

Goa University, Goa, India

2017

Acknowledgement

"Gratitude is a miracle of its own recognition.

It brings out a sense of appreciation and sincerity of a being."

— Auliq-Ice

The completion of PhD has really been a long journey. It's true that "*Life is what happens*" for the reason that life neither stands still, nor waits until you are finished and have time to manage it. Much has happened and changed during the course of time. I owe a great deal of appreciation and gratitude to quite a few people for their contribution in numerous ways.

In the first place I would like to express sincere gratitude to my enthusiastic supervisor, ***Prof. Santosh Kumar Dubey*** for his constant guidance, patience, genuine concern and faith in me. This feat was possible only because of the unconditional support provided by Sir. A person with an amicable and positive disposition, Sir has always made himself available to clarify my doubts despite his busy schedules. It was indeed a great opportunity to work with him and to learn from his research expertise. Thank you Sir, for all your help and support.

I owe my deepest gratitude to ***Prof. M.K. Janarthanam***, Dean, Faculty of Life Sciences and Environment for his valuable advice, kind support and constant motivation. I am grateful to ***Prof. Sanjeev Ghadi*** for being so dedicated to his role as my V.C.'s nominee. I appreciate his contribution of time, insightful questions and ideas to make my PhD experience productive and stimulating. I thank ***Prof. Sarita Nazareth***, Head, Department of Microbiology for providing the academic support and necessary infrastructure to accomplish my research work. I thank all the faculty members, ***Prof. Sandeep Garg, Prof. Irene Furtado, Prof. Saroj Bhosle, Dr. Milind Naik, Dr. Trelita, Dr. Lakshangy Chari, Dr. Priya D'Costa and Dr. Varada Damare*** for their understanding and encouragement.

A journey is easier when you travel together, therefore, I would like to extend huge, warm thanks to my colleagues and friends, ***Kashif, Praveen, Shamshad, Dr. Pramod, Avyleno,***

Aseem, Laxman, Roshan, Md Imran, Mohammad, Kirti, Mira, Prabha, Anoop, Shabnam, Nisha, Kiran, Akshaya, Neha, Sushama, Jyothi, Satyajit, Ashwini, Sajiya, Diviya, Sulochana, Alisha, Sanket, Shruti and Salim. Their precious support, intellectual insights and personal cheering have been of great help during this research. ***Milind Mutnale*** from Centre for Cellular and Molecular Biology deserves my sincere expression of thanks for his help in conducting *in silico* studies and for his constant enthusiasm.

I am grateful to the University Grants Commission, New Delhi for providing financial support as JRF and SRF. I acknowledge the kind help of ***Dr. N. Ramaiah, Mr. Ram Murti Meena and Mr. Girish Prabhu*** from National Institute of Oceanography, Goa for DNA sequencing and X-ray diffraction analysis respectively. I thank ***Dr. R. Mohan and Ms. Sahina Gazi*** from National Centre for Antarctic and Ocean Research, Goa for providing the scanning electron microscopy as well as energy dispersive X-ray spectroscopic facility. I am also thankful to ***Prof. B.R. Srinivasan,*** Head; ***Ms. Mira, Mr. Rahul and Mr. Vishal*** from Department of Chemistry, Goa University for fourier-transform infrared spectroscopic analysis. I thank ***Dr. T.C. Nag*** from All India Institute of Medical Sciences, New Delhi for extending transmission electron microscope facility. I am extremely grateful to ***Dr. Anoop Tiwari*** from the National Centre for Antarctic and Ocean Research for AAS analysis. I owe a great deal of appreciation to ***Dr. Santhakumari and Mr. Yugendra Patil*** from the National Chemical Laboratory, Pune for carrying out the proteomic analysis. I hugely appreciate ***Mr. M. G. Lanjewar*** from the University Science Instrumentation Centre, Goa University for carrying out scanning electron microscopy.

I immensely appreciate the help of our dedicated non-teaching staff, ***Mrs. Saraswati, Mr. Shashi, Ms. Deepashri, Ms. Afra, Mr. Buddhaji, Mr. Dominic, Mr. Narayana, Mr. Tanu, Mr. Rajesh and Mr. Gajanan***.

I am eternally grateful to ***Siddhesh, Parul, Tanvi, Farah and Shalley*** for their support, sincere encouragement, care, love, understanding and unwavering belief in me throughout my research work.

Above all, I owe it all to Almighty God for granting me the wisdom, health and strength to undertake this research task and enabling me to its completion. He has made available his divine intervention in several ways during my challenging times.

Last but not the least, I would like to pay high regards to my parents for their sincere encouragement, inspiration and support to lift me uphill this phase of life. They have supported me in all my pursuits. My Father, ***Mr. R.C. Sharma***, in the first place is the person who put the fundament of my learning character by showing me the joy of intellectual pursuit ever since I was a child. My Mother, ***Mrs. Lalita Sharma***, is the one who sincerely raised me with her care and gentle love. ***Ravi***, my younger brother has been immensely supportive and caring. They all have supported me in every possible way to see the completion of this work.

Jaya Sharma

DEDICATED TO MY FAMILY

ABBREVIATIONS

g	gram	**bp**	base pair
µg	microgram	**kb**	kilobase pair
ng	nanogram	**kDa**	kilodalton
mg	milligram	**nm**	nanometre
µL	microlitre	**ppb**	parts per billion
mL	millilitre	**MW**	molecular weight
dL	decilitre	**Pb**	Lead
cm^3	cubic centimetre	**Fe**	Iron
M	molar	**Mn**	Manganese
mM	millimolar	**Mg**	Magnesium
º	degree	**Cd**	Cadmium
ºC	degree Celsius	**Zn**	Zinc
Å	angstrom	**Cu**	Copper
α	alpha	**Ni**	Nickel
ß	beta	**Co**	Cobalt
Ɵ	theta	**Ca**	Calcium
min^{-1}	per minute	**MTC**	Maximum tolerance concentration
h	hour	**KOH**	Potassium hydroxide
min	minute	**HCl**	Hydrochloride
sec	second	**PBS**	Phosphate buffer saline
rpm	revolutions per minute	**EDTA**	Ethylenediaminetetraacetic acid
3D	three-dimensional	**TAE**	Tris acetate EDTA
TE	Tris-EDTA	**WHO**	World Health Organisation
APS	Ammonium persulphate	**CDC**	Center for Disease Control and Prevention
KBr	Potassium bromide	**APA**	American Pediatric Association
SDS	Sodium dodecyl sulphate	**BLL**	Blood lead level
PAGE	Polyacrylamide gel electrophoresis	**UNEP**	United Nations Environment Programme

ANOVA	Analysis of variance	**IARC**	International agency for research on cancer
$MgCl_2$	Magnesium chloride	**US-EPA**	United States Environmental Protection agency
PCR	Polymerase chain reaction	**ROS**	Reactive oxygen species
MT	Metallothionein	**EPS**	Exopolysaccharide
Bmt	Bacterial metallothionein	**LPS**	Lipopolysaccharide
MHA	Mueller Hinton agar	**CDF**	Cation diffusion facilitator
PYE	Peptone yeast extract	**RND**	Resistance-nodulation-cell division
TBTC	Tributyltin chloride	**SEM**	Scanning electron microscopy
DNA	Deoxyribonucleic acid	**EDX**	Energy-dispersive X-ray spectroscopy
RNA	Ribonucleic acid	**TEM**	Transmission electron microscopy
BLAST	Basic local alignment search tool	**AAS**	Atomic absorption spectroscopy
ATP	Adenosine triphosphate	**XRD**	X-ray diffraction
IDA	Independent data acquisition	**IR**	Infrared
SWATH	Sequential window acquisition of all theoretical data	**FTIR**	Fourier-transform infrared spectroscopy
NMR	Nuclear magnetic resonance spectroscopy	**LC**	Liquid chromatography
XANES	X-ray absorption near edge structure	**MS**	Mass spectrometry
XAFS	X-ray absorption fine structure	**TOF**	Time of flight
MSA	Multiple sequence alignment	**FDR**	False discovery rate

TABLES

CHAPTER I

CHAPTER III

CHAPTER IV

CHAPTER V

CHAPTER VI

FIGURES

CHAPTER I

CHAPTER III

CHAPTER IV

CHAPTER V

CHAPTER VI

Fig. 6.14 Docking of BmtA with nickel (Ni) ion.

Fig. 6.15 Docking of BmtA with calcium (Ca) ion.

CONTENTS

1.1 Introduction

Heavy metals are commonly defined as metals having a specific density of more than 5 g/cm^3. The main threats to human health from heavy metals are associated with exposure to lead, cadmium and mercury (Järup, 2003). Heavy metals that are released into the environment through anthropogenic and industrial activities tend to persist indefinitely, circulating and ultimately accumulating throughout the food chain, thus posing a serious threat to the environment, animals and humans (Volesky and Holan, 1995).

Lead continues to be a significant public health hazard in developing countries. The environmental exposure to lead is associated with air, water as well as soil. The workers get exposed to lead in several occupations viz. motor vehicle assembly, panel beating, battery manufacturing, soldering, lead mining, smelting, lead alloy production, glass, plastic, printing, ceramics and paint industries (Tong et al., 2000). Exposure to lead may result in acute or chronic lead poisoning usually manifested as headache, irritability, abdominal pain, anaemia and other symptoms related to nervous system. Lead encephalopathy is characterized by sleeplessness and restlessness. Long-term lead exposure may also give rise to kidney damage (Landrigan, 1990, 1991).

The entry of lead ions into bacterial cell takes place through common regulatory systems prevalent for various divalent cations or oxyanions since the transmembrane proteins are unable to distinguish them from other cations viz. Fe^{2+}, Mg^{2+}, Mn^{2+} (Nies, 1999). Bacteria have developed and evolved two kinds of resistance mechanisms to block the passive entry of heavy metals inside the cells :

(i) fast, non-specific and proton-motive force based mechanism

(ii) more specific, metal-inducible mechanism usually driven by ATP hydrolysis (Gadd, 1990).

Some prokaryotes possess multiple and even redundant metal resistance systems (Ji and Silver, 1995). Generally, the genes induced by lead encode resistance proteins such as metal-specific efflux pumps, membrane-bound transporters, metal reductases, cytoplasmic or periplasmic metal transport proteins, or metal-sequestering proteins. Bacteria with the ability to modify, extrude out or sequester lead may provide an important and valuable biological tool for removal of toxic lead from lead contaminated terrestrial as well as aquatic environmental sites (Gummersheimer and Giblin, 2003).

1.2 Review of Literature

1.2.1 Lead pollution in the environment

Lead (Pb) is naturally found as the most abundant trace metal in Earth's crust with average concentration of 13 μg g^{-1} (Patel et al., 2006). It is a ubiquitous metal that has been used by the human race since prehistoric times. It is used extensively by various industries due to its unique characteristics viz. high malleability, ductility, softness, poor conductivity, low melting point and corrosion resistance (Flora et al., 2012; Wani and Usmani 2015). Romans extensively used lead in manufacturing water pipes and earthenware containers for wines (Tong et al., 2000; Riva et al., 2012). It tends to persist in the environment therefore, it is a serious global health hazard and has also been listed as a priority pollutant (Sparks, 2005; Gillis et al., 2012). Lead has been identified as 1 of 10 chemicals of major public health concern by the World Health Organisation (WHO). Lead pollution can be defined as the excessive use of lead containing materials that results in toxic emissions of lead.

1.2.2 Sources of lead contamination

Lead contamination can result from both geogenic and anthropogenic activities (Park et al., 2011a). However, geogenic processes viz. volcanic emission, soil erosion or Pb

mobilization from various minerals are minor contributors to environmental Pb pollution (Gadd, 2010; Jaroslawiecka and Piotrowska-Seget, 2014). Major fraction of the environmental lead comes from anthropogenic activities viz. mining, coal combustion, lead smelting, gasoline, motor vehicle assembly, pottery, production of lead-acid batteries, lead arsenate insecticides, manufacturing of glazed ceramics, paints, pigments, stained glass, toys, water pipes, printing, ammunition, jewellery and certain cosmetics (Tong et al., 2000; Wani and Usmani, 2015). Lead exposure is a leading cause of occupational health hazards. Table 1.1 enlists specific industrial operations where workers are commonly exposed to high levels of lead.

Table 1.1 Occupations posing health hazards in workers due to lead exposure. (Hernberg, 1973)

Industrial Operations causing occupational lead exposure to workers	
Primary and secondary lead smelting	Lead mining
Welding and cutting of lead-painted metal constructions	Plumbing
Welding of galvanized or zinc silicate coated sheets, other welding activities	Cable making
Ship breaking	Wire patenting
Non-ferrous founding	Lead casting
Battery manufacture: pasting, assembling, welding of battery connectors	Type founding in printing shops
Production of lead paints	Glass making
Spray painting	Assembling of cars
Mixing (by hand) of lead stabilizers into polyvinyl chloride	Shot making
Mixing (by hand) of crystal glass mass	Lead glass blowing
Sanding or scraping of lead paint	Repair of automobile radiators
Burning of lead in enamelling workshops	Pottery

1.2.3 Toxicology of lead

1.2.3.1 Lead exposure

Lead continues to be a significant public health hazard in developing countries. Environmental exposure to lead is associated with multiple sources viz. petrol, industrial processes, paint, solder in canned foods, water pipes and pathways viz. air, household dust, street dirt, soil, water and food (Fig. 1.1). Lead enters the human body mainly through following routes:

a) *Ingestion* of food, water or dust contaminated with lead due to use of leaded pipes or storage in lead-glazed or lead-soldered containers.
b) *Inhalation* of particulate lead resulting from combustion of lead containing materials or during smelting, battery recycling, leaded aviation fuel or gasoline or stripped paint.
c) *Application* of cosmetics or use of medicines containing lead

Young children are more vulnerable to the toxic effects of lead because their body can absorb higher amount of lead and their organ systems particularly, nervous system is more sensitive in comparison to adults. As per the guidelines of United States Center for Disease Control and Prevention (CDC) and American Pediatric Association (APA) blood level ≥ 10 μg/dL is considered to be of concern for children as well as young women. Occupational lead exposure is considered safe if blood lead level (BLL) doesn't exceed 30 μg/dL (Patrick, 2006). WHO and the United Nations Environment Programme (UNEP) have jointly taken up an initiative which is referred to as "The Global Alliance to Eliminate Lead Paint" in order to prevent children from lead exposure and simultaneously abate occupational lead exposure (http://www.who.int). The International Agency for Research on Cancer (IARC) has classified lead as a "probable human carcinogen" (Rousseau et al., 2005). The United States - Environmental Protection Agency (US-EPA) has established a regulation, "Lead and Copper Rule" so that the concentration of lead in drinking water does not exceed beyond 15 ppb.

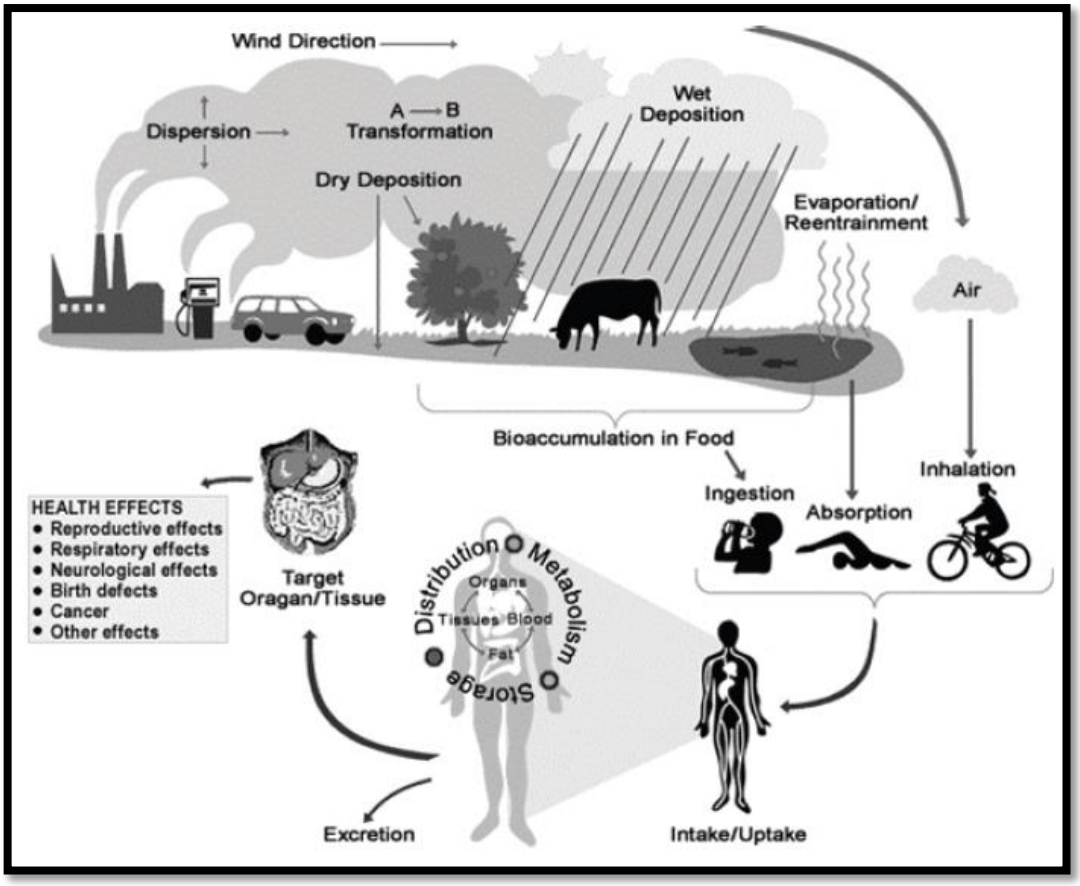

Fig. 1.1 Illustration of lead exposure and its adverse effects on human health.

(Wani and Usmani, 2015)

1.2.3.2 Health hazards of lead

Ingestion or inhalation of lead results in its distribution to various vital organs of the body viz. brain, liver, bones and kidney. It gets accumulated in bones as well as teeth over time. During pregnancy, this lead gets remobilized into the blood stream by resorption and diffusion. This poses risk of exposure to the foetus since lead can cross the placental barrier (Cory-Slechta, 1996). Moreover, children suffering from malnutrition are more vulnerable to lead exposure as their bodies tend to absorb more lead in absence of other nutrients such as calcium. Toxic effects of lead on various organ systems are as follows:

1.2.3.2.1 Nervous system

The main target of lead toxicity is brain, affecting both peripheral and central nervous systems (Cory-Slechta,1996). Children suffer from hyperactivity, irritability, headache, attention deficit disorders, reduction in intelligence quotient, antisocial behaviour, hearing loss, short-term memory and delayed growth (Lanphear et al., 2005; Patrick, 2006; Gillis et al., 2012). Lead toxicity can cause severe manifestations viz. encephalopathy, convulsions, lack of coordination, paralysis, coma and even death (Cleveland et al., 2008).

1.2.3.2.2 Renal system

Lead nephropathy is manifested as glomerular sclerosis, proximal tubular damage and interstitial fibrosis. However, chronic nephropathy is characterised by tubulointerstitial and glomerular changes leading to renal breakdown and hyperuricemia (Patrick, 2006).

1.2.3.2.3 Haematopoietic system

Lead restrains the synthesis of haemoglobin by inhibiting the key enzymes of heme synthesis resulting in anaemia. Moreover, it shortens the life span of the circulating erythrocytes by making the cell membranes more fragile (Flora et al., 2012).

1.2.3.2.4 Reproductive system

Lead exerts negative impact on the reproductive systems of men as well as women. In case of men, lead exposure results in reduced spermatogenesis (sperm count and motility), infertility, changes in prostate function and testosterone levels along with a decreased libido. On the other hand, women suffer from increase in rate of still-births, miscarriages, abortions and reduced fertility (Patrick, 2006; Flora et al., 2012).

1.2.3.2.5 Cardiovascular system

Acute and chronic lead poisoning may show potentially lethal manifestations in the form of hypertension, ischemic coronary heart disease and other cardiovascular diseases (Navas-Acien et al., 2007).

1.2.3.3 Mechanism of lead toxicity

Lead toxicity occurs as a result of inhibition of enzyme activity, modifications in the conformation of nucleic acids and proteins, disruption of oxidative phosphorylation and membrane functions as well as variations in the osmotic balance (Jaroslawiecka and Piotrowska-Seget, 2014). The development of opiate system is also adversely affected by lead. Moreover lead, being a divalent cation shows strong binding with the sulfhydryl groups of proteins. It also interferes with the neuronal signalling by mimicking calcium ions. It prevents the entry of calcium into cells and causes distortion of mitochondrial cristae thereby inhibiting the respiration process (Needleman, 2004). In the presence of lead, there is generation of reactive oxygen species (ROS) while there is depletion of the antioxidant reserves (Flora et al., 2007; 2012). Table 1.2 clearly depicts the two different forms of lead poisoning.

Table 1.2 Different forms of lead poisoning (Flora et al., 2012).

S. N.	Types of lead poisoning	Exposure	Lead levels (µg/dL)	Clinical symptoms
1.	Acute poisoning	Intense exposure of short duration	100-120	Muscle pain, fatigue, abdominal pain, headache, vomiting, seizures and coma
2.	Chronic poisoning	Repeated low-level exposure over a prolonged period	40-60	Persistent vomiting, encephalopathy, lethargy, delirium, convulsions and coma

1.2.4 Lead resistance in bacteria

1.2.4.1 Overview

Lead is not required for any biological function in bacteria and is toxic even at minute concentrations but it enters the cells by various pathways meant for uptake of other essential divalent metal ions viz. Zn and Mn (Bruins et al., 2000). In spite of its toxicity, certain lead resistant microorganisms specially, bacteria have been isolated from either lead contaminated wastes (soil, water) or from the plants growing in those contaminated areas. Among these, *Bacillus megaterium*, *B. cereus*, *Pseudomonas putida*, *P. marginalis*, *P. vesicularis*, *P. aeruginosa*, *Aeromonas caviae*, *Providencia alcalifaciens*, *Enterobacter cloacae*, *Bacillus cereus*, *Vibrio harveyi*, *Staphylococcus aureus*, *Citrobacter freundii*, *Cupriavidus metallidurans*, *Burkholderia cepacia*, *and Klebsiella aerogenes* are known to tolerate considerable amount of lead. They employ various resistance mechanisms such as production of exopolymers, intracellular as well as extracellular precipitation of lead, intracellular sequestration by metallothioneins, biotransformation of lead compounds, binding with siderophores and efflux of lead mediated by P-type ATPases as shown in Fig. 1.2 (Levinson et al., 1996; Levinson and Mahler, 1998; Roane, 1999; Mire et al., 2004; Gadd, 2010, Naik and Dubey, 2011; Naik, et al., 2012 a, b, c, d; Naik and Dubey, 2013; Shamim et al., 2013; Gupta et al., 2014; Jaroslawiecka and Piotrowska-Seget, 2014; Kang et al., 2015; Pan et al., 2017).

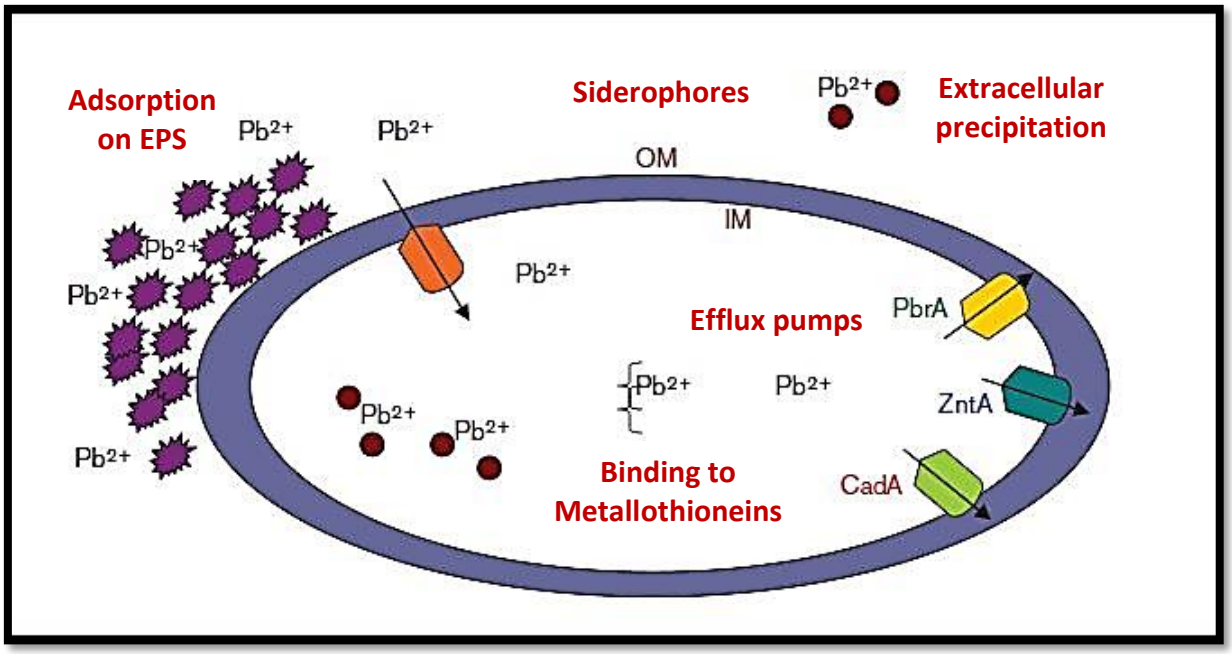

Fig. 1.2 Mechanisms of lead resistance employed by bacteria.

(Jaroslawiecka and Piotrowska-Seget, 2014)

1.2.4.2 Exopolymeric substances and cell wall

Several bacterial strains are capable of synthesizing exopolymeric substance (EPS) which consists of polysaccharides, proteins, nucleic acids, uronic acids and humic acids. EPS can chelate the metal cations and reduce their bioavailability thereby alleviating the toxicity to bacterial cells (Bruins et al., 2000). Roane (1999) had shown production of an exopolymer by *Pseudomonas marginalis* as a lead resistance mechanism. There are reports of EPS facilitated Pb binding in bacteria viz. *Halomonas* sp., *Bacillus* sp., *Paenibacillus jamilae* and *Pseudomonas* sp. (Salehizadeh and Shojaosadati, 2003; Perez et al., 2008; Amoozegar et al., 2012).

Bacterial cell wall also restricts the movement of lead ions into the cell as the functional groups present on the cell wall interact with the metal ions. In case of Gram positive bacteria, peptidoglycan, teichoic acid as well as teichuronic acid are involved in lead binding whereas in Gram negative bacteria, lipopolysaccharide (LPS) is mainly responsible for it (Beveridge and Fyfe, 1985). The major functional groups that participate in lead binding in *Bacillus* sp. and *Pseudomonas* sp. include amide, sulphonamide, hydroxyl, amino, carboxyl, phosphate and carbonyl (Cabuk et al., 2006, Gabr et al., 2008).

1.2.4.3 Precipitation of lead

Several bacteria are known to interact with lead forming insoluble complexes, thus employing precipitation as a mechanism to reduce lead toxicity. Bacterial strains viz. *Citrobacter freundii, Vibrio harveyi* and *Providencia alcalifaciens* 2EA are well known to precipitate lead extracellularly as lead phosphates (Aickin and Dean, 1979; Aickin et al., 1979; Levinson and Mahler, 1998; Mire et al., 2004; Naik et al., 2012a). On the other hand, several bacterial strains immobilize lead intracellularly in various forms viz. lead phosphate by *Burkholderia cepacia, Staphylococcus aureus*; lead carbonate by *Enterobacter cloacae*; lead

hydroxyapatite by *Bacillus cereus* 12-2; lead sulphide by *Klebsiella aerogenes* and *Rhodobacter sphaeroides* (Aiking et al., 1985; Levinson et al., 1996; Levinson and Mahler, 1998; Templeton et al., 2003; Bai and Zhang, 2009; Kang et al., 2015; Chen et al., 2016).

1.2.4.4 Metallothioneins in intracellular metal sequestration

Metallothionein (MT) is a family of low molecular weight (MW range : 6-14 kDa), cysteine rich, metal induced proteins found in both eukaryotes and prokaryotes (Kagi, 1991; Klaassen et al., 1999; Cobbett et al., 2002; Achard-Joris et al., 2007; Atanesyan et al., 2011). These are capable of binding both physiologically required metals viz. zinc, copper, selenium as well as xenobiotic metals viz. cadmium, lead, mercury, silver and arsenic through thiol groups of cysteine residues thus, facilitating detoxification of toxic heavy metals (Hamer, 1986; Dunn et al., 1987; Cajaraville et al., 2000; Enshaei et al., 2010; Murthy et al., 2011). The metallothionein gene, *smtA* was first characterized from the cyanobacterium, *Synechococcus* PCC7942 whereas Pseudothionein, a histidine containing cadmium binding protein was isolated and characterized from *Pseudomonas putida* (Huckle et al., 1993; Ji and Silver, 1995; Blindauer, 2011). Presence of *smtA* gene that encodes bacterial metallothionein have also been reported in *Salmonella choleraesuis* and *Proteus penneri*, whereas *bmtA* gene encoding bacterial metallothionein has been reported in *Pseudomonas aeruginosa* (Blindauer et al., 2002; Blindauer, 2008, 2011; Naik et al., 2012b). The copper-binding MT has also been reported in the pathogen, *Mycobacterium tuberculosis* (Gold et al. 2008).

1.2.4.5 Efflux mediated resistance mechanism

Bacteria possess specific proteins to export the metal ions outside the cell. These include P-type ATPases, cation diffusion facilitator (CDF) proteins and CBA efflux pumps belonging to resistance-nodulation-cell division (RND) superfamily (Nies and Silver, 1995;

Nies, 1999, 2003; Coombs and Barkay, 2005). P_{IB}-type ATPases, a subfamily of P-type ATPases regulate the export of heavy metal ions from cytoplasm to periplasmic space using energy from ATP hydrolysis, while proton motive force drives the CDF transporters for expelling toxic metal ions (Fig. 1.3). On the other hand, CBA transporters use a chemiosmotic gradient to efflux metal ions from both cytoplasm and periplasm to outside the cell (Hynninen, 2010). Efflux of Pb^{2+} ions has been reported by PbrA of *Cupriavidus metallidurans* CH34, CadA ATPase of *S. aureus* which is a cadmium translocating P-type ATPase as well as ZntA ATPase of *Escherichia coli* which is a cadmium and zinc transporting ATP dependent pump (Silver, 1996; Silver and Phung, 1996; Rensing et al., 1998, Hynninen et al., 2009). Several proteins viz. ZitB, CzcD and ZntA involved in zinc, cadmium resistance respectively belong to the family of cation diffusion proteins (Anton et al., 2004; Haney et al., 2005; Silver and Phung, 2005). CzcCBA1 belongs to group of CBA transporters and facilitates the export of lead ions from cells of *Pseudomonas putida* KT2440 (Hynninen, 2010; Piotrowska-Seget, 2014).

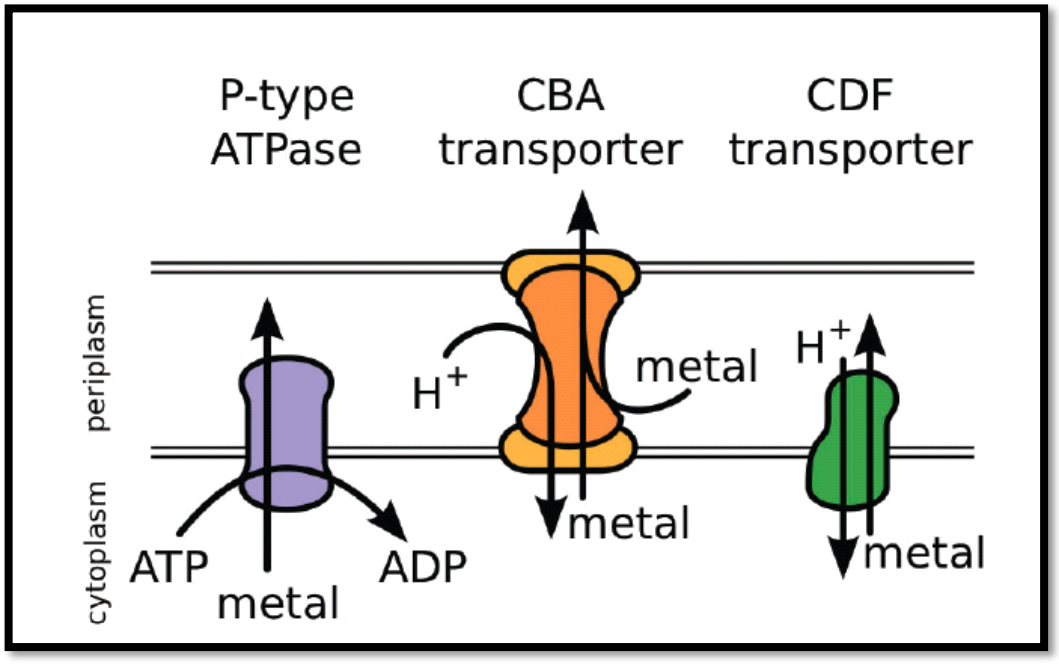

Fig. 1.3 Efflux systems found in bacteria to combat lead toxicity (Hynninen, 2010).

1.2.4.6 Siderophores and pigments

Siderophores are organic compounds synthesized by bacteria in order to chelate iron with a high afffinity. Apart from iron, these molecules are able to chelate other metal ions like Pb^{2+} as well (Saha et al., 2012). Pyoverdine and pyochelin are the main siderophore pigments produced by *Pseudomonas* and they are also implicated in binding with Pb^{2+} (Braud et al., 2010). It is interesting to note that *Pseudomonas aeruginosa* strain 4EA showed enhanced siderophore production in presence of 0.8 mM lead nitrate (Naik and Dubey, 2011). Moreover, synthesis of red and red-brown pigments in presence of lead nitrate by *P. vesicularis* and *Streptomyces* sp has also been reported (Zanardini et al., 1997). Therefore, siderophores and bacterial pigments also play an important role in protecting the bacterial cells from lead toxicity.

1.2.4.7 Lead resistance Operon *(pbr* operon)

Metal resistance genes are known to be located on chromosome, plasmid or transposon forming gene clusters or operons (Trevors et al., 1985; Silver and Walderhaug, 1992; Rouch et al., 1995; Silver, 1996). *Cupriavidus metallidurans* strain CH34 contains two megaplasmids, pMOL28 and pMOL30 that govern resistance to 20 heavy metals (Monchy et al., 2007; Janssen et al., 2010). Borremans et al. (2001) reported the first operon conferring resistance to lead in *C. metallidurans* CH34 (previously known as *Ralstonia metallidurans*, *Alcaligenes eutrophus* and *Wautersia metallidurans*) from *mer-pbr-czc* island of pMOL30. Genes present on *pbrTRABCD* operon are located on two divergently transcribed regions and govern lead resistance (Fig. 1.4).

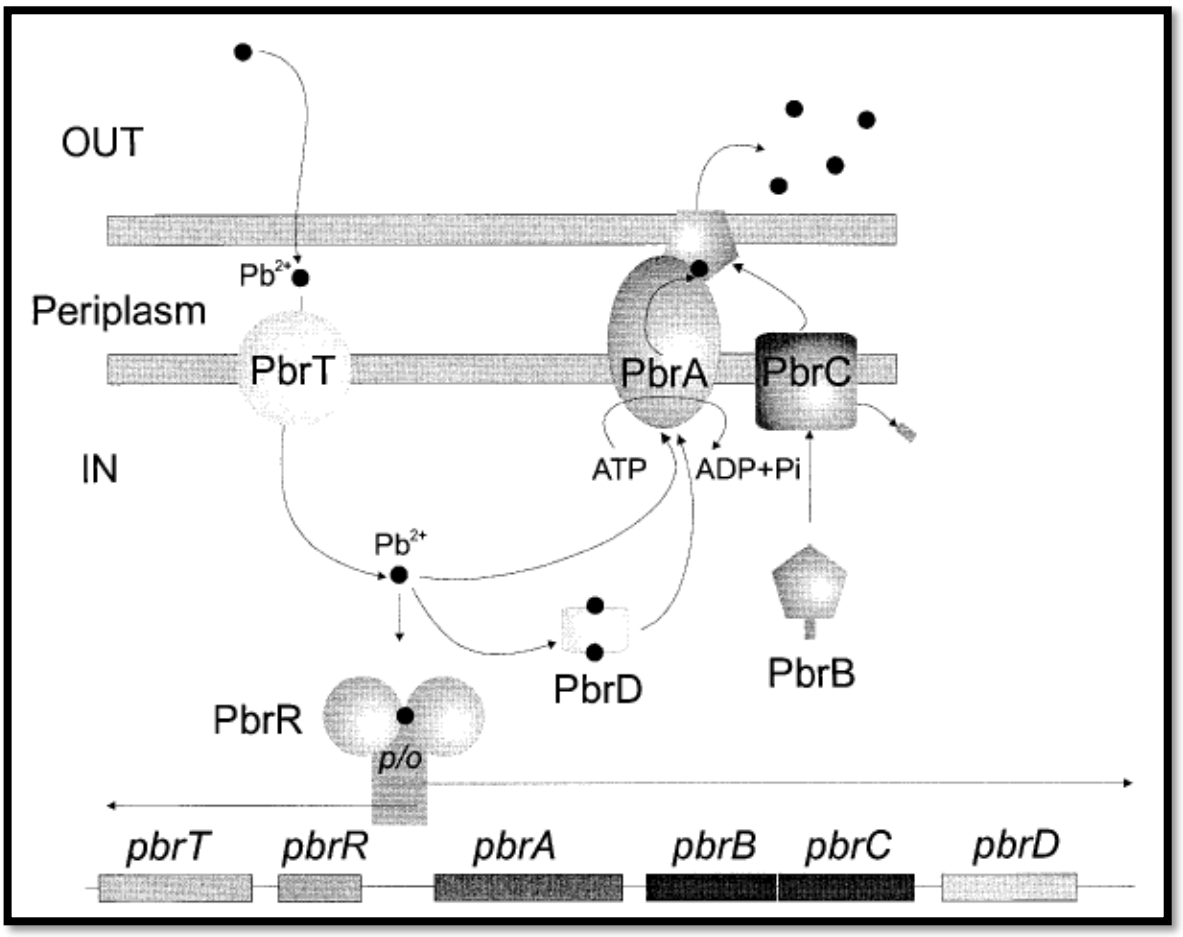

Fig. 1.4 *pbr* operon of *Cupriavidus metallidurans* CH34 (Borremans et al., 2001).

The proteins encoded by *pbr* operon are PbrT, a membrane protein responsible for influx of Pb^{2+} in the cytoplasm; PbrR, a positive transcriptional regulator; PbrA, a P-type ATPase involved in the efflux of lead ions from cytoplasm to periplasm; PbrB, an undecaprenyl pyrophosphate phosphatase that facilitates precipitation of lead; PbrC, a pro-lipoprotein signal peptidase and PbrD, facilitates lead sequestration in the cytoplasm (Fig. 1.5). Some of these genes are also found in various other bacterial strains (Fig. 1.6).

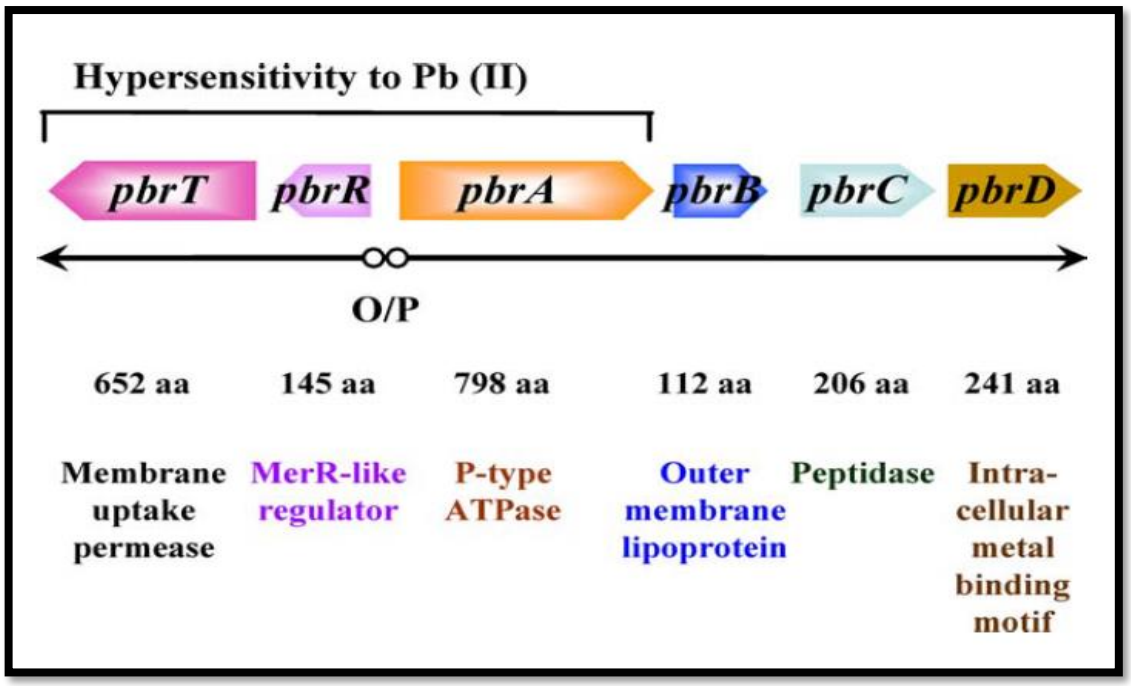

Fig. 1.5 Proteins encoded by the *pbr* operon (Silver and Phung, 2005).

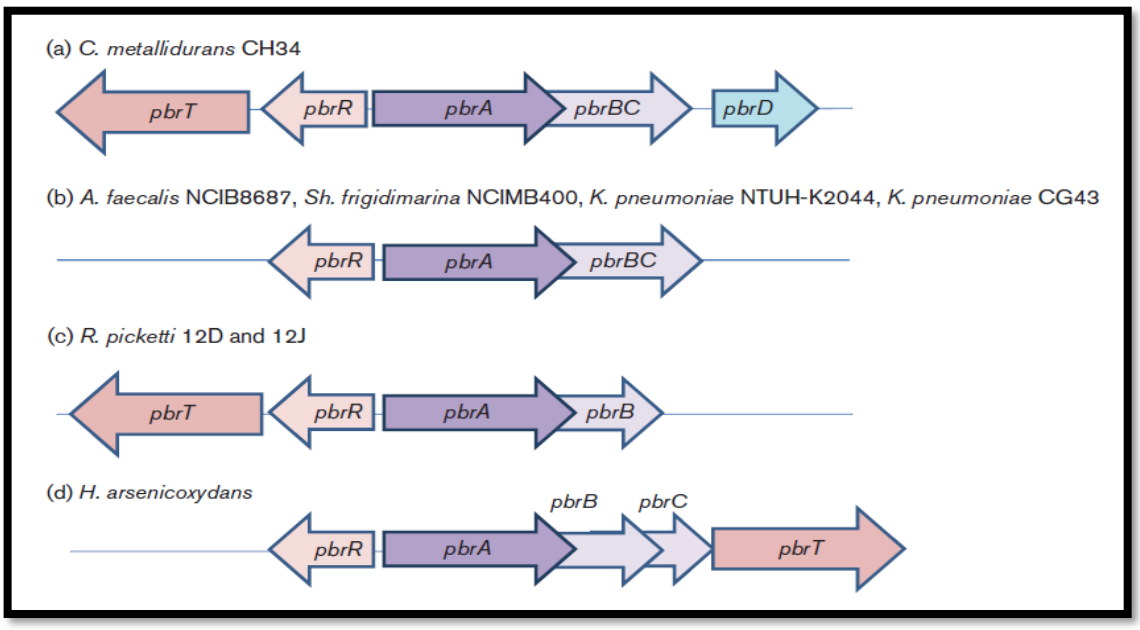

Fig. 1.6 *pbr* genes in various bacteria (Jaroslawiecka and Piotrowska-Seget, 2014).

1.2.4.7.1 Mechanism of **PbrA** *and* **PbrB** *mediated lead resistance*

Hynninen et al. (2009) showed that lead resistance in *C. metallidurans* CH34 is achieved through the cooperation of PbrA, a Pb/Zn/Cd-translocating ATPase and PbrB which is an undecaprenyl pyrophosphate phosphatase. Pb^{2+} ions enter the bacterial cells by means of various transporters including those for essential metals. This initiates the transcription of *pbr* operon. PbrA effluxes out the Pb^{2+} ions from cytoplasm to the periplasmic space, whereas PbrB generates inorganic phosphates by dephosphorylating other substrates. Consequently, the lead ions present in the periplasm get sequestered as phosphate salt. Thus, the bacterial cells are protected from harmful effects of lead (Fig. 1.7).

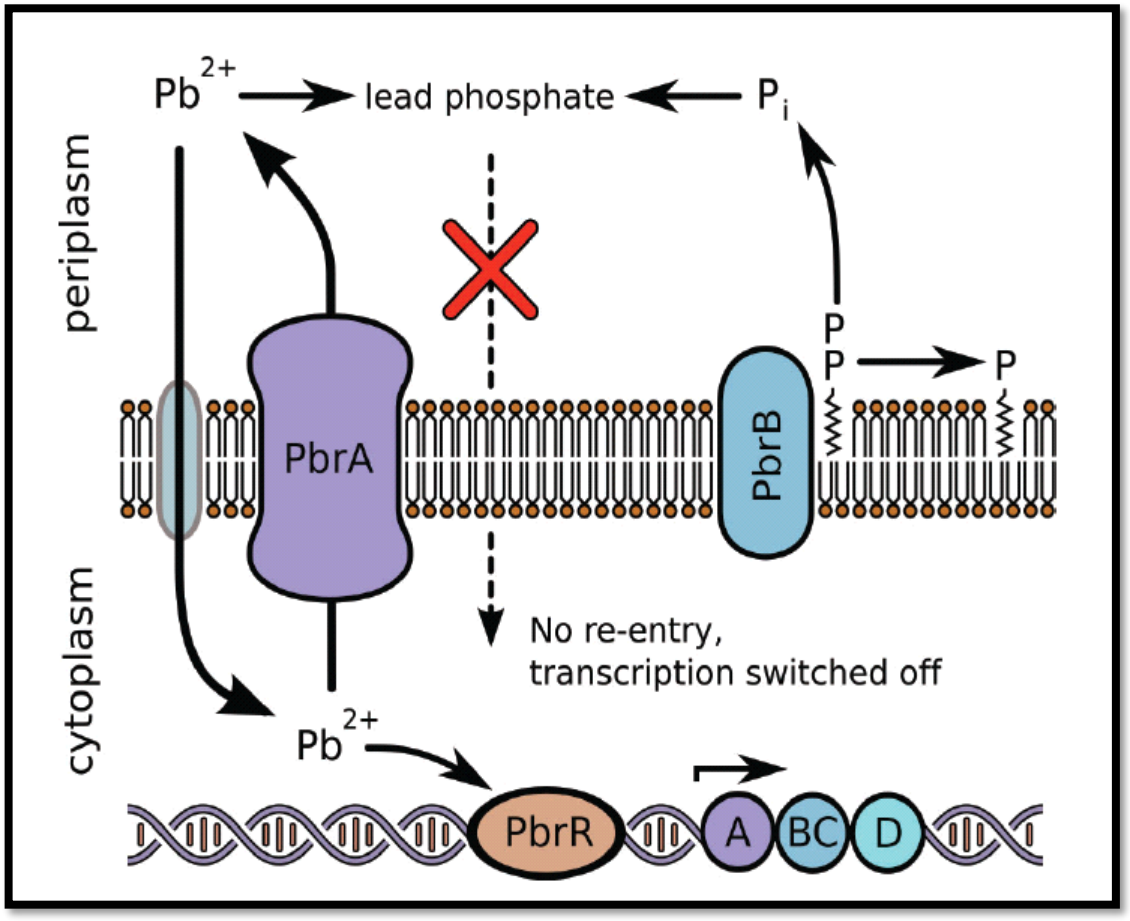

Fig. 1.7 Mode of action for the *pbr* resistance determinants (Hynninen et al., 2009).

1.2.4.8 Regulatory proteins

Various metallo-regulatory proteins belonging to MerR family regulate the concentration of lead ions in the bacterial cell (Brown et al., 2003). PbrR of *C. metallidurans* CH34 is a MerR-like protein (Borremans et al., 2001). It has been shown that PbrR binds lead(II) almost 1000-fold more selectively over other metal ions such as mercury, cadmium, zinc, cobalt, nickel, copper and silver (Chen and He, 2008). CmPbrR and its two homologues, CmPbrR2 (formerly PbrR691) and CmPbrR3 are the only Pb^{2+}-specific regulatory proteins reported from nature (Chen et al., 2007). ZntR is another transcriptional regulator belonging to MerR family. It regulates the expression of ZntA which is known to efflux out Zn^{2+}, Cd^{2+} and Pb^{2+} in *E. coli* (Binet and Poole, 2000). CadC from *S. aureus* and CmtR from *M. tuberculosis* are regulatory proteins from the SmtB/ArsR family. Likewise, CadA is a Zn^{2+}/ Cd^{2+}/Pb^{2+} translocating P_{IB}-type ATPase and CmtR is a cadmium/lead detecting transcriptional repressor (Busenlehner et al., 2003, Cavet et al., 2003, Jaroslawiecka and Piotrowska-Seget, 2014).

We are aware that microorganisms including bacteria adopt numerous mechanisms to alleviate lead toxicity. Therefore, these microbes may be used as biological tools either to sense this environmental pollutant or for it's bioremediation.

There is not enough information available illustrating the lead resistance mechanisms in bacteria at molecular level. Therefore, keeping in view these facts and in order to explore novel mechanisms governing lead resistance in bacteria following objectives were proposed:

1. ***Screening and identification of lead resistant bacterial isolates.***
2. ***To determine whether the resistance to lead is conferred by plasmid or genomic DNA.***
3. ***To explore the mechanisms of lead resistance viz. intracellular sequestration, surface adsorption and precipitation.***
4. ***To study the proteomic profile of lead resistant bacteria.***
5. ***To examine the presence of metallothionein (MT) genes in lead resistant bacteria.***

2.1 Sampling and enrichment

Soil samples were collected from the waste dump of a battery manufacturing industry in Corlim, Goa, India in sterile polypropylene tubes. The samples were enriched by incubating 1.0 g soil in 10.0 mL nutrient broth (Appendix A) supplemented with 1.0 mM lead nitrate (Appendix B) in an incubator-shaker at 30^{o}C for 24 h at 150 rpm.

2.2 Screening of lead resistant bacteria

Following enrichment, appropriate dilutions of the samples were plated on M9 minimal medium agar plates (Sambrook et al., 1989) (Appendix A) supplemented with 1.5 mM lead nitrate. The agar plates were incubated at 30^{o}C for 48 h. Morphologically distinct bacterial colonies were selected for further purification in order to obtain axenic cultures which were maintained on nutrient agar supplemented with 1 mM lead nitrate.

2.3 Determination of maximum tolerance concentration (MTC*)*

In order to determine the maximum tolerance concentration (MTC) of lead for the bacterial isolates, a defined minimal medium composed of (per litre): $C_6H_{12}O_6$ (glucose), 1.0 g; $C_6H_5O_7Na_3$ (sodium citrate), 0.5 g; $(NH_4)_2SO_4$ (ammonium sulphate), 1.0 g; $MgSO_4.7H_2O$ (magnesium sulphate), 0.1 g and $Na_5O_{10}P_3$ (sodium tripolyphosphate), 0.1 g with pH 6.0 was used (Appendix A). Sodium tripolyphosphate being an organic source of phosphate was incorporated in the medium in order to enhance the bioavailability of lead (Roane, 1999). Agar plates with the defined minimal medium supplemented with an increasing concentration of lead nitrate ranging from 0 to 4.5 mM were spot inoculated. These plates were incubated at 30^{o}C for 48 h and were observed for visible bacterial colonies.

2.4 Plasmid profile

Lead resistant bacterial isolates were grown overnight in nutrient broth (Appendix A) supplemented with 1 mM lead nitrate. Plasmid DNA from these isolates was isolated using Gen Elute^{TM} Plasmid Miniprep kit (Sigma-Aldrich, USA), electrophoresed on 0.8% agarose gel with ethidium bromide (Appendix C) and visualized using gel documentation system (Syngene G:BOX, UK).

2.5 Morphological and biochemical characterisation

The lead resistant isolates were subjected to gram staining and were observed using a microscope at 1000X magnification (Nikon H600L, Japan). Additionally, the KOH string test was performed in order to confirm the Gram character of the bacterial isolates (Powers, 1995). In this test, a drop of 3% KOH (Appendix B) was placed on a clean glass slide and a loopful of bacterial culture was added and mixed thoroughly. The organism was considered Gram negative if the mixture turned highly viscous within 60 sec leading to formation of strings. Biochemical identification was performed using a microbiological kit (Himedia, India) in order to tentatively identify the selected bacterial isolates based on Bergey's Manual of Systematic Bacteriology (Holt et al., 1994).

2.6 Antibiotic susceptibility

Mueller Hinton agar (MHA) (Appendix A) was used to assess the sensitivity of selected lead resistant bacterial isolates to various antibiotics by Kirby-Bauer disc diffusion test (Bauer et al., 1966). Overnight grown bacterial cultures were spread plated on MHA plates to get uniform lawn of bacterial cells and antibiotic octa-discs (Himedia, India) were placed on them. The agar plates were incubated at 30^{o}C for 24 h and zone diameter of clearance due to different antibiotics was recorded.

2.7 Extraction of genomic DNA

Genomic DNA of overnight grown bacterial strains was isolated using Dneasy® Blood & Tissue Kit (Qiagen, Hilden, Germany), analysed using 0.8% agarose gel electrophoresis and visualized by gel documentation system (Syngene G:BOX, UK). The genomic DNA was further quantified and the purity was also checked using NanoDrop 2000c spectrophotometer (Thermofisher Scientific, USA).

2.8 PCR amplification and DNA sequencing of 16S rRNA gene

PCR amplification of 16S ribosomal RNA (16S rRNA) gene was performed using Jump Start Red *Taq* ReadyMix (Sigma - Aldrich, USA) and universal primers 27F and 1495R (Appendix E). The thermal cycler program comprised of an initial denaturation step of 5 min at 95°C followed by 30 cycles of 1 min denaturation at 95°C, 1 min annealing at 55°C and elongation at 72°C for 1 min followed by a final extension step of 5 min at 72°C (Nexus Gradient Mastercycler, Eppendorf, Germany). The resulting PCR amplicon was analysed on 0.8% agarose gel followed by purification using a Strata Prep PCR Purification kit (Agilent Technologies, USA). The purified DNA of 16S rRNA gene amplicon was subsequently sequenced using an automated DNA sequencer.

2.9 Bioinformatic analysis of 16S rRNA gene

The DNA sequence of 16S rRNA gene was subjected to BLAST analysis and was subsequently submitted to Genbank (Altschul et al., 1990). A phylogenetic dendrogram was also constructed by neighbor-joining method using MEGA 7.0 package (Kumar et al., 2016).

2.10 Growth behaviour of selected bacterial isolates in presence of lead

The selected bacterial isolates were grown overnight and 2% inoculum was used for flasks containing defined minimal medium amended with 0.2% glucose along with variable concentration of lead nitrate in the range of 0 to 0.8 mM. The flasks were incubated under constant shaking condition at 150 rpm, 30^{o}C for 48 h. The absorbance of culture suspension was recorded at 600 nm within definite time intervals (12 h) using a Biospectrometer (Eppendorf, Germany) in order to determine the growth.

2.11 PCR amplification of *pbrR* gene

pbrR gene was amplified using Jump Start Red *Taq* ReadyMix (Sigma - Aldrich, USA) and gene specific primers: *pbrR1* and *pbrR2* (Appendix E) (Wei et al., 2014). Both genomic and plasmid DNAs were used separately as templates for carrying out polymerase chain reaction (PCR). The PCR conditions consisted of an initial denaturation step of 4 min at 96°C followed by 35 cycles of 1 min denaturation at 96°C, 1 min annealing at 51°C and 1 min elongation at 72°C with a final extension step of 5 min at 72°C. The PCR amplicon was analysed on a 1% agarose gel followed by visualization using gel documentation system (Syngene G:BOX, UK).

2.12 SEM-EDX analysis

The selected bacterial isolates were grown in a minimal medium supplemented with 0.2% glucose with lead nitrate (0.5 mM and 0.8 mM separately) as test and without lead nitrate as control for 48 h under constant shaking at 150 rpm and at 30^{o}C. Bacterial cell pellet was obtained by centrifugation at 3,000 rpm for 10 min (Eppendorf, Germany) followed by washing with 0.1 M phosphate buffered saline (PBS) with pH 7.4 (Appendix B). Bacterial cells were smeared on cover slips and overnight fixation was done in 2.5% glutaraldehyde

(prepared in PBS). The cells were subjected to critical drying in acetone series from 20% to 100%. The cells were viewed under scanning electron microscope (JEOL JSM-6360 LV, USA) and electron dispersive spectroscopic analysis of the cells was performed simultaneously.

2.13 Transmission Electron Microscopy (TEM)

Transmission electron microscopy of the bacterial isolate grown with and without lead nitrate was done by harvesting cells at 3,000 rpm for 10 min followed by washing with 0.1 M PBS (pH 7.4). The cell pellet obtained was resuspended and fixed in a mixture of 2% para-formaldehyde and 2.5% glutaraldehyde prepared in PBS for 2 to 3 h at 4^{o}C. Bacterial cells were again centrifuged at 3,000 rpm and the fixative was replaced by 0.5 ml of 0.1 M PBS. Samples were sectioned and analysed by TEM (Morgagni 268D, Fei Electron Optics, USA).

2.14 Atomic Absorption Spectroscopy (AAS)

Bacterial cells were grown with and without lead nitrate (0.5 mM) in minimal medium supplemented with 0.2% glucose in 500 ml flasks for 48 h at 150 rpm and 30^{o}C. The cells were harvested, dried and ground to obtain a fine powder. The samples were subjected to wet digestion using nitric acid (50%) followed by filtration. Lead analysis was performed using Atomic Absorption Spectrometer (Thermo Fisher Scientific, USA) by furnace method at a wavelength of 217 nm. The amount of lead internalised by the bacterium was calculated as mg Pb^{2+}/g dry weight of the biomass using standards.

2.15 X-ray Diffraction (XRD) analysis

Bacterial cells exposed to 0.5 mM lead nitrate and control (without lead nitrate) were centrifuged at 10,000 rpm for 10 min followed by washing with 0.1 M PBS (pH 7.4). Subsequently the cell pellet obtained was kept for drying at 45°C for 48 h. The dried pellet was pulverized to form a fine powder which was further used to make a film on a glass slide for X-ray diffraction analysis (Panalytical X'pert-pro diffractometer, Japan). The XRD measurements were accomplished in a continuous-scan mode with Cu-Kα radiation (1.540 Å) and 2θ ranged from 10° to 80° by a step of 0.2°.

2.16 Fourier Transformed Infrared Spectroscopy (FTIR)

The 48h grown bacterial cultures in presence and absence of lead nitrate were centrifuged at 10,000 rpm for 10 min followed by washing with 0.1 M PBS (pH 7.4). The cell pellet was dried in an incubator at 45^{o}C for 48 h. The dried pellet was subjected to grinding using an agate mortar in order to obtain a fine powder. Sample was pressed into a sample holder after grinding in excess of finely ground KBr. The infrared spectrum was displayed in the range of 4000-400 cm^{-1} by instrument, IR Prestige-21 (Shimadzu, Japan).

2.17 Phosphatase assay

Whole cell protein of the bacterial cells grown in presence (0.2 and 0.5 mM) and absence of lead nitrate was extracted as per the standard protocol of Laemmli (1970) and used to estimate phosphatase activity. Phosphatase assay was performed by modifying the protocol of Sand et al. (2015). Para-nitrophenol (pNP) was used for preparation of a standard curve (Appendix). Para-nitrophenyl phosphate (pNPP) was added to the reaction mix to a final concentration of 5 mM in 50 mM sodium acetate buffer (pH 5.5). The reaction was initiated by addition of 500 µg of extracted protein followed by an incubation at 37^{o}C for 10 min. The

reaction was terminated by adding 800 µl of 2 N NaOH and the absorbance was recorded at 405 nm using Biospectrometer (Eppendorf, Germany). Phosphatase activity was defined as nmoles of para-nitrophenol generated min^{-1} at 37^{o}C.

2.18 Statistical analysis

Experimental data were statistically analysed using one-way ANOVA in GraphPad Prism 7.03 (GraphPad Software, La Jolla California, USA). The results were considered significant if $p < 0.05$.

2.19 Proteomic analysis

2.19.1 Extraction of whole cell protein

Bacterial cells were grown up to mid-log phase in presence (0.2 mM) as well as absence of lead nitrate. 50 mg cell pellet was taken for proteomic analysis after harvesting cell suspension at 10,000 rpm for 10 min at room temperature. The cell pellet was washed with 0.1 M PBS (pH 7.4) twice followed by addition of 20 µL protease inhibitor cocktail mix and 100 µL PBS along with lysozyme at a final concentration of 0.2 mg/mL followed by mixing. The microfuge tubes containing the mix were incubated at 37^{o}C, 700 rpm for 30 min. The tubes were centrifuged at 10,000 rpm, room temperature for 5 min. The pellet was resuspended in 0.1% *Rapi*Gest SF buffer (Waters, USA) prepared in 50 mM ammonium bicarbonate. The bacterial cells were sonicated for 30 sec on ice. The tubes were recentrifuged at 10,000 rpm for 10 min at 4^{o}C. Subsequently, clean microfuge tubes were used to collect the supernatant which was centrifuged again at 16,000 rpm, 4^{o}C for 60 min. The protein was collected as the supernatant in clean microfuge tubes.

2.19.2 Quantification of protein

Protein samples were quantified by Bradford assay (Bradford, 1976). Bovine serum albumin was used to prepare a standard curve for protein estimation (Appendix D). The extracted protein from the control and lead exposed cells was quantified.

2.19.3 Qualitative analysis of protein

Protein sample containing 15 µg protein was mixed and heated with 6X sample solubilizing buffer (Appendix D) and analysed using 12% sodium dodecyl sulphate-polyacrylamide gel electrophoresis (SDS-PAGE) in 1X Tris-glycine electrophoresis buffer (Appendix D) at 100V using BIORAD Mini PROTEAN Tetra System (Sambrook et al., 1989). The gel was stained overnight using freshly prepared 0.05% Coomassie Brilliant blue R250 followed by thorough de-staining by keeping in de-staining solution on a rocker till it became clear (Appendix D).

2.19.4 In- Solution digestion

The extracted protein was subsequently subjected to in-solution digestion using trypsin (Deshmukh et al., 2017). Initially, the protein samples were concentrated to 100 µL using spin column with MW cut off of 3000 Daltons. The solution was subsequently heated at 80^{o}C for 15 min and maintained at 500 rpm. Later on, 3 µL of 100 mM dithiothreitol was added and heated at 60^{o}C for 15 min at 500 rpm. The pH of solution was checked following which 3 µL of 200 mM iodoacetamide was added and incubated in dark for 30 min at RT. Eventually 2 µL of 1 µg/µL trypsin was added and incubated overnight at 37^{o}C, 500 rpm. Finally, 2 µL of concentrated HCl was added to the tubes which were incubated at 37^{o}C for 20 min before centrifugation. Clean up of the digested peptides was performed by Zip Tips C_{18} (Millipore, Merck, Germany) followed by reconstitution in 3% acetonitrile containing 0.1% formic acid.

2.19.5 LC-MS/MS analysis

The peptides were analysed using a Micro LC 200 (Eksigent, Dublin, CA) and TripleTOF 5600 (AB Sciex, USA). The sample parameters applied include cysteine alkylation by iodoacetamide, digestion with trypsin and search effort was set to rapid. Identification and quantification of the peptides was achieved by means of Independent Data Acquisition (IDA) and Sequential Window Acquisition of All Theoretical Data (SWATH) respectively against the Uniprot database of the respective bacterium (Gillet et al., 2012). False discovery rate analysis (FDR) was set to <1% on protein level using ProteinPilot software. Quantitative analysis of the proteins was performed in PeakView followed by MarkerView analysis (Sciex, USA).

2.20 Cell motility assay

1 µL overnight grown bacterial culture was spot inoculated on PYE soft agar (Appendix A) containing 0.25% agar supplemented with 0, 0.5 and 1 mM lead nitrate. The plates were observed to check the growth rings after 16 h of incubation at 30^{o}C.

2.21 PCR amplification of *smtAB* gene

Amplification of *smtAB* gene was performed using Jumpstart Red *Taq* ReadyMix (Sigma-Aldrich, USA) and gene specific primers: *smt1* and *smt2* (Appendix E) (Naz et al., 2005) procured from Sigma-Aldrich, India. The PCR reaction conditions comprised of initial denaturation step of 5 min at 94°C, followed by 35 cycles of 1 min denaturation at 94°C, 45 sec annealing at a temperature gradient (50°C to 60°C), and 1 min elongation at 72°C followed by a final extension of 5 min at 72°C. Subsequently the PCR product was analysed on 1% agarose gel.

2.22 PCR amplification of *bmtA* gene

The isolated plasmid DNA was taken as a template for *bmtA* gene amplification using gene specific primers: P3 and P4 (Appendix E) (Blindauer et al., 2002) synthesized by Sigma-Aldrich, India. The PCR amplification was carried out using Jumpstart Red *Taq* ReadyMix (Sigma-Aldrich, USA) with addition of 1.5 mM $MgCl_2$ since the optimum $MgCl_2$ required for the PCR reaction was 2.25 mM. The PCR reaction conditions comprised of an initial denaturation step of 5 min at 94°C, followed by 30 cycles of 1 min denaturation at 94°C, 45 sec annealing at 59°C and 1 min elongation at 72°C followed by a final extension of 5 min at 72°C. The PCR product was analysed on 1.5% agarose gel (Appendix C), purified by Strata Prep PCR purification kit (Agilent Technologies, USA).

2.23 DNA sequencing of *bmtA* and phylogenetic analysis of BmtA

The *bmtA* amplicon was sequenced using an automated sequencer. The DNA sequence was subjected to BLASTx, compared with the closely related sequences followed by construction of a dendrogram using Mega 7.0 package by neighbour-joining method. The *bmtA* gene sequence has been submitted to the Genbank.

2.24 Homology modelling of BmtA

The three-dimensional model of BmtA (Accession no. WP_003100805) was constructed using I-TASSER suite which also predicted the secondary structure of this protein (Yang et al., 2015). Modelled structures were assessed using the protein structure and model assessment tools viz. QMEAN score (Benkert et al., 2008) and Gromos (van Gunsteren et al., 1996) at the Swiss model server. They were further analysed by programs viz. PROCHECK (Laskowski et al., 1993), VERIFY3D (Eisenberg and Luthy, 1997) and ERRAT (Colovos and Yeates, 1993) of the verification server, SAVES (Dawar et al., 2013).

2.25 *In silico* docking studies of BmtA and metal ions

The BmtA protein was docked against various metal ions viz. Pb, Zn, Cd, Ni, Co, Cu and Ca in order to understand the binding and interactions of these metal ions with various amino acid residues of BmtA using Patchdock server (Schneidman-Duhovny et al., 2005) (http://bioinfo3d.cs.tau.ac.il/PatchDock/). Subsequently the structures were viewed by PyMOL and Discovery Studio.

3.1 Isolation of lead resistant bacterial strains

A battery waste site was selected from industrial area of Goa for collection of soil samples since batteries are a major source of lead contamination in the environment nowadays. Minimal medium (M9) agar plate supplemented with 1.5 mM lead nitrate displayed 28 morphologically distinct bacterial colonies.

3.2 Maximum tolerance concentration (MTC) of lead

Bacterial isolates screened from battery waste of Goa when checked for their lead tolerance in a defined minimal medium resulted in 11 lead resistant bacterial strains showing tolerance of >2 mM lead nitrate which have been listed in Table 3.1. Most of them could tolerate within a range of 3 to 4 mM which is significantly high concentration. Earlier reports suggest that lead resistant bacteria generally tolerate lead in the range of 0.5 - 3.7 mM. For instance, the minimum inhibitory concentration was found to be 0.6 mM for *Bacillus megaterium*, 2.5 mM for *Pseudomonas marginalis* (Roane, 1999; Das et al., 2016), 1.21 mM for *Agrobacterium tumefaciens* and 3.62 mM for *Acinetobacter* sp. (Zhang et al., 2011). However, it is not appropriate to compare our results with previous studies because there are various factors such as media composition, strength of medium, complexation, organic nutrients and availability of lead in the medium that alter the MTC values up to a great extent (Kamala-Kannan and Krishnamoorthy, 2006; Govarthanan et al., 2013). Interestingly, the lead resistant bacterial strains demonstrated various alterations in colony morphology viz. brownish pigmentation, presence of a clear zone surrounding the colony and formation of a precipitation ring on exposure to lead nitrate (Fig. 3.1). Red-brown pigmentation has also been reported in *Pseudomonas vesicularis* and *Streptomyces* sp. on exposure to lead (Zanardini et al., 1997).

Table 3.1 Bacterial isolates showing MTC >2 mM for lead.

S.N.	Lead resistant bacterial isolates	MTC (mM)
1	SJ2A	3
2	SJ3A	3
3	SJ4	3.5
4	SJ7A	3.5
5	SJ11	4
6	SJ20	3
7	SJ28	4
8	SJ29	4
9	SJ37B	4
10	SJ42	3
11	KS2	3.5

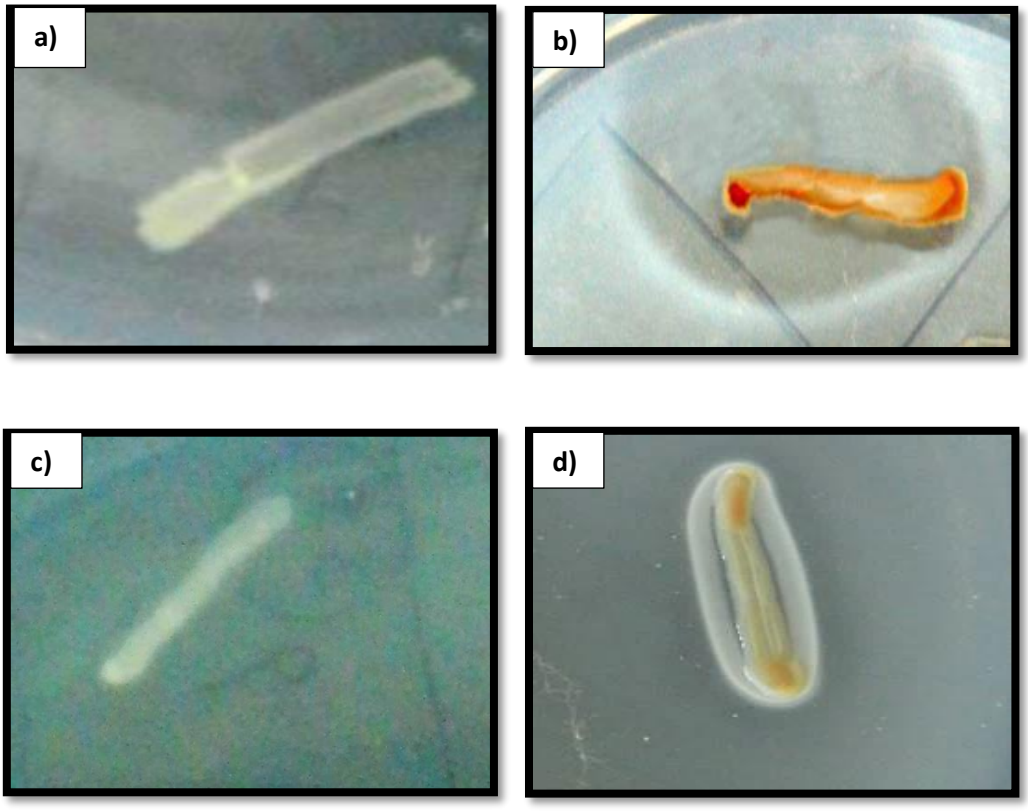

Fig. 3.1 Alterations in colony morphology of bacterial isolates on exposure to lead.

a), b) Controls of bacterial strains SJ2A and SJ11 respectively (without lead nitrate)

c), d) Zone of clearance in case of strain SJ2A and formation of a precipitation ring in case of strain SJ11 (exposed to 2 mM lead nitrate) respectively.

3.3 Plasmid profile

Heavy metal resistance in bacteria is known to be governed by plasmids (Silver and Misra, 1988). This prompted us to screen the lead resistant isolates for occurrence of any plasmids. Interestingly out of 11, three lead resistant bacterial isolates showed presence of plasmids of varying sizes (Fig. 3.2). Earlier studies in *C. metallidurans* CH34 have described presence of mega-plasmids, pMOL28 and pMOL30 which contain at least 7 genetic determinants conferring resistance to several toxic heavy metals such as zinc, cadmium, mercury, cobalt, nickel and lead (Mergeay et al., 1985; Borremans et al., 2001). Genes, *pbtTFYRABC* located on plasmid pA81 of *Achromobacter xylosoxidans* A8 are also involved in governing resistance to Pb^{2+} and Cd^{2+} (Hložková et al., 2013**)**. Therefore, possibly the plasmids present in the lead resistant isolates SJ2A, SJ3A and SJ20 are also responsible for their resistance to high concentrations of lead. Based on MTC values, alterations in colony morphology as well as presence of plasmids, bacterial isolates, SJ2A, SJ3A, SJ20 and SJ11 were selected for further identification using biochemical tests.

3.4 Morphological and biochemical characterisation

All the selected bacterial isolates were Gram negative rods. The Gram character was confirmed by KOH string test since the mixture of cells and 3% KOH turned highly viscous within a few seconds resulting in appearance of strings. Subsequently, all the three bacterial isolates SJ2A, SJ3A and SJ20, were tentatively identified as *Providencia* sp. belonging to the family Enterobacteriaceae based on biochemical tests though they depicted different plasmid profiles (Table 3.2). On the other hand, the isolate SJ11 was not found to belong to Enterobacteriaceae family. Therefore, the lead resistant bacterial isolates, SJ2A and SJ11 were selected for further characterization.

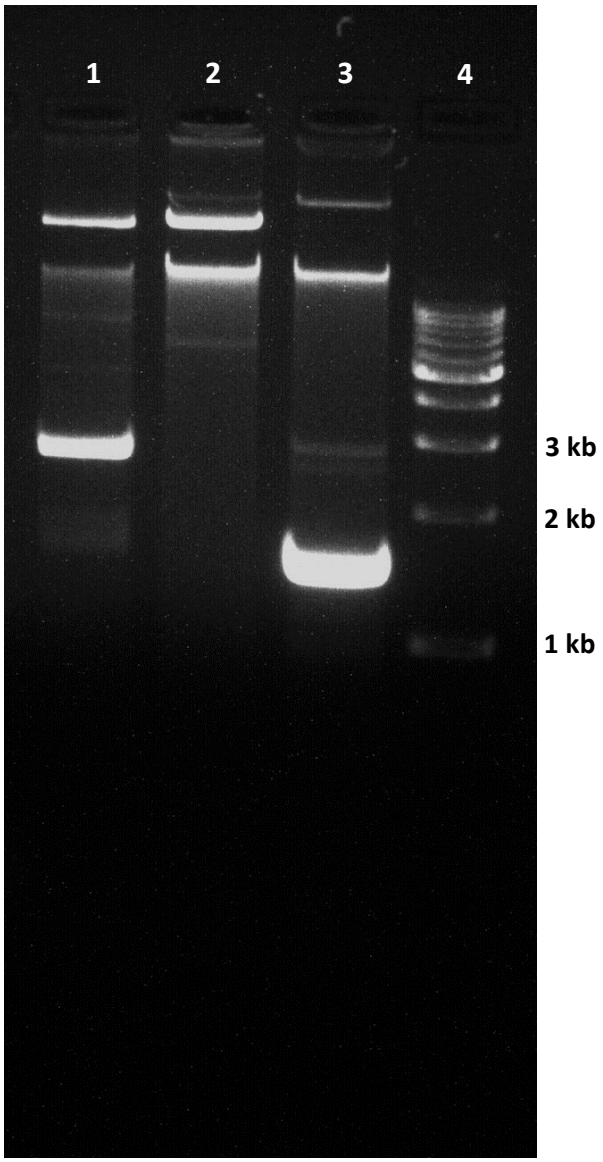

Fig. 3.2 Plasmid profile of lead resistant bacterial isolates.

Lane 1: Isolate SJ2A

Lane 2: Isolate SJ3A

Lane 3: Isolate SJ20

Lane 4: 1 kb DNA ladder

Table 3.2 Biochemical characteristics of lead resistant bacterial isolates.

S.N.	Biochemical tests	SJ2A	SJ3A	SJ11	SJ20
1	ONPG	-	-	-	-
2	Lysine utilization	-	-	-	-
3	Ornithine utilization	+	+	-	+
4	Urease	-	+	-	+
5	Phenylalanine deamination	+	+	-	+
6	Nitrate reduction	+	+	-	+
7	H_2S production	-	-	-	-
8	Citrate utilization	-	+	+	-
9	Voges Proskauer's	-	-	-	-
10	Methyl red	+	+	-	+
11	Indole	-	-	-	-
12	Malonate utilization	-	-	-	-
13	Esculin hydrolysis	-	-	-	-
14	Oxidase	-	-	+	-
15	Catalase	+	+	+	+
	Sugar fermentation tests				
1	Arabinose	+	+	-	+
2	Xylose	-	-	+	-
3	Adonitol	+	+	-	+
4	Rhamnose	-	-	-	-
5	Cellobiose	-	-	-	-
6	Melibiose	-	-	-	-
7	Saccharose	-	-	-	-
8	Raffinose	-	-	-	-
9	Trehalose	+	+	-	+
10	Glucose	+	+	+	+
11	Lactose	-	-	-	-

+ Positive; - Negative

3.5 Antibiotic susceptibility

It is a well known fact that genes encoding heavy metal resistance and various antibiotics coexist on chromosomal/plasmid genome (Silver and Phung, 1996, Lupo et al., 2012). In fact, genes governing heavy metal efflux are located on the R plasmids thus, conferring metal resistance (Martinez et al., 2009). It is interesting to note that the plasmid carrying isolate, SJ2A was resistant to various antibiotics (Table 3.4) viz. bacitracin (10 Units), ampicillin (10µg), cephalothin (30µg), penicillin-G (10 Units), polymyxin-B (300 Units), cloxacillin (5µg), erythromycin (15µg) and colistin sulphate (25µg). On the other hand, isolate SJ11 also demonstrated resistance to several antibiotics viz. gentamicin (10µg), ampicillin (10µg), cephalothin (30µg), colistin sulphate (25µg), kanamycin (30µg) and amikacin (10µg). Susceptibility of these lead resistant bacterial isolates to certain antibiotics viz. sulphatriad (200µg), carbenicillin (100µg), co-trimazine (25µg), streptomycin (10µg), ciprofloxacin (10µg) and neomycin (30µg) was evident from the diameter of clearance zone surrounding the respective antibiotic disc (Fig. 3.3).

Table 3.4 Susceptibility of lead resistant isolates SJ2A and SJ11 against various antibiotics.

Antibiotic	Concentration (per disc)	Response of isolates	
		SJ2A	SJ11
Ampicillin (AMP)	10µg	R	R
Cephalothin (CEP)	5µg	R	R
Colistin sulphate (CL)	25µg	R	R
Gentamicin (GEN)	10µg	S	R
Streptomycin (S)	10µg	S	S
Ciprofloxacin (CIP)	10µg	S	S
Kanamycin (K)	30µg	S	R
Tetracycline (TE)	30µg	R	R
Neomycin (N)	30µg	S	S
Polymyxin-B (PB)	300 Units	R	S
Penicillin-G (P)	10 Units	R	R
Co-Trimoxazole (COT)	25µg	S	S
Chloramphenicol (C)	30µg	R	R
Bacitracin (B)	10 Units	R	R
Erythromycin (E)	15µg	R	R
Oxytetracycline (O)	30µg	R	R
Cloxacillin (COX)	5µg	R	R
Clindamycin (CD)	2µg	R	R
Amikacin (AK)	10µg	S	R
Sulphatriad (S3)	200µg	S	S
Carbenicillin (CB)	100µg	S	S
Co-Trimazine (CM)	25µg	S	S

S- Susceptible; R- Resistant

a)

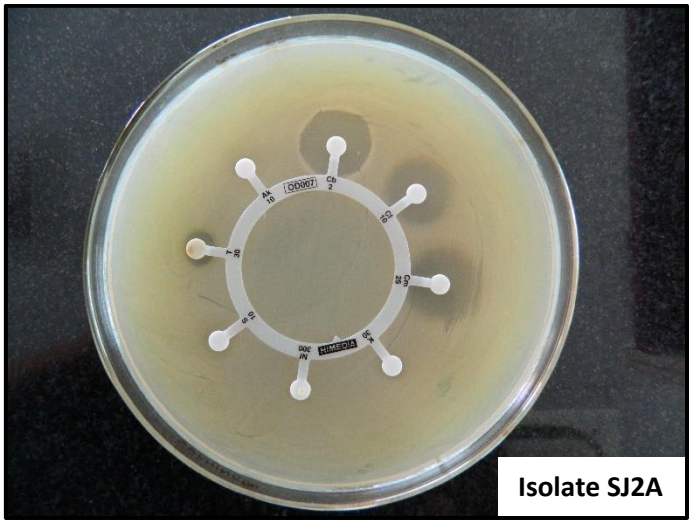

b)

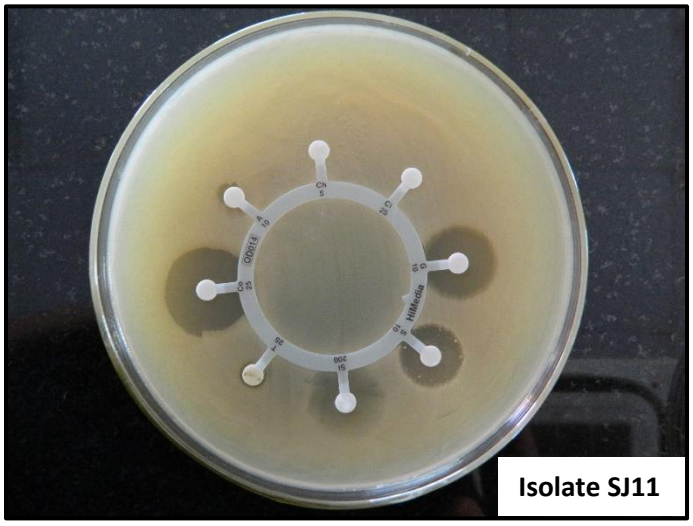

Fig. 3.3 Mueller Hinton agar plates depicting antibiotic susceptibility of the lead resistant bacterial isolates, SJ2A and SJ11. The clear zones surrounding the antibiotic discs indicate susceptibility of the bacterial isolates.

3.6 Extraction of genomic DNA

A distinct band of genomic DNA was observed on the agarose gel (Fig. 3.4). The quality and purity ratios have been shown in Table 3.5. The agarose gel evidently showed that the DNA isolated was of very good quality and free from any RNA contamination. However, the $A_{260/280}$ and $A_{260/230}$ values did not reflect the purity of DNA. This could be due to interference by certain chemicals such as guanidine hydrochloride or guanidine isocyanate which were present in the genomic DNA isolation kit.

3.7 Amplification and sequence analysis of 16S rRNA

Amplicon of 16S rRNA gene (1.5 kb) was observed on 0.8% agarose gel (Fig. 3.5). The isolate SJ2A was identified as *Providencia vermicola* based on DNA sequencing of this gene followed by BLAST analysis. The 16S rRNA gene sequence has been deposited in Genbank as *Providencia vermicola* strain SJ2A with an accession number KT799659 (https://www.ncbi.nlm.nih.gov/nuccore/KT799659.1). The phenogram of *P. vermicola* strain SJ2A (Fig. 3.6) clearly showed its close relatedness to other strains of *Providencia* sp. Similarly, BLAST analysis of 16S rDNA sequence of SJ11 confirmed it to be *Achromobacter xylosoxidans* and the sequence is now available in Genbank with an accession number KT807473 (https://www.ncbi.nlm.nih.gov/nuccore/931255884). The phenogram of *A. xylosoxidans* strain SJ11 indicates that the bacterium shows maximum homology with *A. xylosoxidans* strain NA20 and *A. insolitus* strain Y2P1 (Fig. 3.7).

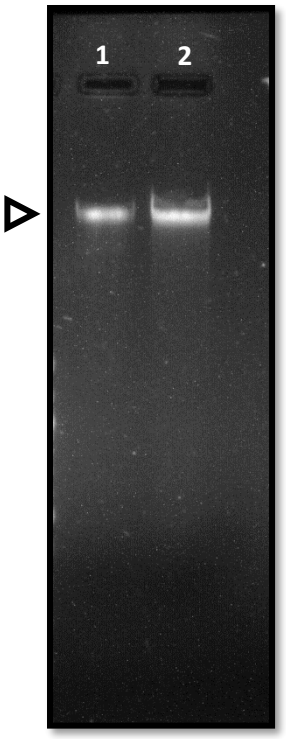

Fig. 3.4 Genomic DNA isolated from the lead resistant bacterial isolates.

Lane 1: Genomic DNA of isolate SJ2A

Lane 2: Genomic DNA of isolate SJ11

Table 3.5 Quantity and purity of isolated genomic DNA.

Bacterial Isolates	DNA concentration (ng/µL)	A 260/280	A 260/230
SJ2A	54.3	2.24	0.87
SJ11	52.7	2.26	1.25

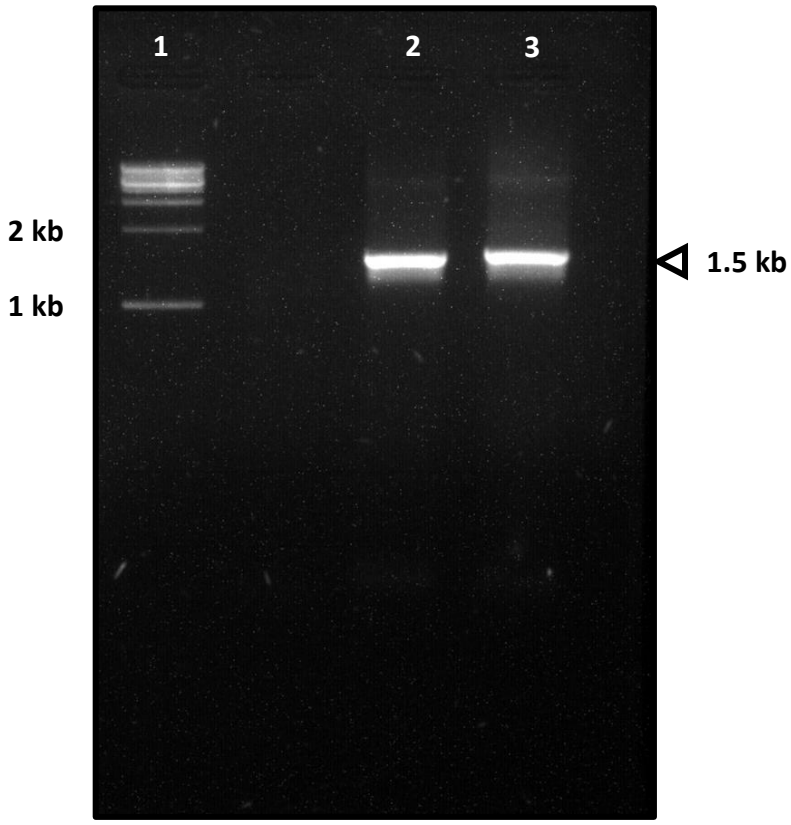

Fig. 3.5 16S rRNA gene amplicon on 0.8% agarose gel.

Lane 1: 1 kb DNA ladder

Lane 2: 16S rRNA gene amplicon from isolate SJ2A

Lane 3: 16S rRNA gene amplicon from isolate SJ11

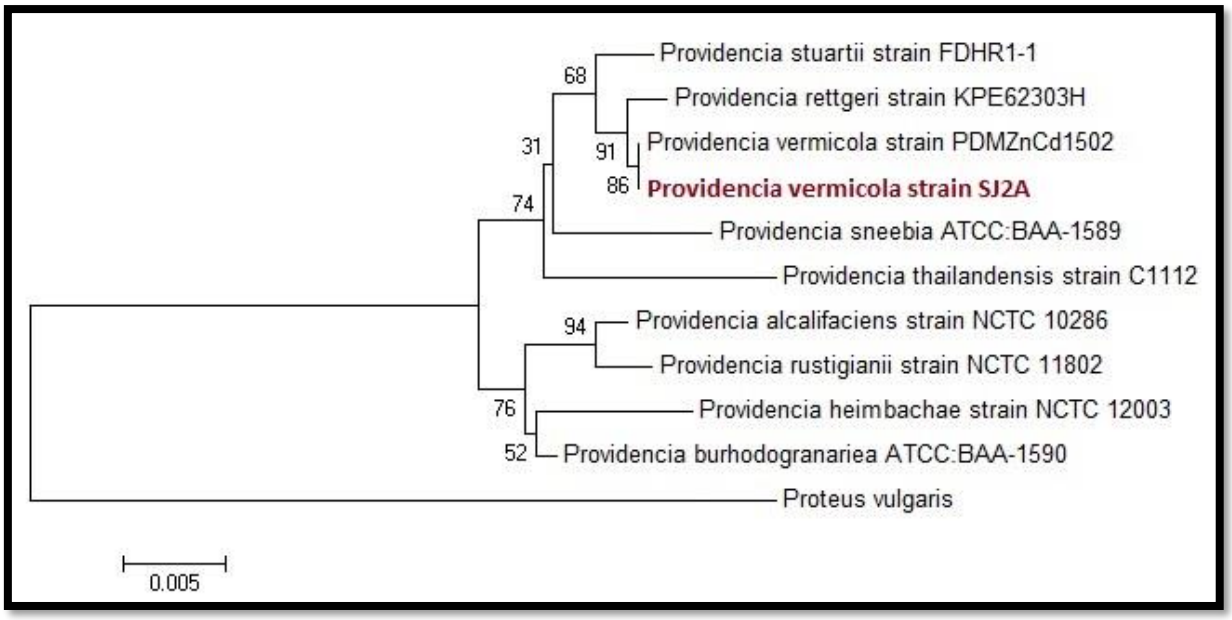

Fig. 3.6 Phylogenetic tree showing relationship of the lead resistant bacterial isolate *Providencia vermicola* strain SJ2A with other strains of *Providencia* sp. using neighbour-joining method. The bootstrap values were based on 10000 replicates.

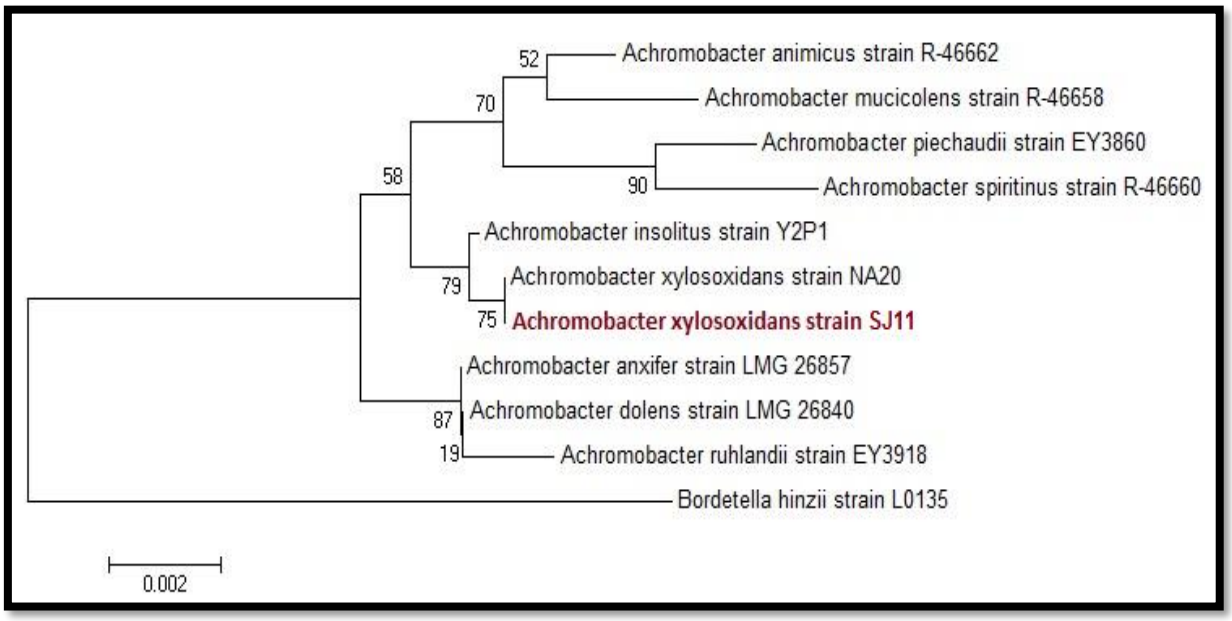

Fig. 3.7 Phylogenetic tree showing relationship of the lead resistant bacterial isolate *Achromobacter xylosoxidans* strain SJ11 with other strains of *Achromobacter* sp. using neighbour-joining method. The bootstrap values were based on 10000 replicates.

Summary

Lead resistant bacterial strains were isolated from the waste site of a battery manufacturing industry in Goa. The maximum tolerance concentration for these bacterial strains ranged from 3 to 4 mM in defined minimal medium. Interestingly, a few strains demonstrated alterations in colony characteristics viz. pigmentation, zone of clearance and precipitation ring on exposure to lead nitrate. The bacterial isolates SJ2A, SJ3A and SJ20 clearly showed multiple bands for plasmids. Subsequently, the potential lead resistant bacterial isolates, SJ2A and SJ11 were identified as *Providencia vermicola* and *Achromobacter xylosoxidans* respectively, based on biochemical tests and 16S rDNA sequencing. Furthermore, these bacterial strains were characterised to explore the lead resistance mechanisms.

4.1 Growth behaviour of the selected bacterial isolates in presence of lead

The bacterial isolates, *P. vermicola* strain SJ2A and *A. xylosoxidans* strain SJ11 could tolerate upto 0.8 mM lead nitrate in a defined minimal medium (Fig. 4.1, 4.2). MTC values were comparatively less in liquid medium as compared to the solid medium due to the fact that the bioavailability of lead increases by several fold in the liquid medium. Growth for both the bacterial isolates was inversely proportional to the concentration of lead in the medium. Interestingly, the bacterium, *A. xylosoxidans* strain SJ11 also demonstrated formation of a visible white precipitate in presence of 0.5 mM lead nitrate (Fig. 4.3).

4.2 PCR amplification of *pbrR* gene

A *pbrR* amplicon of approximately 500 bp was obtained by using gene specific primers (Fig. 4.4). *pbrR* is well known to encode PbrR protein which regulates the lead induced transcription of *pbr* operon and it has also been used for construction of lead biosensor (Borremans et al., 2001; Wei et al., 2014). Interestingly, in case of *P. vermicola* strain SJ2A, *pbrR* was amplified from genomic as well as plasmid DNA. This suggested that both plasmid as well as chromosomal genome play an important role in conferring lead resistance in this organism. Another bacterial strain, *A. xylosoxidans* strain SJ11 did not harbour any plasmid therefore, amplification of gene from the chromosomal DNA indicates that lead resistance is governed solely by the genes located on chromosomal genome.

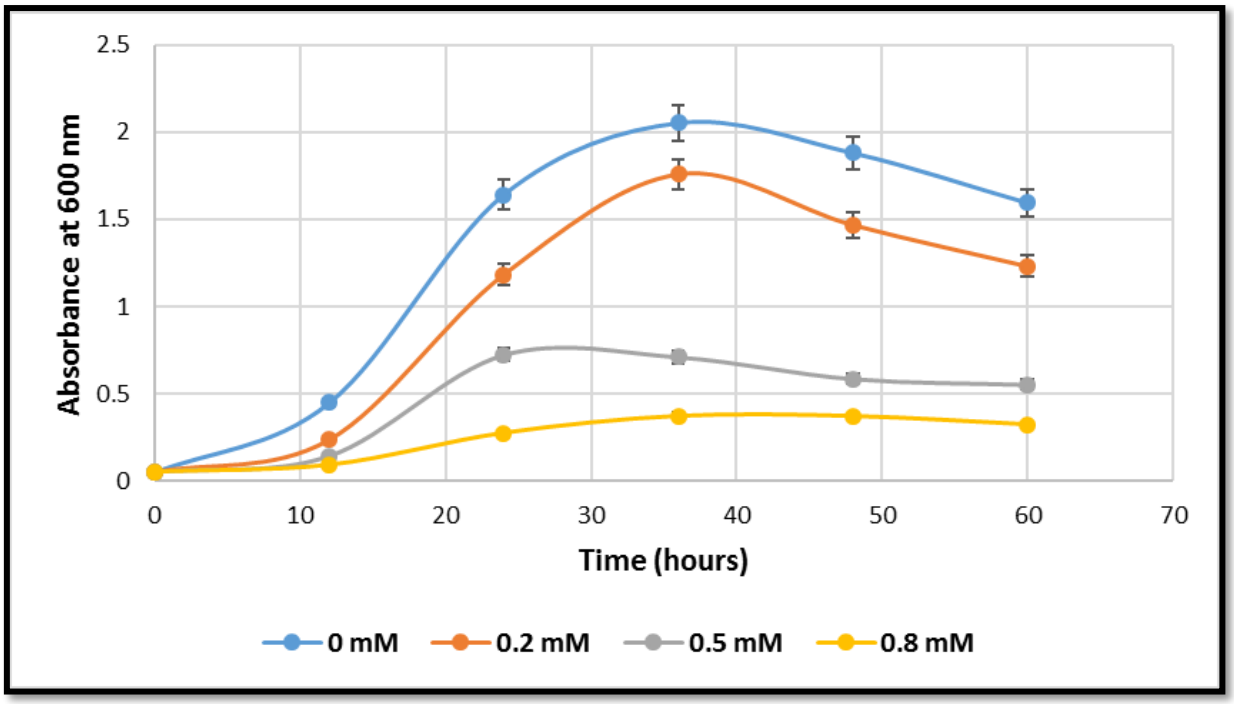

Fig. 4.1 Growth behaviour of *Providencia vermicola* strain SJ2A in presence of varying concentrations (0 to 0.8 mM) of lead nitrate.

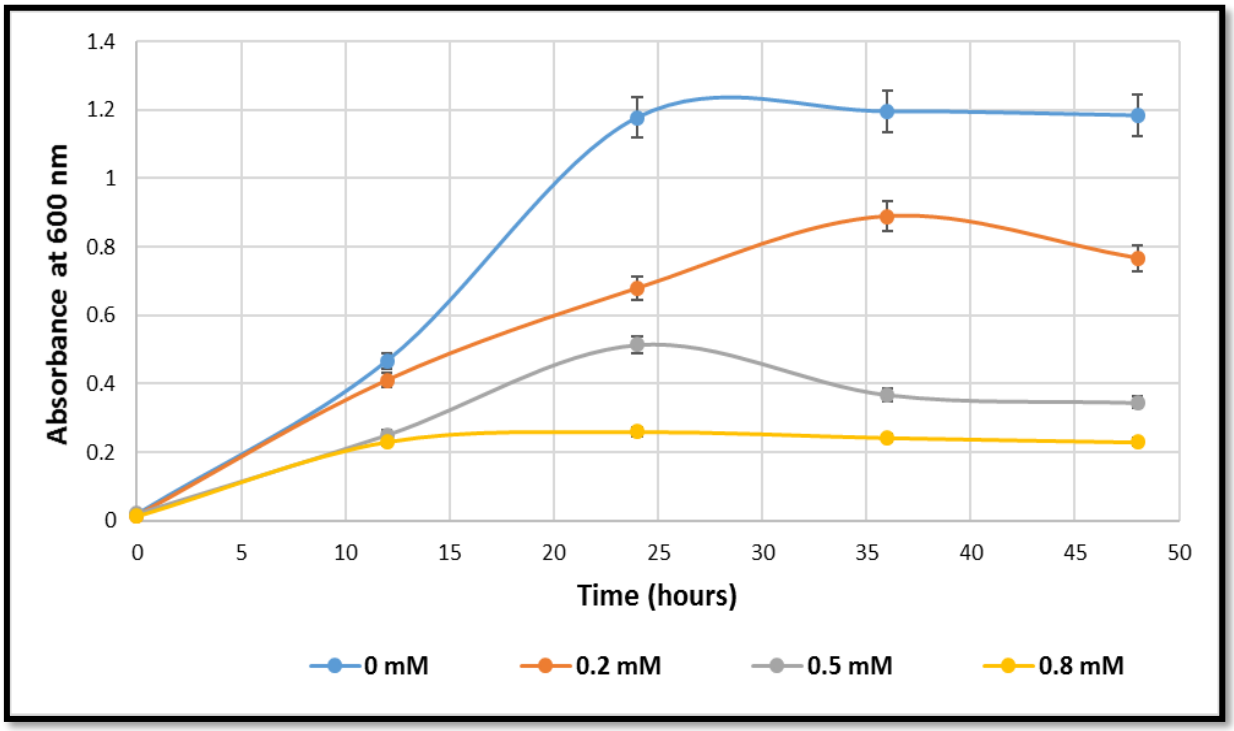

Fig. 4.2 Growth behaviour of *Achromobacter xylosoxidans* strain SJ11 in presence of varying concentrations (0 to 0.8 mM) of lead nitrate.

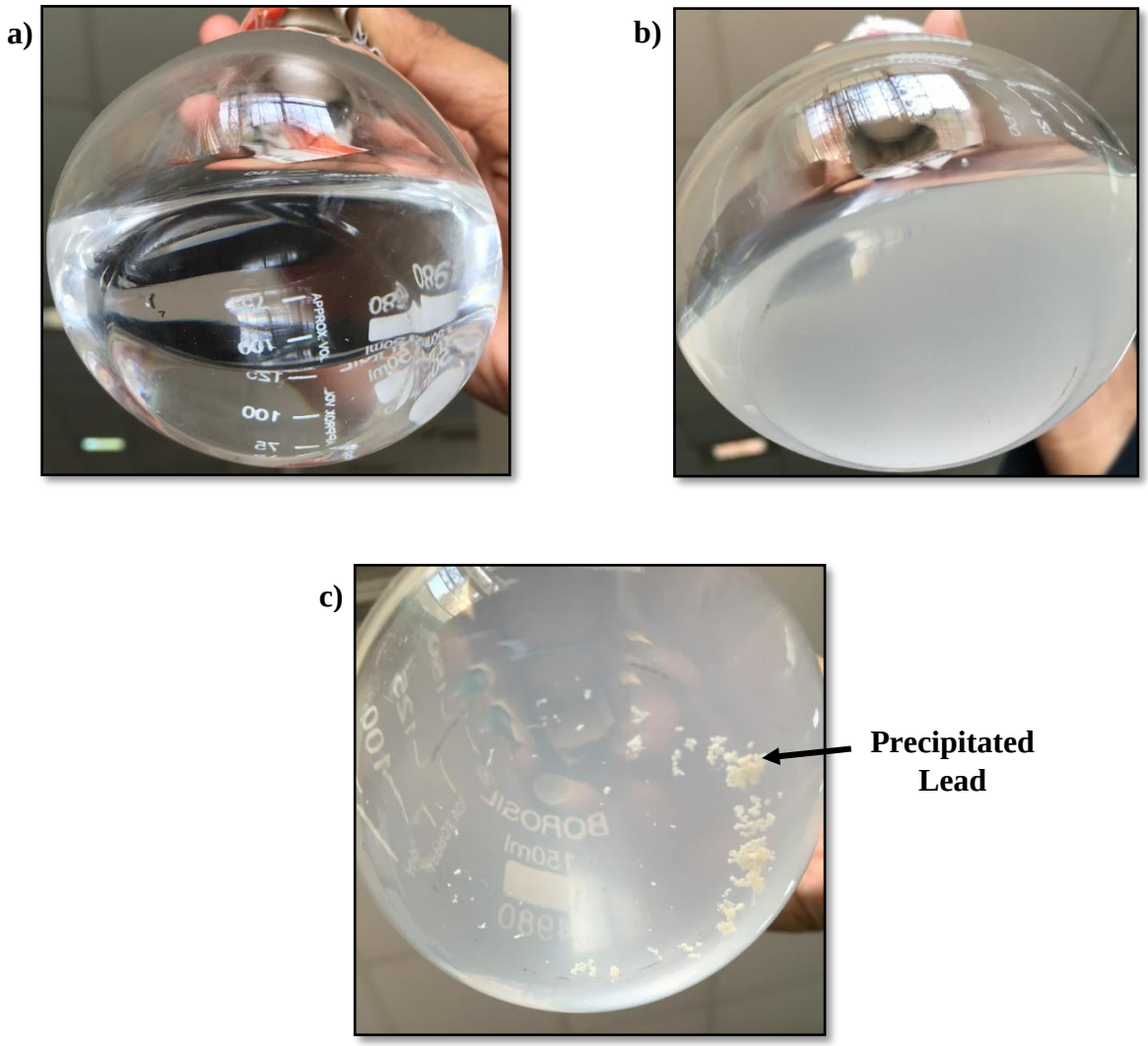

Fig. 4.3 Lead precipitation by *A. xylosoxidans* strain SJ11 in defined minimal medium.

a) Medium without lead nitrate and bacterial culture

b) Medium without lead nitrate containing bacterial culture

c) Medium supplemented with 0.5 mM lead nitrate containing bacterial culture showing lead precipitation

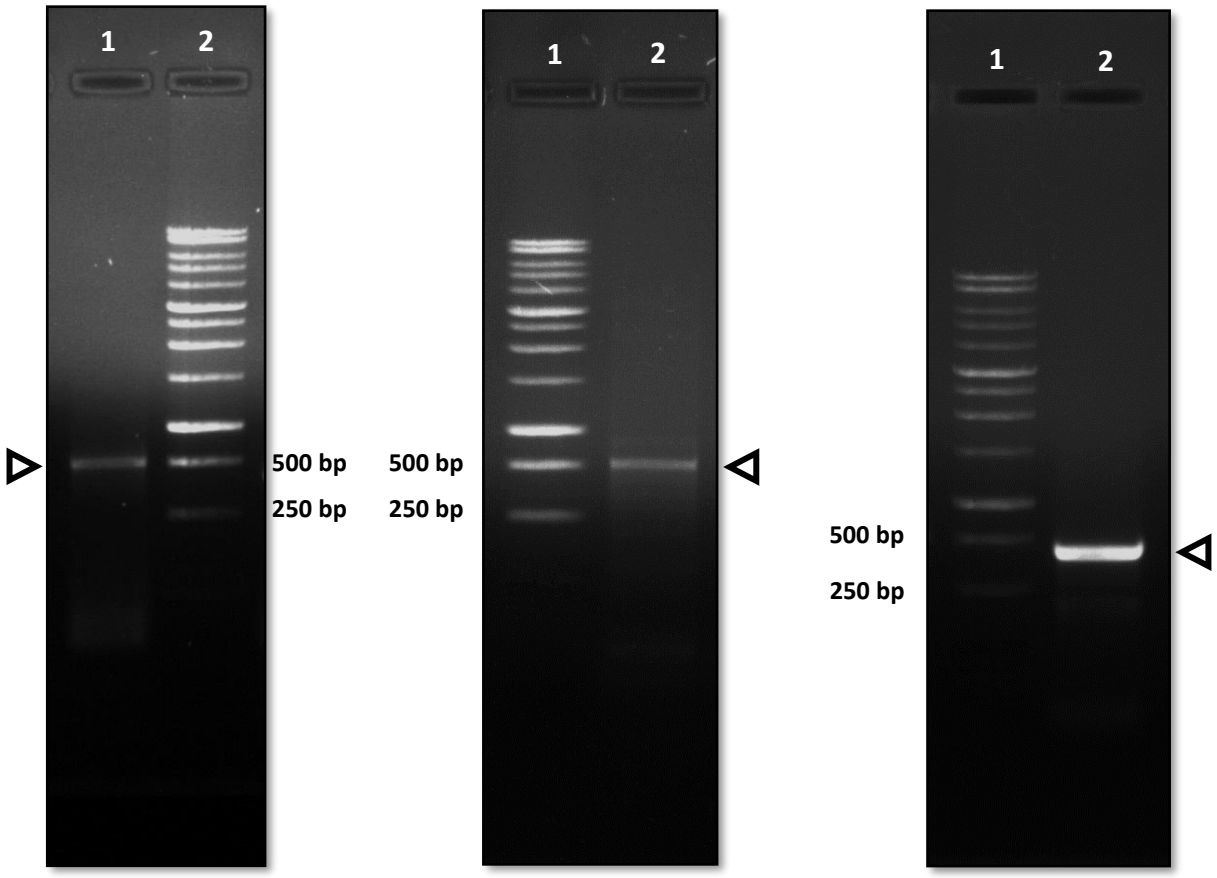

Fig. 4.4 *pbrR* gene amplicon on 1% agarose gel.

a) Lane 1: *pbrR* amplicon using *P. vermicola* strain SJ2A genomic DNA as template; Lane 2: 1 kb DNA ladder

b) Lane 1: 1 kb DNA ladder; Lane 2: *pbrR* amplicon using *P. vermicola* strain SJ2A plasmid DNA as template

c) Lane 1: 1 kb DNA ladder; Lane 2: *pbrR* amplicon using *A. xylosoxidans* strain SJ11 genomic DNA as template

4.3 Mechanism of lead resistance in *P. vermicola* strain SJ2A

4.3.1 SEM-EDX Analysis

The cells of *P. vermicola* strain SJ2A showed a unique alteration pattern in the cell morphology due to lead exposure. In presence of 0.8 mM lead nitrate, the cells tend to become filamentous and appear as long inter-connected chains, approximately 7 to 8 times longer than the usual size (Fig. 4.5). The septum formation seems to be inhibited and therefore daughter cells fail to separate resulting in long chains of bacterial cells. It has been reported that bacteria use filamentation of cells as a strategy to overcome stress condition such as antibiotic therapies (Justice et al., 2008). Similar pattern of filamentation has been observed in *Aeromonas caviae* strain KS-1 when exposed to TBTC (Shamim et al., 2013). Transformation of cells from rods to inter-connected chains of cells reduces the surface area exposed to the toxic metals thus alleviating their lethal effects.

Electron dispersive X ray spectroscopy did not show any considerable adsorption of lead onto the bacterial cell surface (Fig. 4.6). This suggested that intracellular uptake of lead could be a preferred lead resistance mechanism in *P. vermicola* strain SJ2A.

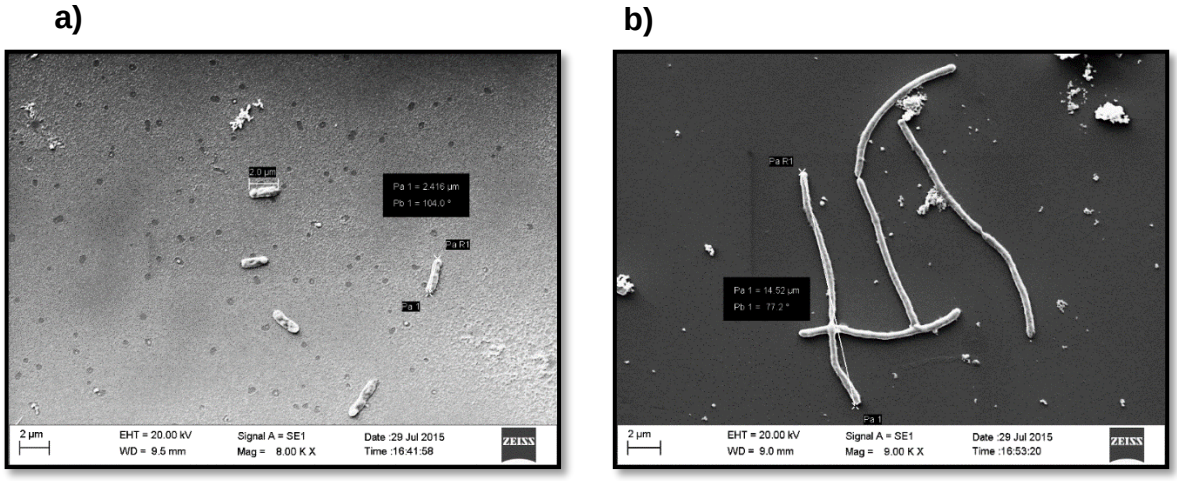

Fig. 4.5 Scanning electron micrographs of cells of *P. vermicola* strain SJ2A.

a) Bacterial cells without lead nitrate exposure (rod shaped)

b) Bacterial cells exposed to 0.8 mM lead nitrate (filamentous)

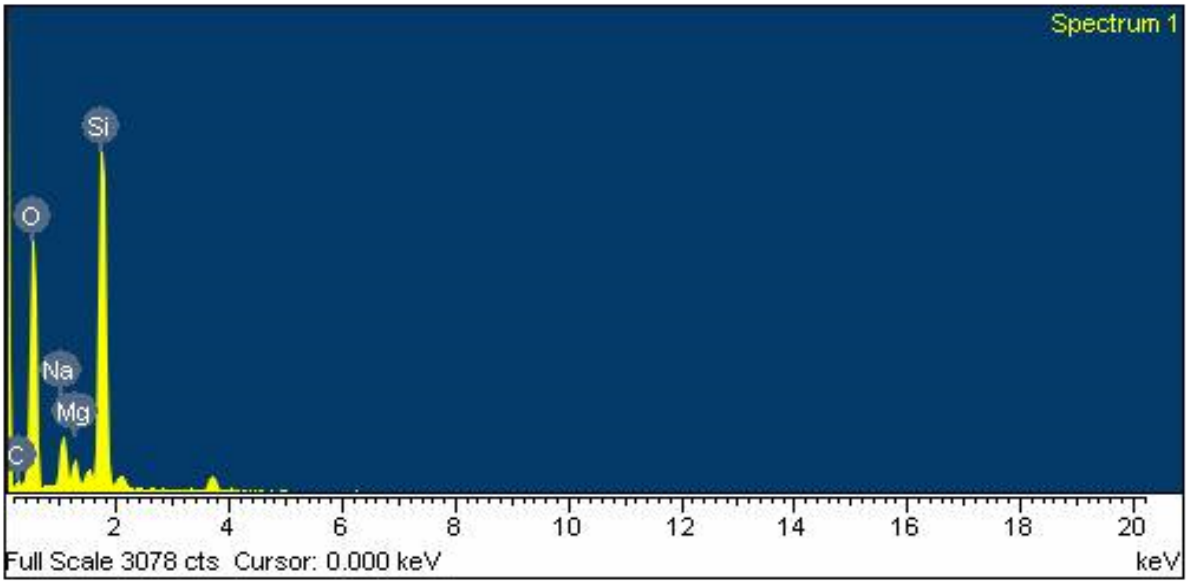

Fig. 4.6 Electron dispersive X- ray spectrum of *P. vermicola* strain SJ2A cells exposed to 0.8 mM lead nitrate in minimal medium.

Element	Weight%	Atomic%
C K	13.95	18.95
O K	69.73	71.10
Na K	2.89	2.05
Mg K	1.15	0.77
Si K	12.29	7.14
Totals	100.00	

4.3.2 TEM Analysis

There was negligible surface adsorption of lead on *P. vermicola* strain SJ2A cells which is evident from EDX analysis. Therefore, TEM analysis was carried out to confirm the intracellular uptake of lead. TEM analysis demonstrated that the cells exposed to lead showed a distinct darkening pattern wherein the cells were dark only at the periphery thereby, suggesting that lead accumulated specifically in the periplasmic space of the bacterium (Fig. 4.7). There are only few reports of intracellular lead accumulation, for instance, in the membrane fraction of *Bacillus thuringiensis* and within the cytoplasm of *Bacillus megaterium*, *Staphylococcus aureus* (Levinson and Mahler, 1998; Roane, 1999; Guo et al., 2010) but there is no report of periplasmic lead accumulation in bacteria so far. However, uranium sequestration in the bacterial cell periphery has been reported recently (Islam and Sar, 2016). Several efflux pumps viz. CadA, ZntA, PbrA are known to facilitate active transport of the metal ions from the cell cytoplasm to the cell exterior or the periplasmic space (Nies, 2003; Hynninen et al., 2009). Therefore, there is a possible involvement of such efflux pumps in mobilization of lead ions into the periplasmic space of this bacterial isolate.

4.3.3 AAS

Atomic absorption spectroscopy interestingly demonstrated internalisation of 155.12 mg Pb^{2+}/g biomass of *P. vermicola* strain SJ2A. There are very few reports indicating intracellular bioaccumulation of lead in bacteria viz. *Staphylococcus aureus*, *Bacillus megaterium* and *B. thuringiensis* (Levinson et al., 1996; Roane, 1999; Guo et al., 2010). *B. thuringiensis* has been found to accumulate 80.5% lead in the membrane fraction whereas *B. megaterium* reduced the bioavailable lead upto 50% (Park et al., 2011a).

a)

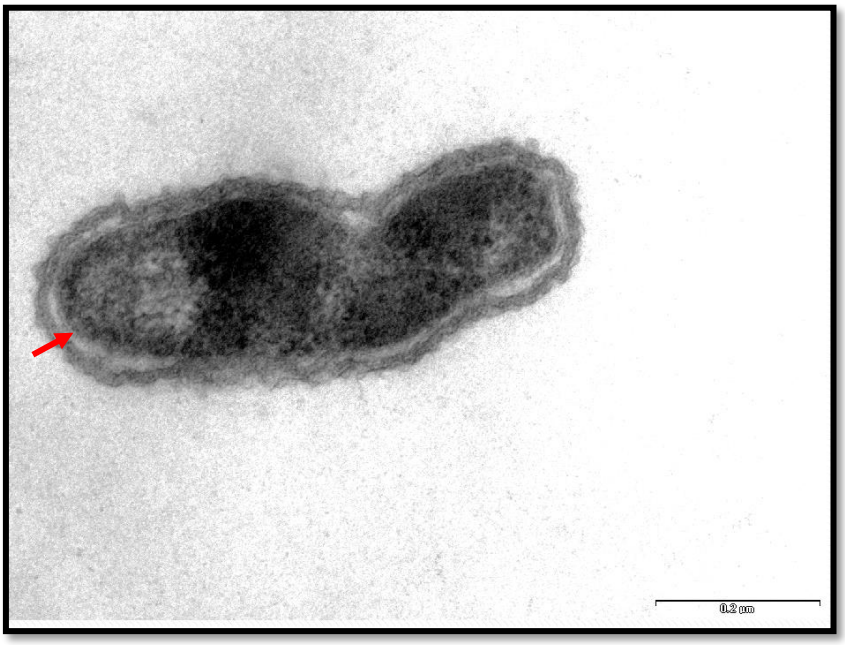

b)

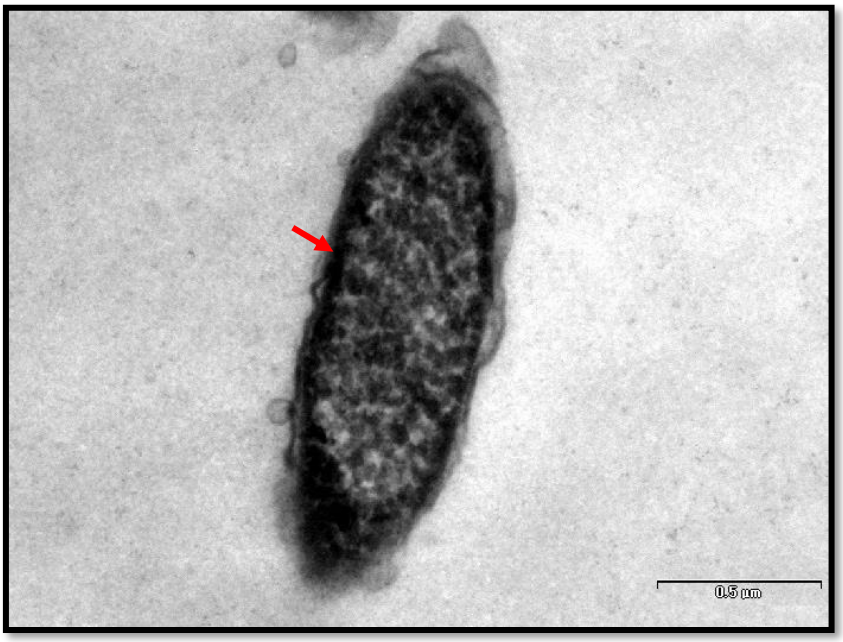

Fig. 4.7 Transmission electron micrographs of cells of *P. vermicola* strain SJ2A.

a) Bacterial cells without lead nitrate exposure showing clear periplasm

b) Bacterial cells exposed to 0.8 mM lead nitrate showing periplasm with dark granules

4.3.4 XRD Analysis

X-ray diffraction data on analysis using X powder software displayed certain peaks present exclusively in the sample consisting of bacterial cells exposed to lead nitrate (Fig. 4.8). X'Pert High Score Plus was employed to compare these peaks with the standards from International Centre for Diffraction Data. The peaks corresponding to a 2θ value of 20.8°, 23.3°, 27.7°, 30.2°, and 43.8° with d-spacing of 4.2, 3.8, 3.2, 2.9 and 2.06 respectively as per Bragg's law clearly indicated presence of lead sulfite (JCPDS reference card: 00-037-0004) in an orthorhombic crystal system within the bacterial cells exposed to lead nitrate. This clearly confirmed that lead is being sequestered by the cells of *P. vermicola* strain SJ2A in the form of lead sulfite ($PbSO_3$) which has been reported for the first time (Sharma et al., 2017). XRD has been used earlier to confirm the accumulation of lead as apatite in *Enterobacter* sp., pyromorphite, $Pb_5(PO_4)_3(OH)$ in *Burkholderia cepacia*, and lead phosphate, $Pb_9(PO_4)_6$ in *Vibrio harveyi* as well as *Providencia vermicola* strain 2EA (Templeton et al., 2003; Mire et al., 2004; Park et al., 2011b; Naik et al., 2012a).

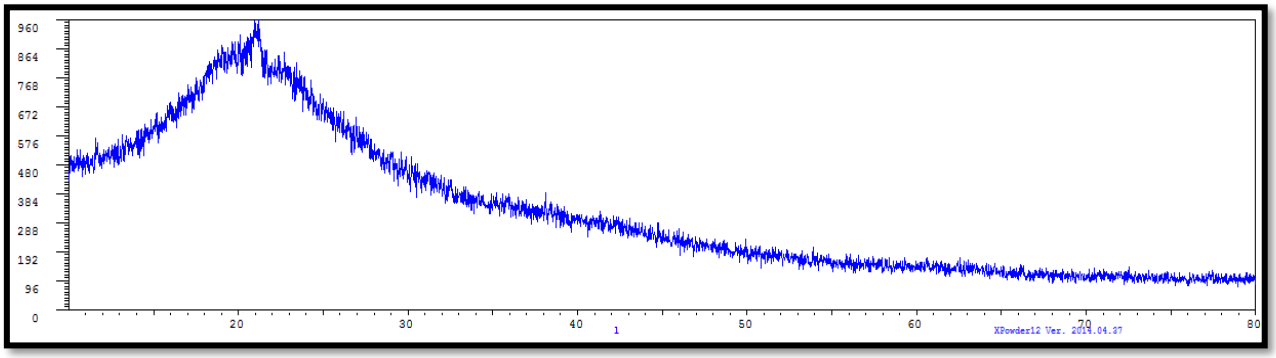

a)

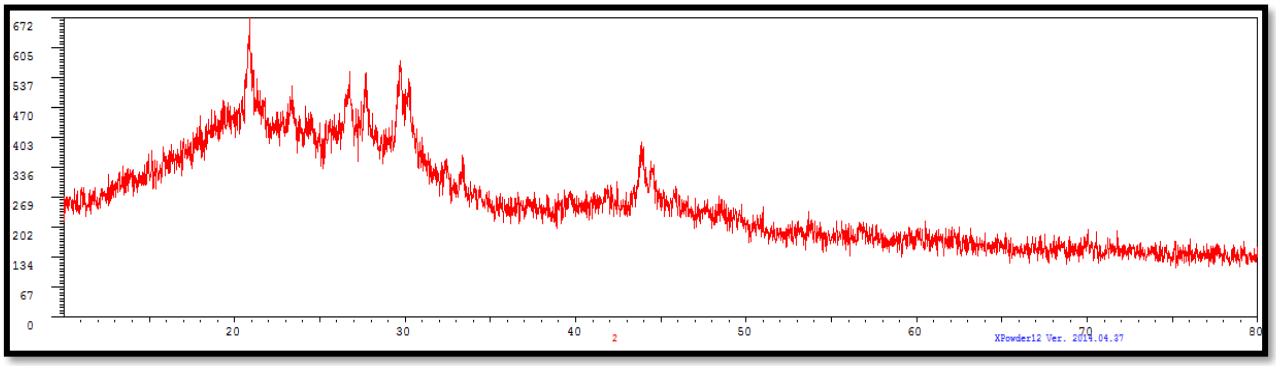

b)

Fig. 4.8 X-ray diffractogram of *P. vermicola* strain SJ2A.

a) Cells without lead exposure (control)

b) Cells exposed to lead nitrate

4.3.5 FTIR Analysis

FTIR analysis of control as well as lead-exposed bacterial cells was performed in order to reveal the functional groups interacting with lead ions (Fig. 4.9). Analysis of the IR spectra clearly indicated shifting and sharpening of various peaks that can be assigned to characteristic functional groups present in the biomolecules of bacterial cells following lead accumulation (Table 4.1). A significant sharpening of bands at 2922 cm^{-1} as well as 2852 cm^{-1} in the lead-exposed cells as compared to the control reflects a major involvement of fatty acids of various membrane phospholipids in metal binding (Naumann, 2000). The peak shift from 1658 cm^{-1} to 1656 cm^{-1} could be attributed to α-helical secondary structures of proteins suggesting the role of proteins in binding of metal (Choudhary and Sar, 2009). A clear shift of the band from 1440 cm^{-1} to 1458 cm^{-1} indicates the interaction of metal with peptidoglycan, phospholipids and lipo-polysaccharides since this band is a characteristic of the scissoring motion of $-CH_2$ groups usually present in these biomolecules. The band shift to a lower energy level, that is, from 1074 cm^{-1} to 1068 cm^{-1} is a result of the stretching vibrations in phosphate groups of the nucleic acids or phospholipids (Jiang et al., 2004). Therefore, IR anaylsis clearly demonstrated that membrane components viz. phospholipids, LPS, peptidoglycan as well as proteins were the key biomolecules involved in interaction with lead ions. This is in agreement with the results of TEM analysis of cells exposed to lead which clearly indicated sequestration of lead mostly in the periplasmic space.

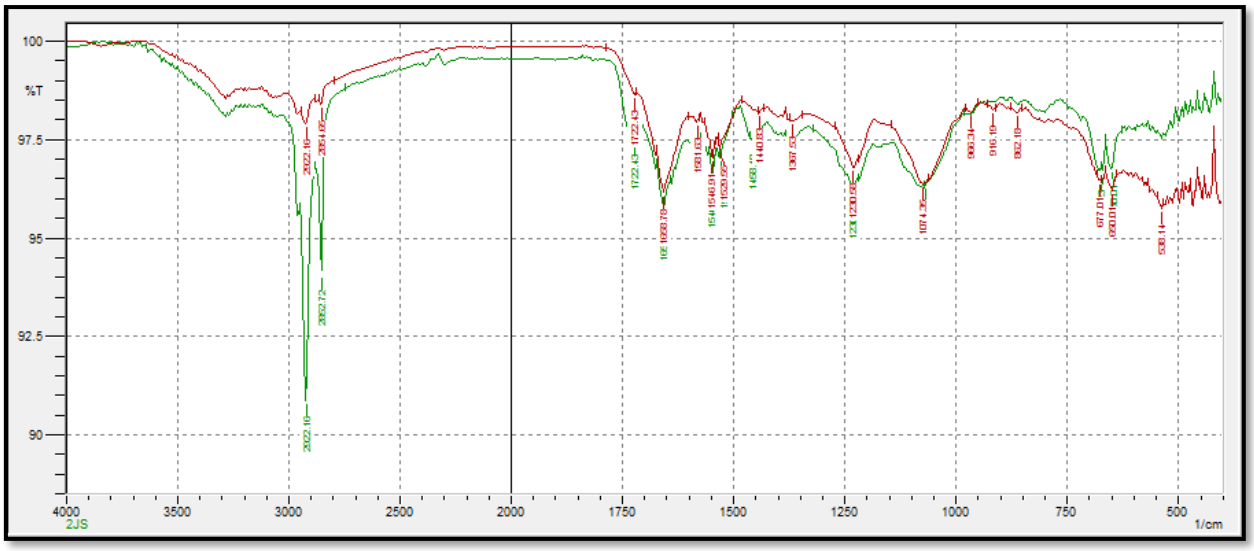

Fig. 4.9 IR spectra of *P. vermicola* strain SJ2A.

Red: Cells without exposure to lead nitrate (control); green: cells exposed to lead nitrate

Table 4.1 Major peak changes observed in FTIR spectra of *P. vermicola* strain SJ2A after lead exposure and the functional groups involved in metal binding.

Control cells (cm^{-1})	Lead-exposed cells (cm^{-1})	Functional groups
2922	2922	C-H asymmetric stretching $>CH_2$ in fatty acids
2852	2852	C-H asymmetric stretching $>CH_2$ in fatty acids
1658	1656	Amide I of α-helical structures
1440	1458	C-H deformation of $>CH_2$ in lipids proteins
1074	1068	P=O symmetric stretching in DNA, RNA and phospholipids

4.4 Mechanism of lead resistance in *A. xylosoxidans* strain SJ11

4.4.1 SEM-EDX Analysis

Scanning electron micrographs of *A. xylosoxidans* strain SJ11 cells revealed a very interesting phenomenon where the bacterial cells fused forming an aggregate on exposure to lead along with the presence of a distinct precipitate (Fig. 4.10). SEM analysis of the precipitate showed presence of cuboidal particles while energy dispersive X-ray spectroscopic analysis demonstrated a significant amount of lead i.e., 48.5 as weight % in the precipitate (Fig. 4.11). Additionally, phosphorus and chlorine were also detected in the precipitate though these elements were absent in the control. Previously, *Citrobacter freundii* showed precipitation of the lead on the cell surface (Aickin and Dean, 1979; Aickin et al., 1979) whereas *Pseudomonas marginalis* (Roane, 1999) demonstrated sequestration of lead in an extracellular polymer. In addition, Naik et al. (2012a) suggested formation of an extracellular brown precipitate of lead by *Providencia alcalifaciens* strain 2EA.

4.4.2 TEM Analysis

The transmission electron micrographs evidently revealed that there was no change in the cells of *A. xylosoxidans* strain SJ11 even after exposure to lead nitrate negating the possibility of any intracellular uptake of lead (Fig. 4.12). This confirmed our hypothesis that the bacterium employed extracellular precipitation of lead as an imperative mechanism to tolerate high levels of lead.

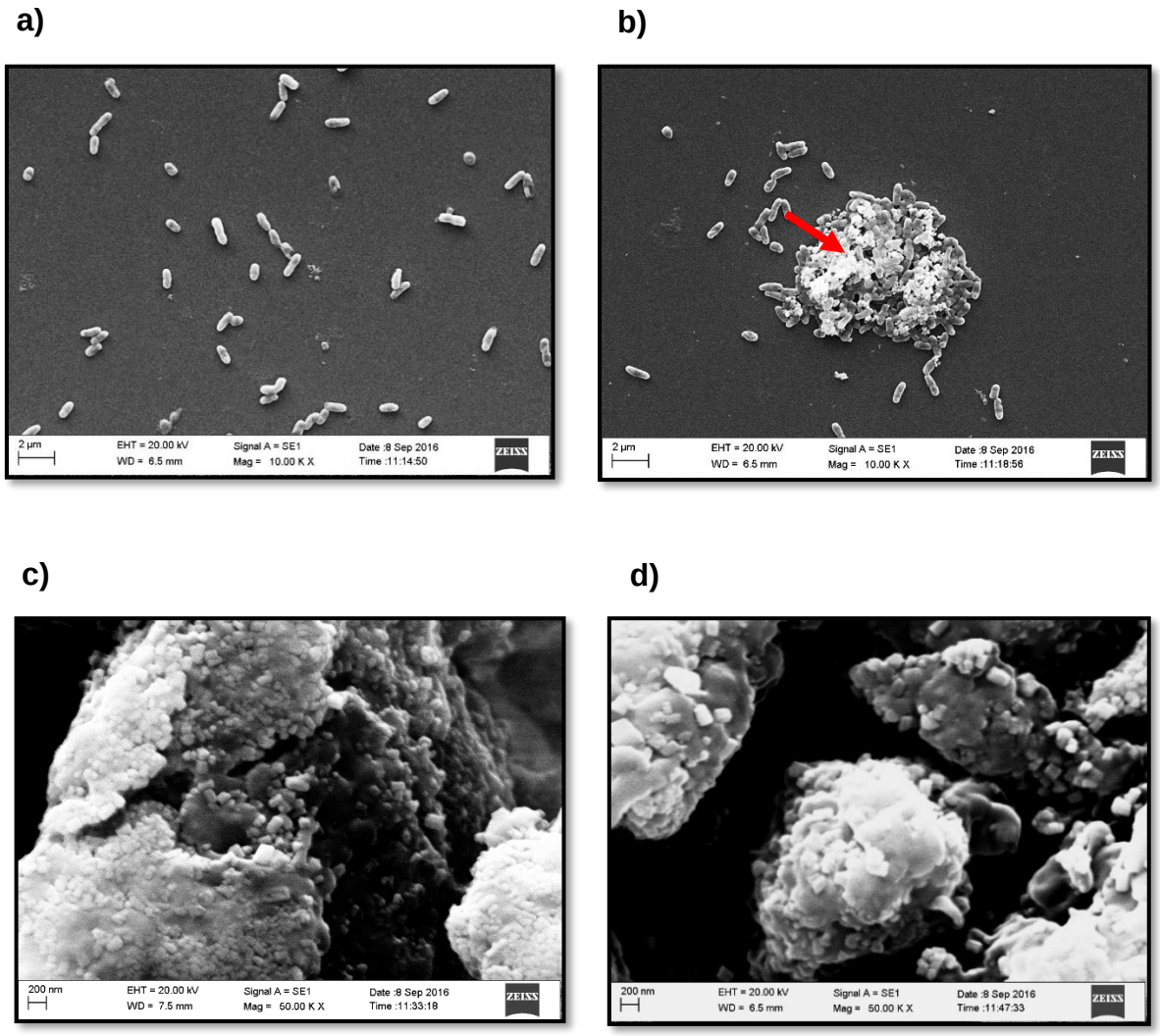

Fig. 4.10 Scanning electron micrographs of cells of *A. xylosoxidans* strain SJ11.

a) Bacterial cells without lead (control)

b) Bacterial cells exposed to 0.5 mM lead nitrate showing precipitation (precipitate has been marked with an arrow)

c) and d) Extracellular precipitate.

a)

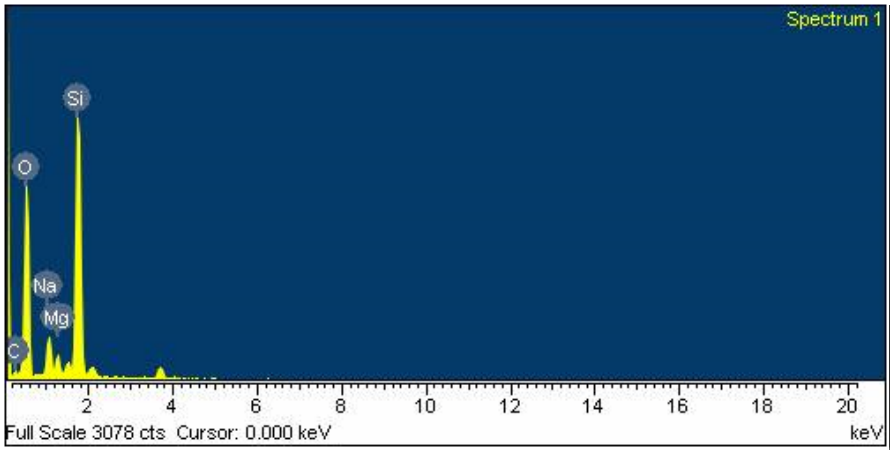

Element	Weight%	Atomic%
C K	10.07	14.51
O K	62.72	67.82
Na K	5.31	3.99
Mg K	1.96	1.39
Si K	19.95	12.29
Totals	100.00	

b)

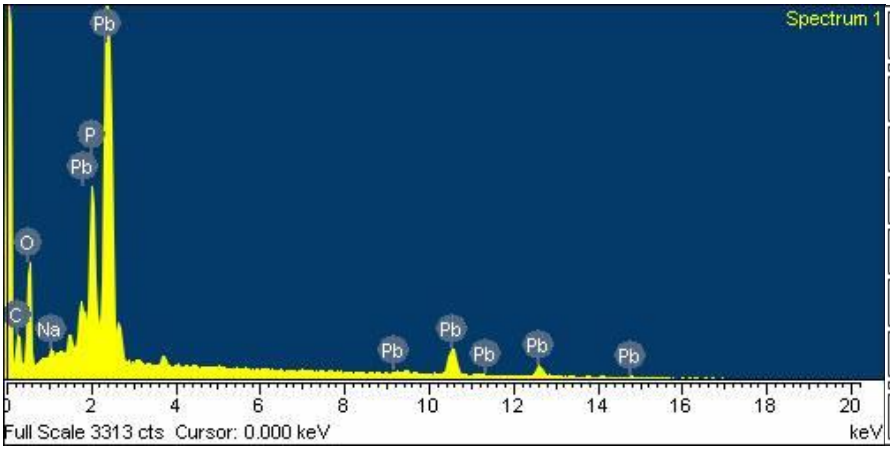

Element	Weight%	Atomic%
C K	16.56	38.50
O K	27.83	48.57
Na K	0.51	0.62
P K	5.14	4.63
Cl K	1.47	1.15
Pb M	48.49	6.53
Totals	100.00	

Fig. 4.11 Electron diffraction X-ray spectroscopic analysis.

a) Bacterial cells grown in absence of lead nitrate (control)

b) Lead precipitate obtained when the bacterial cells were grown in minimal medium supplemented with 0.5 mM lead nitrate

a) **b)**

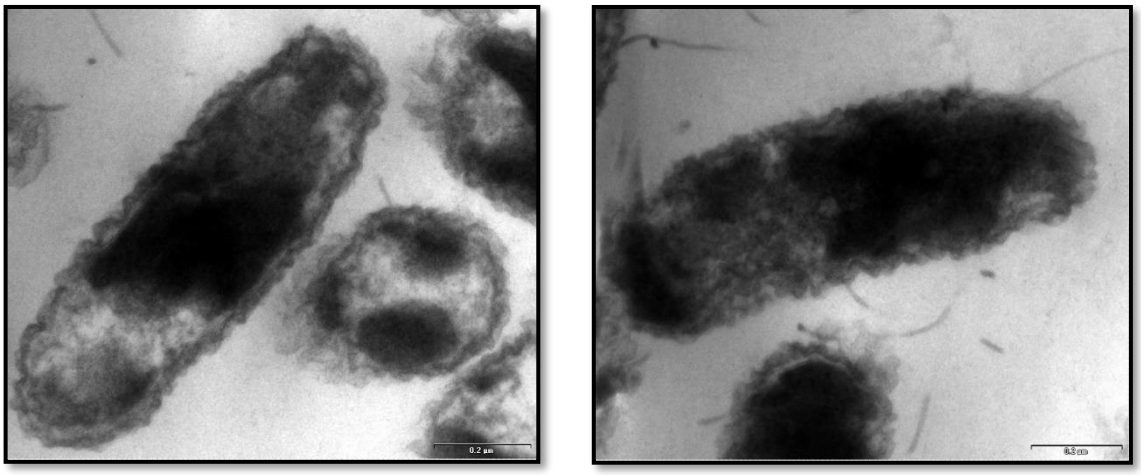

Fig. 4.12 Transmission electron micrographs of cells of *A. xylosoxidans* strain SJ11.

A) Bacterial cells without lead nitrate exposure

B) Bacterial cells exposed to 0.5 mM lead nitrate

4.4.3 XRD Analysis

X- ray diffraction analysis was performed using X powder software in order to find out the exact composition of the white precipitate since EDX had indicated presence of lead, phosphorus and chlorine. XRD demonstrated various peaks corresponding to a 2θ value of 30.14^o, 21.49^o, 30.9^o, 43.8^o, 27.2^o and 26.3^o with a d-spacing of 2.96, 4.13, 2.88, 2.06, 3.27, 3.38 respectively as per Bragg's law (Fig. 4.13). X'Pert High Score Plus was employed to compare these peaks with the standards from International Centre for Diffraction Data which clearly confirmed formation of pyromorphite, a lead chloride phosphate [$Pb_5(PO_4)_3Cl$] (JCPDS reference card: 00-019-0701) in a hexagonal crystal system. This indicates that *A. xylosoxidans* strain SJ11 could efficiently convert the soluble lead from surroundings into an insoluble form thereby reducing the toxicity of lead. There are reports in which the chemical nature of lead precipitate has been elucidated. For instance, $PbHPO_4$ has been reported in the case of *C. freundii* (Aickin et al., 1979), $Pb_9(PO_4)_6$ in *V. harveyi* (Mire et al., 2004) as well as *P. alcalifaciens* 2EA (Naik et al., 2012a); $Pb_5(PO_4)_3(OH)$ in *B. cepacia* (Templeton et al., 2003); $Pb_3(PO_4)_2$ in *S. aureus* (Levinson et al., 1996); Pb-apatite in *Enterobacter* sp. (Govarthanan et al., 2013), Pb-hydroxyapatite in *Bacillus cereus* 12-2 (Chen et al., 2016), PbS in *Rhodobacter sphaeroides* (Bai and Zhang, 2009) and $PbSO_3$ in *Providencia vermicola* strain SJ2A (Sharma et al., 2017).

4.4.4 AAS Analysis

The amount of lead present in the precipitate (pyromorphite) was quantified by atomic absorption spectroscopy to be 465.8 mg/g. This demonstrated that the precipitate contained a significant amount of lead accounting to nearly 47% of the compound.

a)

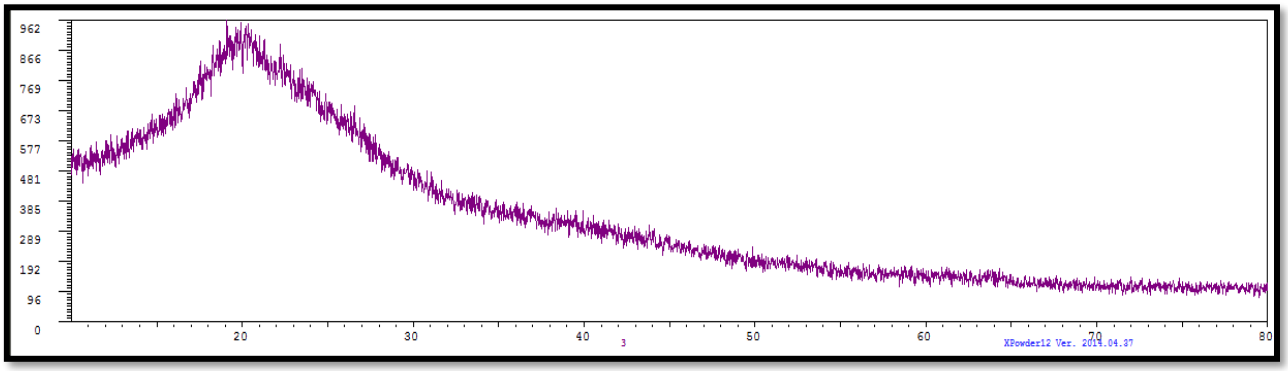

b)

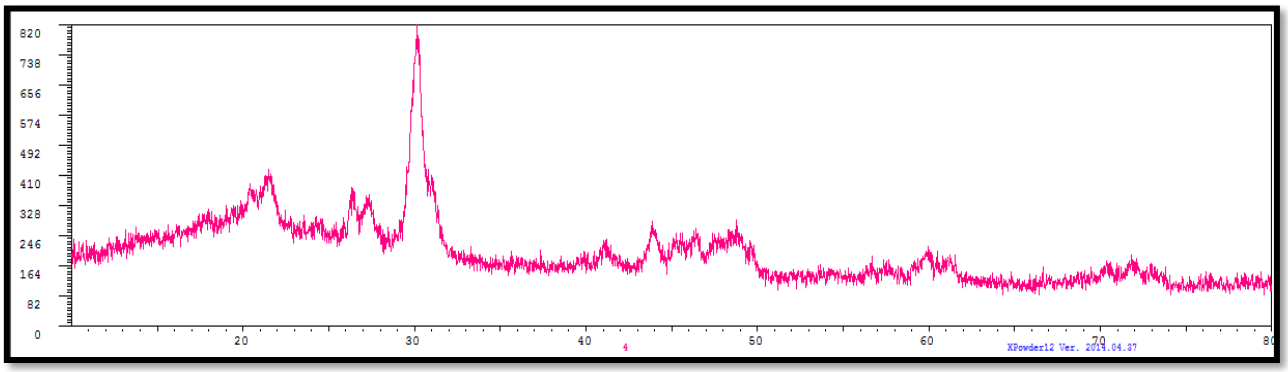

Fig. 4.13 X-ray diffractogram of *A. xylosoxidans* strain SJ11.

a) Bacterial cells without lead exposure; b) Bacterial cells exposed to 0.5 mM lead nitrate

4.4.5 FTIR Analysis

Fourier transformed infrared spectroscopy of *A. xylosoxidans* strain SJ11 cells was performed to identify the functional groups associated with lead resistance (Fig. 4.14). Analysis of the IR spectra indicated shifting and sharpening of various peaks when compared to the control which could be assigned to characteristic functional groups present in the biomolecules of bacterial cells involved in lead precipitation. The major peak changes have been listed in Table 4.2. FTIR peaks lying in the spectral region from 1080 to 970 cm^{-1} showed a significant increase in the intensity which in turn corresponds to symmetric stretching vibrations in phosphate groups (Naumann, 2000). A clear shift in the peak from 1080 to 1041 cm^{-1} evidently showed an interaction of the metal with phosphate groups. This depicted that the phosphate groups played a substantial role in precipitation of lead. Moreover, there was a shift from 1533 to 1525 cm^{-1} that could be attributed to alteration in the secondary structure of proteins due to interaction with lead indicating a probable role of enzymes in the lead precipitation process. Similar alterations in the IR spectra were observed in a uranium resistant strain of *Pseudomonas aeruginosa* (Chaudhary and Sar, 2011).

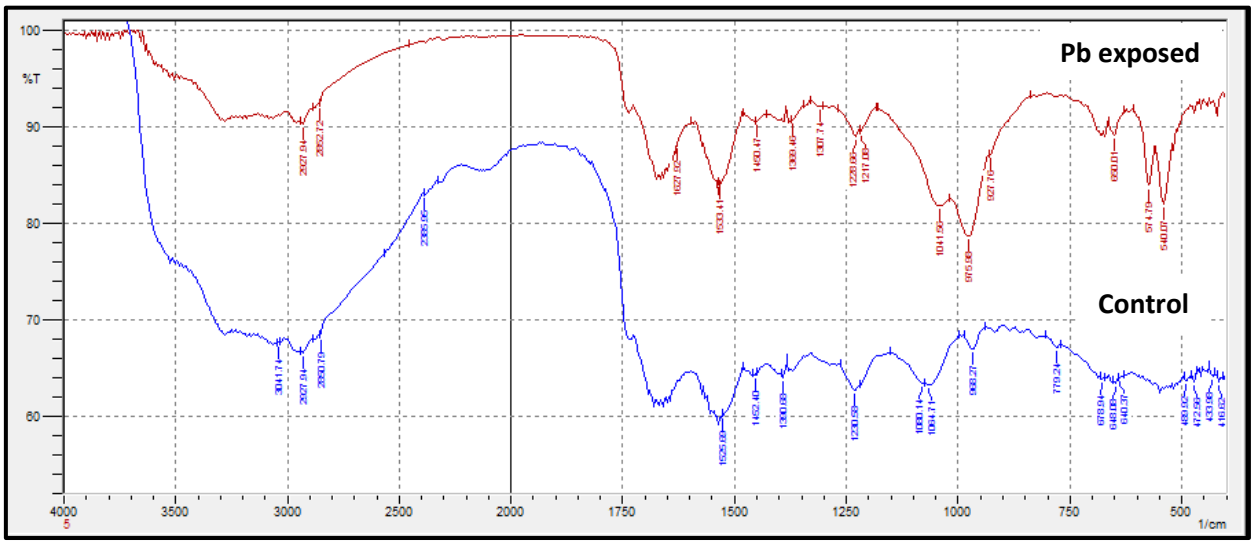

Fig. 4.14 IR spectra of *A. xylosoxidans* strain SJ11.

Bacterial cells without exposure to lead nitrate (blue); bacterial cells exposed to 0.5 mM lead nitrate (red)

Table 4.2 Major peak changes observed in *A. xylosoxidans* strain SJ11 following precipitation of lead and the functional groups involved.

Control cells (cm^{-1})	Lead-exposed cells (cm^{-1})	Functional groups
1525	1533	Amide II of proteins
1080	1041	P=O symmetric stretching of $>PO_2^-$
968	976	P=O symmetric stretching of $>PO_2^-$
548	575, 540	Heavy metal oxides, Pb—O

4.4.6 Phosphatase assay

A remarkable increase was observed in the phosphatase activity, i.e., 66.6% in presence of 0.2 mM lead nitrate and 160% when the cells were exposed to 0.5 mM lead nitrate (Table 4.3). The free phosphorus liberated by the action of phosphatase could combine with lead ions leading to formation of pyromorphite. Phosphatase mediated precipitation of uranium has previously been reported in case of *Citrobacter* sp. (Macaskie et al., 2000).

Table 4.3 Phosphatase activity of *A. xylosoxidans* strain SJ11 grown with and without lead.

Concentration of lead nitrate (mM)	**Enzyme activity (Mean ± SD[a], nmoles μg^{-1} min^{-1})**
0 (Control)	20.63 ± 1.93
0.2	34.36 ± 2.25
0.5	53.63 ± 1.28

[a]The mean and standard deviation of triplicate determinations ($p < 0.0001$; F: 315.7).

Summary

Lead resistance mechanisms were investigated in the selected bacterial strains. *Providencia vermicola* strain SJ2A carried the *pbrR* gene on plasmid as well as chromosomal genome. Scanning electron micrographs of bacterial cells exposed to lead revealed a unique alteration in the cell morphology from rods to long inter-connected filaments while electron dispersive X-ray spectroscopy clearly indicated no significant lead adsorption. However, transmission electron micrographs of the bacterial cells exposed to lead evidently demonstrated periplasmic sequestration of lead which was also supported by fourier transformed infrared spectroscopic analysis. The bacterium internalised 155.12 mg Pb^{2+}/g biomass as determined by atomic absorption spectroscopy which was subsequently identified as lead sulfite by X-ray diffraction studies.

Another lead resistant bacterium, *Achromobacter xylosoxidans* strain SJ11 was found to form a precipitate in presence of lead nitrate which was also evident from the scanning electron micrographs. Energy dispersive X-ray spectroscopic analysis revealed the presence of lead (48.5 by weight %) along with phosphorus and chlorine in the precipitate. Transmission electron microscopy of bacterial cells negated the possibility of intracellular lead uptake confirming extracellular precipitation as a predominant mechanism of lead resistance in this strain. The extracellular precipitate was identified as pyromorphite [$Pb_5(PO_4)_3Cl$] by X-ray diffraction analysis. This was also corroborated by fourier transformed infrared spectroscopy indicating a significant involvement of phosphate groups in binding with lead. Atomic absorption spectroscopic analysis clearly demonstrated that 465.8 mg Pb^{2+}/g was precipitated by the bacterial cells which is highly significant. Moreover, there was a remarkable increase (i.e. 160%) in phosphatase enzyme activity substantiating the role of phosphatase in lead precipitation.

5.1 Quantification of extracted protein

Whole cell protein extracted from bacterial cells grown with and without lead resulted in a good yield of protein although the yield from lead exposed cells was comparatively less than the unexposed cells (Table 5.1). We chose the concentration of lead as 0.2 mM for exposure since the bacterial cells were required to experience stress caused by lead but at the same time, the particular concentration should not inhibit the bacterial growth significantly. SDS-PAGE analysis of the protein extracted from control and lead exposed cells helped in the assessment of protein quality. It was also interesting to note that the differential expression of proteins in response to lead was evident from SDS-PAGE (Fig. 5.1). This further ensured that the samples could be processed further for LC-MS/MS analysis.

Table 5.1 Concentration of the protein extracted from lead resistant bacterial isolates. (Bradford assay)

Bacterial isolates	Sample	Protein concentration (µg/mL)
***Providencia vermicola* strain SJ2A**	Control	2.105
	Cells exposed to 0.2 mM lead	1.865
***Achromobacter xylosoxidans* strain SJ11**	Control	4.7733
	Cells exposed to 0.2 mM lead	3.4097

5.2 LC-MS/MS Analysis

There are very few reports elucidating biochemical mechanisms of lead resistance in bacteria (Borremans et al., 2001, Hynninen et al., 2009, 2010; Sharma et al., 2006) and this prompted us to explore lead responsive proteins in the lead resistant bacterial isolates extensively. This would enable us to decipher the role of proteins in rendering lead resistance.

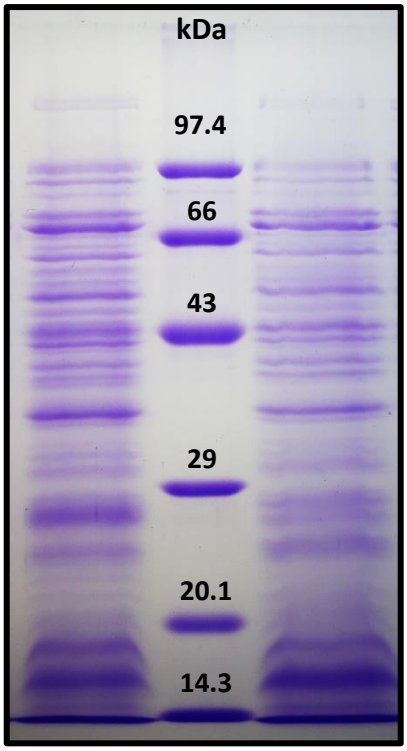

Fig. 5.1 SDS-PAGE analysis representing the quality assessment of extracted protein.

Lane 1: Protein extracted from control cells

Lane 2: Protein molecular weight marker

Lane 3: Protein extracted from cells exposed to 0.2 mM lead

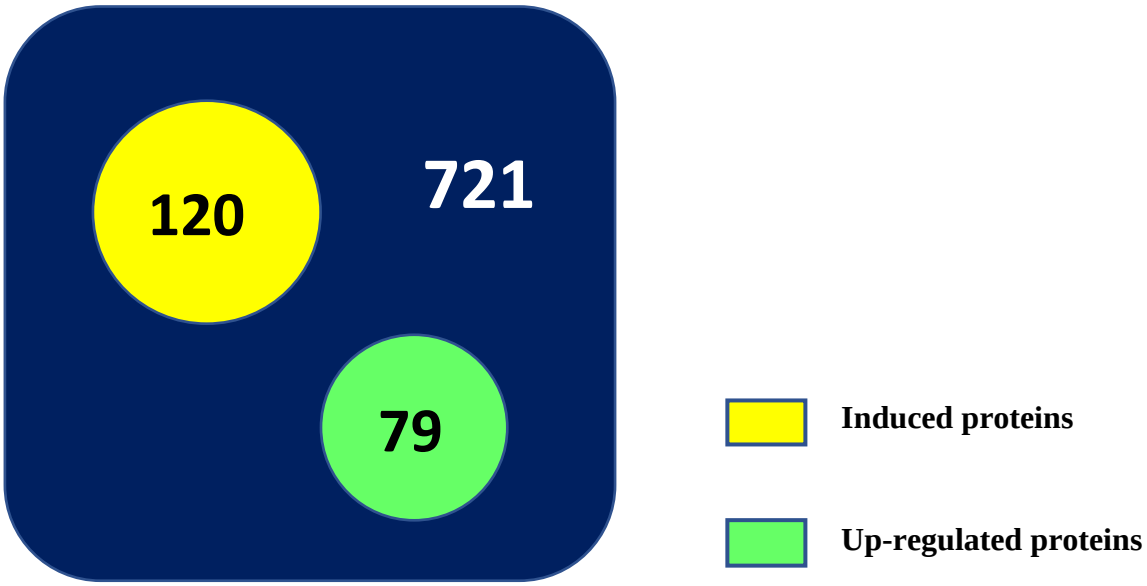

Fig. 5.2 Illustration depicting the distribution of proteins identified in *P. vermicola* strain SJ2A exposed to lead.

5.2.1 Proteomic analysis of *Providencia vermicola* strain SJ2A

Total 857 and 721 proteins were identified with an FDR of 1% in case of unexposed and cells exposed to 0.2 mM lead respectively. Out of these 721 proteins identified in the lead exposed bacterial cells, 120 were induced while 79 were up-regulated (Fig. 5.2). The proteins were categorized as *induced* when they were observed only in presence of lead and *up-regulated* if they exhibited an increase in expression due to lead (Tables 5.2 and 5.3). These were further classified based on their biological context in order to gain an insight into the difference in protein expression due to lead exposure.

Our analysis revealed that the induced and up-regulated proteins govern diverse cellular functions. The major group of induced proteins (Fig. 5.3) were involved in nitrogen metabolism (18%), oxidation-reduction processes (16%), regulatory functions (13%), transport (9%) and stress response (9%). Similarly, up-regulated proteins comprised of the ones governing nitrogen and carbon metabolism (36%), transcription-translation (15%) and stress responses (Fig. 5.4). Interestingly, lipopolysaccharide associated proteins constituted 6% of the total up-regulated proteins which further corroborated the lead resistance mechanism of periplasmic sequestration exhibited by this organism.

Another protein, BolA was observed in lead exposed cells. This protein has recently been identified as a transcriptional factor in *Escherichia coli* which is responsible for inhibition of flagellar biosynthesis (Dressaire et al., 2015). In addition, induced proteins viz. co-chaperones, zinc/cadmium/mercury/lead-transporting ATPase, cadmium-exporting ATPase, copper-sensing regulators, metal ABC transporter periplasmic protein, cupredoxin-like domain protein, efflux transporter (RND family), glutaredoxin-like protein, glutathione-dependent thiol reductase and bacterioferritin could facilitate the resistance mechanism in this bacterium to combat lead stress (Table 5.2).

Amongst the up-regulated proteins, stress responsive proteins such as chaperonin and metal binding protein ZinT demonstrated a significant increase in protein expression i.e., 10.3 and 9.5 fold respectively, substantiating their role in governing lead resistance (Table 5.3). We also observed up-regulation of the elongation factor, Tu which reflects the adaptation strategy of the bacterium as it is responsible for enhancing the overall protein synthesis. Previously, increase in the expression of elongation factor, Tu has been observed for *Pseudomonas fluorescens* in presence of cobalt (Sharma et al., 2006). Hence, the proteins that were found to be induced or up-regulated probably assist in rendering lead resistance to *P. vermicola* strain SJ2A.

Table 5.2 List of proteins induced in *P. vermicola* strain SJ2A on exposure to lead.

Carbon metabolism
• 2,3-butanediol dehydrogenase
• Acetoin reductase
• Acyl-[ACP]-phospholipid O-acyltransferase
• EF_0830/AHA_3911 family protein
• NAD-dependent malic enzyme
• PTS system N-acetyl glucosamine specific transporter subunits IICBA
• PTS system sugar transporter subunit IIA
• Succinate dehydrogenase hydrophobic membrane anchor subunit
• Sugar-binding domain protein
• UDP-N-acetylmuramate-L-alanyl-gamma-D-glutamyl-meso-2,6-diaminoheptandioate ligase
Protein metabolism
• 2-oxoglutaramate amidase
• Amidohydrolase family protein
• Aminopeptidase B
• Aspartate aminotransferase
• Cysteine desulfurase activator complex subunit SufB

• Cysteine desulfurase, sulfur acceptor subunit CsdE
• Cytosol nonspecific dipeptidase
• Endothelin-converting protein 1
• FtsH protease regulator HflK
• N-substituted formamide deformylase
• Penicillin-binding protein activator LpoA
• Peptidase family M13
• Peptidase, M16 family
• PTS IIA-like nitrogen-regulatory protein PtsN
• PTS system nitrogen regulatory protein IIA(Ntr)
• Pyridoxal phosphate-dependent enzyme, D-cysteine desulfhydrase family
• Sensor protein CpxA
• Serine acetyltransferase
• Two-component sensor histidine kinase
• Two-component sensor protein
• Xaa-His dipeptidase
Fatty acid metabolism
• 3-ketoacyl-(Acyl-carrier-protein) reductase
• 3-oxoacyl-[acyl-carrier-protein] reductase
• Bifunctional protein Aas
• Putative oxoacyl-(Acyl carrier protein) reductase
Nucleotide metabolism
• 2',3'-cyclic-nucleotide 2'-phosphodiesterase
• Bifunctional 2',3'-cyclic nucleotide 2'-phosphodiesterase/3'-nucleotidase periplasmic protein
• Class Ia ribonucleotide reductase, beta subunit
• dITP/XTP pyrophosphatase
• Endoribonuclease
• Nucleoprotein/polynucleotide-associated enzyme
• Orotidine 5'-phosphate decarboxylase

• Ribonucleoside-diphosphate reductase, beta subunit-like protein
DNA repair and replication
• DNA gyrase inhibitor YacG
Translation and transcription
• Ribosomal silencing factor RsfS
• Ribosome-associated protein
• S4 domain protein
• Translation initiation factor Sui1
Response to stress
• Cadmium-exporting ATPase
• Co-chaperone YbbN
• Copper-sensing histidine kinase
• Copper-sensing two-component system response regulator
• Cupredoxin-like domain protein
• Heavy metal transporting ATPase
• Metal ABC transporter periplasmic protein/surface antigen
• Metallo-beta-lactamase domain protein
• Universal stress protein F
• Zinc ABC transporter ATPase (Fragment)
• Zinc/cadmium/mercury/lead-transporting ATPase
Cell division
• Cell division protein BolA
• Cell division protein DedD
• Cell division protein FtsH
• Cell division protein ZipA
Regulatory functions
• AepA family exoenzyme regulatory protein
• Anti-sigma-E factor RseA
• BolA-like protein
• HTH-type transcriptional repressor PurR
• HU-beta family DNA-binding protein

• Modulator of FtsH protease HflK
• MrpJ family protein
• Quorum-sensing regulator protein G
• Response regulator homolog
• SspA
• TraM protein DNA-binding domain protein
• Transcription repressor
• Transcriptional regulator, Spx/MgsR family
• Transcriptional regulatory protein PhoP
• Two-component system response regulator OmpR
• Virulence transcriptional regulatory protein PhoP
Oxidation-Reduction
• ArsC family reductase
• ATP synthase epsilon chain
• Bacterioferritin
• Coproporphyrinogen-III oxidase
• Fe-S assembly protein IscX
• Fe-S metabolism protein SufE
• Glutamine-dependent NAD(+) synthetase
• Glutaredoxin-like protein
• Glutathione-dependent thiol reductase
• Iron-sulfur cluster assembly ATPase protein
• Iron-sulfur cluster assembly scaffold protein IscU
• NADH pyrophosphatase
• NADH-quinone oxidoreductase subunit E
• NDH-1 subunit E
• Peptide methionine sulfoxide reductase MsrB
• Sulfite reductase [NADPH] hemoprotein beta-component
• Tat pathway signal sequence domain protein
• Thiosulfate sulfurtransferase
• YciK family oxidoreductase

Transporter
• ATP-binding cassette protein, ChvD family
• Efflux transporter, RND family, MFP subunit
• Heme/hemoglobin transport protein
• Hemin transport protein HmuS
• Multidrug efflux pump subunit AcrA
• Multidrug transporter
• OmpA-like transmembrane domain protein
• Outer membrane channel protein
• Periplasmic binding protein
• Putative ATP-dependent transporter SufC
• Type I secretion outer membrane protein, TolC family
Others
• LppC
• Molybdenum cofactor biosynthesis protein MoaE
• Outer membrane lipoprotein, Slp family
• Outer membrane protein A
• PF04320 family protein
• PF09831 family protein
• Putative cytoplasmic protein
• Putative reductase
• UPF0434 protein PROSTU_01760
• WxcM-like protein
• YfhG lipoprotein

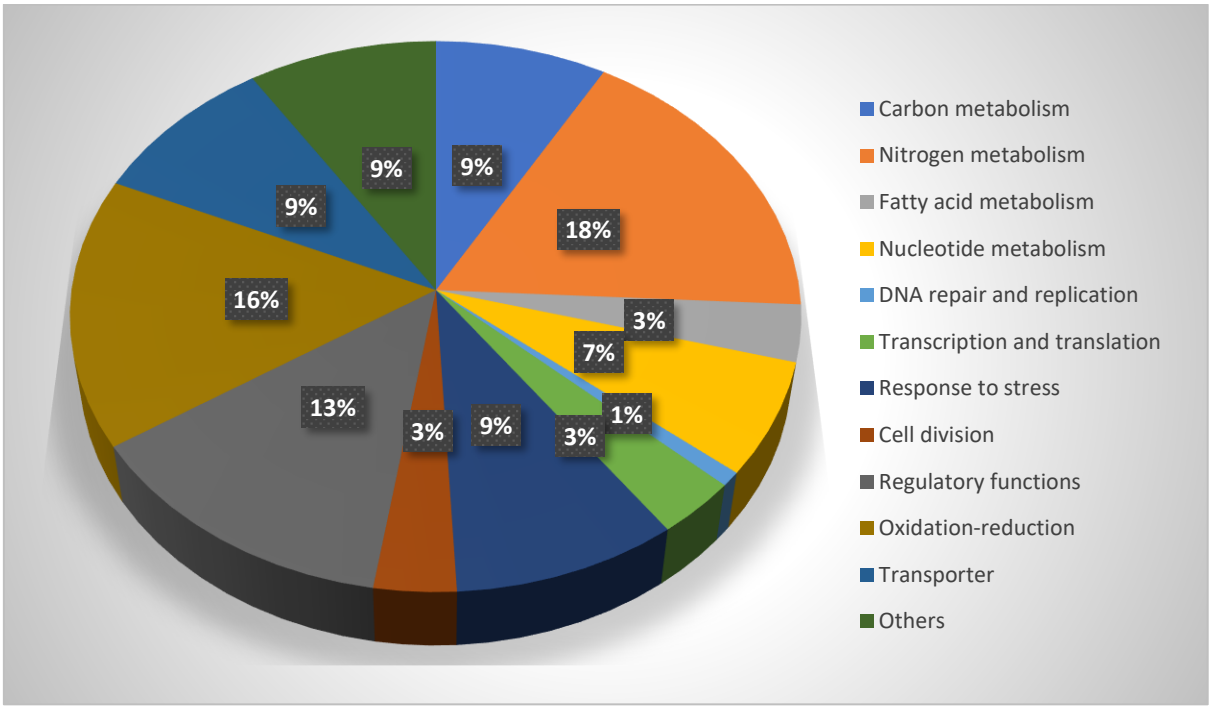

Fig. 5.3 Induced proteins from *P. vermicola* strain SJ2A were classified based on their involvement in various biological processes.

Table 5.3 List of proteins up-regulated in *P. vermicola* strain SJ2A on exposure to lead and the fold change in expression.

Proteins	Fold change
Carbon metabolism	
• 1,4-dihydroxy-2-naphthoyl-CoA synthase	2.06
• 2-dehydro-3-deoxyphosphooctonate aldolase	1.8
• Aspartate ammonia-lyase	2.0
• Bifunctional protein HldE	1.83
• D-hexose-6-phosphate mutarotase	1.69
• Malate dehydrogenase	2.21
• Probable malate:quinone oxidoreductase	2.13
• PTS N-acetyl glucosamine transporter subunit IIABC	2.57
• Ribose-5-phosphate isomerase A	1.68
• Ribulose-phosphate 3-epimerase	4.57
• Triosephosphate isomerase	1.75
Nitrogen metabolism	
• 4-hydroxy-tetrahydrodipicolinate synthase	2.19
• ATP phosphoribosyltransferase	3.26
• ATP-dependent protease ATPase subunit HslU	2.3
• ATP-dependent protease subunit HslV	1.66
• Branched chain amino acid aminotransferase	1.99
• D-3-phosphoglycerate dehydrogenase	1.86
• Glutamate dehydrogenase	1.68
• Glutamine synthetase	37.67
• Histidine biosynthesis bifunctional protein HisB	3.03
• Histidine biosynthesis bifunctional protein HisIE	3.05
• Histidinol dehydrogenase	8.44
• Histidinol-phosphate aminotransferase	2.39
• Imidazole glycerol phosphate synthase subunit HisF	2.4
• O-acetylhomoserine aminocarboxypropyltransferase	1.63

• Peptide deformylase	5.9
• Tryptophan synthase beta chain	1.51
• Urease alpha subunit	1.82
Fatty acid metabolism	
• 3-oxoacyl-[acyl-carrier-protein] synthase 2	1.99
Nucleotide metabolism	
• dTDP-3-amino-3,6-dideoxy-alpha-D-galactopyranose transaminase	1.81
• Guanylate kinase	1.53
• Hypoxanthine phosphoribosyltransferase	2.81
• Phosphoribosylformylglycinamidine synthase	1.77
• Uracil phosphoribosyltransferase	1.6
DNA repair and replication	
• Ribonucleoside-diphosphate reductase subunit beta	3.12
Translation and transcription	
• 30S ribosomal protein S7	3.32
• 30S ribosomal protein S9	1.63
• 50S ribosomal protein L5	1.59
• 50S ribosomal protein L22	1.55
• 50S ribosomal protein L35	1.94
• 50S ribosomal protein L36	2.02
• DNA-directed RNA polymerase subunit beta'	8.68
• Elongation factor Tu (Fragment)	2.23
• Peptide chain release factor 1	2.12
• Translation initiation factor IF-1	1.69
• Translation initiation factor IF-3	1.57
• tRNA-specific 2-thiouridylase MnmA	1.88
Response to stress	
• 60 kDa chaperonin	10.33
• Chaperone protein DnaJ	1.59
• Metal-binding protein ZinT	9.49

• Osmotically inducible protein Y	1.76
• Putative fimbrial chaperone	1.74
• Universal stress protein UspA	2.48
• Zinc ABC transporter substrate-binding protein	1.84
LPS associated	
• Lipoprotein	1.91
• Murein lipoprotein	1.7
• Outer membrane protein assembly factor BamA	1.82
• Peptidoglycan-binding protein	1.87
• Signal recognition particle protein	1.82
Regulatory functions	
• DNA-binding protein	2.2
• DNA-binding response regulator	1.65
• Leucine responsive regulatory protein	1.69
• Putative DNA-binding transcriptional regulator	2.83
Oxidation-Reduction	
• NAD(P)-dependent oxidoreductase	2.9
• Superoxide dismutase [Cu-Zn]	1.81
Transporter	
• Colicin I receptor	5.43
• Iron ABC transporter substrate-binding protein	2.04
• Phosphate-specific transport system accessory protein PhoU	1.5
• TonB-dependent siderophore receptor	2.34
Others	
• Bifunctional polymyxin resistance protein ArnA	3.12
• Membrane protein insertase YidC	1.5
• Pantothenate synthetase	2.03
• Probable 4-deoxy-4-formamido-L-arabinose-phosphoundecaprenol deformylase ArnD	1.78
• Sulfurtransferase	1.56

• Thiamine biosynthesis protein ThiS	2.17
• Thiamine pyrophosphate enzyme, N-terminal TPP binding domain protein	2.1
• Thiazole synthase	1.73
• Uncharacterized protein	2.55
• UPF0250 protein A3Q29_02040	7.64

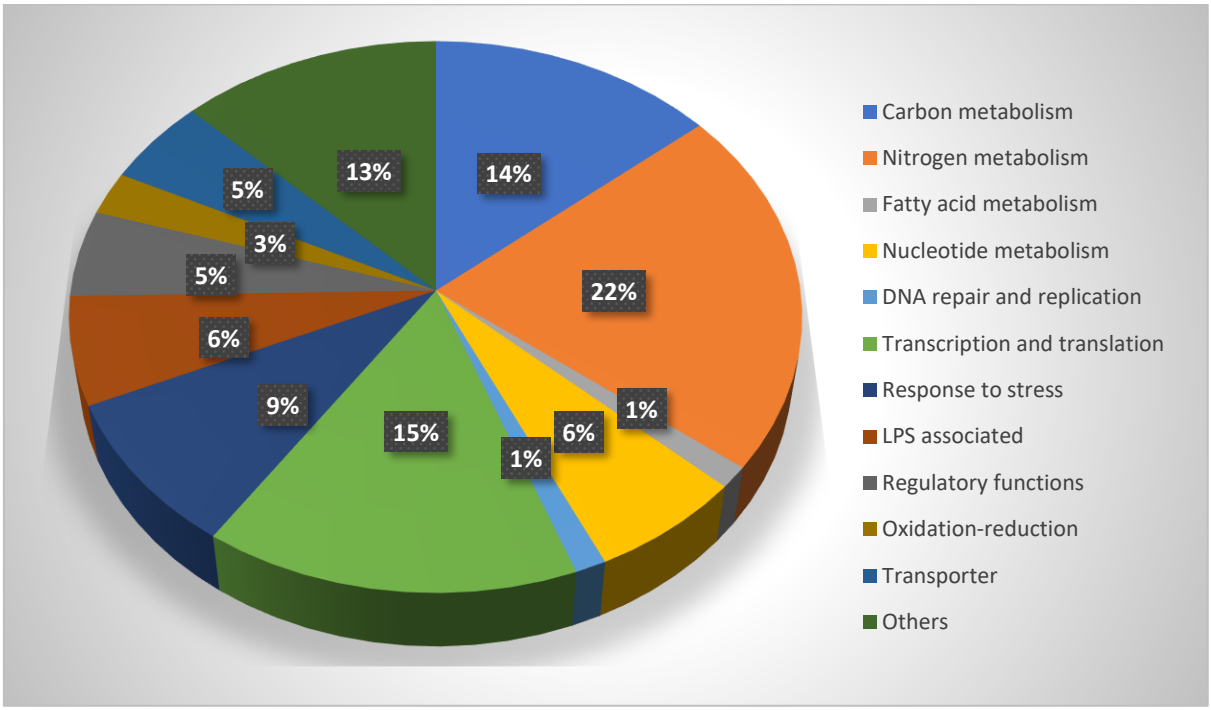

Fig. 5.4 Up-regulated proteins from *P. vermicola* strain SJ2A were classified based on their involvement in various biological processes.

5.2.2 Proteomic analysis of *Achromobacter xylosoxidans* strain SJ11

Total 1179 proteins were identified with confidence (FDR 1%) by mass spectrometry across the samples, of which 688 proteins belonged to the bacterial cells exposed to 0.2 mM lead. Of these 688 proteins, 38 were analysed to be induced while 79 were the proteins that were up-regulated in presence of lead (Fig. 5.5).

The proteins were classified based on their involvement in various biological processes. The analysis clearly revealed that most of the induced proteins (Fig. 5.6) contribute to catabolism (24%), transport (21%), biosynthesis (16%), stress response (16%) and oxidation-reduction processes (10%). While a major group of up-regulated proteins have a role in transcription as well translation (24%), biosynthesis (23%), catabolism (15%), transport (13%), stress response (11%) and redox processes (6%) as depicted in Fig. 5.7.

Some of the induced proteins of relevance in lead resistance (Table 5.4) include Cd(II)/Pb(II)-responsive transcriptional regulator, mercuric resistance operon regulatory protein, MerR family transcriptional regulator, cation efflux system protein, cobalt-zinc-cadmium resistance protein CzcC, copper-transporting P-type ATPase and chemotaxis protein. On the other hand, in case of up-regulated proteins (Table 5.5) several proteins showed a significant increase in their expression viz. elongation factor G (42.2 fold), 2-oxoglutarate dehydrogenase (35.4 fold), thiol reductant ABC transporter CydC (30.8 fold), phosphoenolpyruvate synthase (24 fold) and DNA gyrase (20.8 fold).

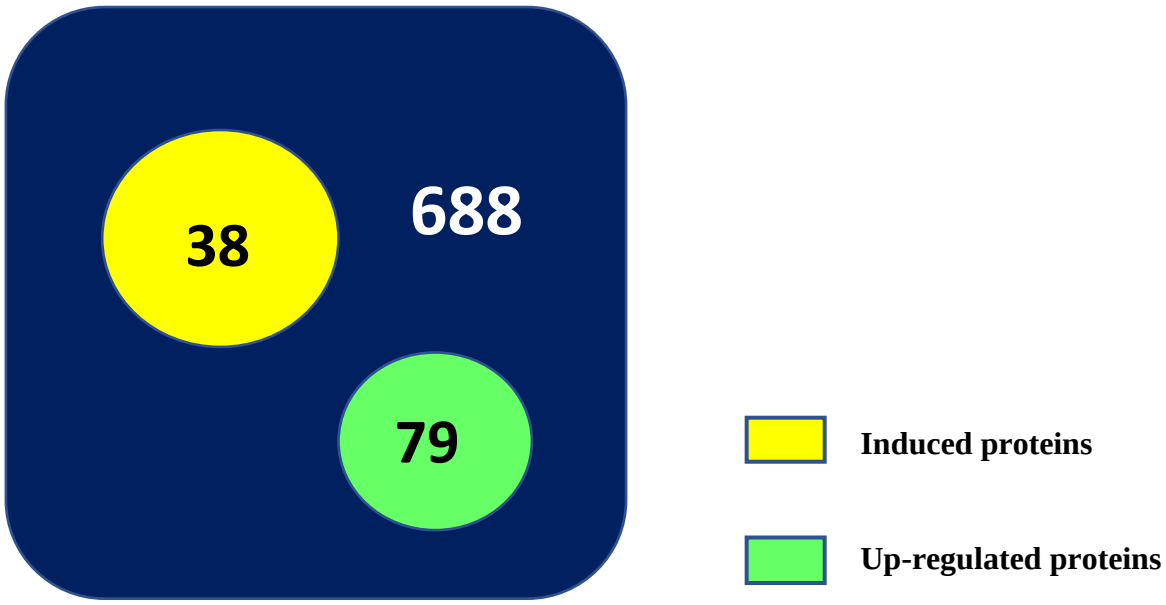

Fig. 5.5 Illustration depicting the distribution of proteins identified in *A. xylosoxidans* strain SJ11 exposed to lead.

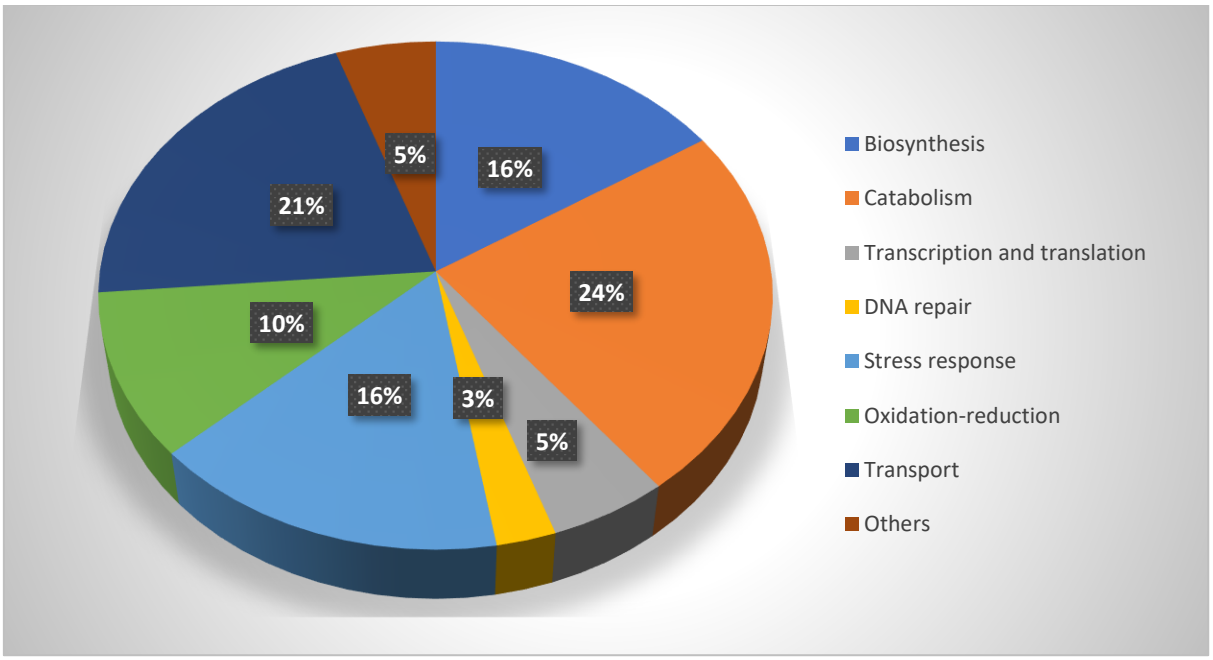

Fig. 5.6 Induced proteins from *A. xylosoxidans* strain SJ11 were classified based on their involvement in various biological processes.

Interestingly, there were certain proteins which are usually implicated in heavy metal resistance such as the ferric hydroxamate uptake protein (12.5 fold), glutathione-binding protein gsiB (7.53 fold), GroES protein (8.69 fold), chaperone protein ClpB (8.28 fold), glutathione S-transferase (2.86 fold), GST-like protein yfcG (6.66 fold), methyl-accepting chemotaxis protein (8.62 fold), organic hydroperoxide resistance protein (8.28 fold), chemotaxis protein CheA (4.43 fold) and a protein phosphatase CheZ (1.73 fold). The proteins CheA and CheZ are well known for their roles in chemotaxis (Zhao et al., 2002). Binding of chemical molecules to the transmembrane receptors leads to autophosphorylation of CheA which further transfers the phosphoryl group to CheY. Phosphatase, CheZ is responsible for dephosphorylation of CheY—P (Baker et al., 2006; Silversmith et al., 2008; Silversmith, 2010). The phosphorus liberated by the action of phosphatase is free to combine with lead ions thus, leading to formation of pyromorphite. Therefore, we hypothesize it as a mechanism for lead precipitation by *A. xylosoxidans* strain SJ11.

Table 5.4 List of proteins induced in *A. xylosoxidans* strain SJ11 on exposure to lead.

Biosynthesis
• 1, 3-oxoacyl-[acyl-carrier-protein] reductase 5
• GTP cyclohydrolase 1 type 2 homolog
• Polyprenyl synthetase family protein
• Flavin prenyltransferase UbiX
• Polyketide cyclase
• Phosphoheptose isomerase
Catabolism
• Metalloprotease TldD
• Protease prtS
• Bifunctional aconitate hydratase 2/2-methylisocitrate dehydratase
• Isochorismatase

• Isochorismatase family
• Mandelate racemase/muconate lactonizing enzyme, N-terminal domain protein 3
• Dehydratase family protein 1
• Bifunctional D-altronate/D-mannonate dehydratase
• Histidine ammonia-lyase
Transcription and translation
• Cys-tRNA(Pro)/Cys-tRNA(Cys) deacylase ybaK
• GntR family transcriptional regulator
DNA repair
• DNA repair protein
Stress response
• Cd(II)/Pb(II)-responsive transcriptional regulator
• DnaJ domain protein
• Mercuric resistance operon regulatory protein
• MerR family transcriptional regulator
• General stress protein CsbD
• YicC family protein
Oxidation-Reduction
• Berberine and berberine like
• Flavin reductase
• Rubredoxin
• Electron transfer flavoprotein subunit alpha 1
Transport
• Bacterial extracellular solute-binding family protein 8
• Bacterial extracellular solute-binding protein, family 7 family protein 3
• Molybdate ABC transporter substrate-binding protein
• Methyl-accepting chemotaxis protein II 1
• Cation efflux system protein CzcC
• Cobalt-zinc-cadmium resistance protein CzcC

• Copper-transporting P-type ATPase
• Ligand-gated channel protein
Others
• Flagellar hook-length control protein
• Alpha-2-macroglobulin

Table 5.5 List of proteins up-regulated in *A. xylosoxidans* strain SJ11 on exposure to lead and the fold change in expression.

Proteins	Fold change
Biosynthesis	
• Phosphoenolpyruvate synthase	23.95
• 3-oxoacyl-[acyl-carrier-protein] synthase 3	7.05
• Phosphomethylpyrimidine synthase	7.05
• Acetyl-CoA carboxylase biotin carboxylase subunit	6.98
• Acetylglutamate kinase	8.3
• Acyl-[acyl-carrier-protein]-UDP-N-acetylglucosamine O-acyltransferase	10.35
• Adenylosuccinate lyase	7.3
• Aerobactin synthase IucC	6.88
• Argininosuccinate lyase	7.3
• Aspartate carbamoyltransferase catalytic chain	6.88
• Cyclopropane mycolic acid synthase 1	2.93
• Glutamine-fructose-6-phosphate aminotransferase [isomerizing]	4.91
• Glycerol kinase	6.27
• O-acetylhomoserine aminocarboxypropyltransferase	5.31
• Putative uroporphyrinogen-III C-methyltransferase	17.06
• Sulfate adenylyltransferase subunit 1	19.97
• Tryptophan synthase beta chain	7.26

• Uridylate kinase	3.94
Catabolism	
• 2-methylisocitrate lyase	3.39
• 2-oxoglutarate dehydrogenase E1 component	35.39
• Carboxymethylenebutenolidase	3.7
• Citrate synthase	4.66
• Dihydrolipoyllysine-residue succinyltransferase component of 2-oxoglutarate dehydrogenase complex	5.36
• L-lactate dehydrogenase	9.12
• Probable succinyl-CoA:3-ketoacid-coenzyme A transferase subunit A	9.65
• Succinate dehydrogenase flavoprotein subunit	4.97
• Succinate--CoA ligase [ADP-forming] subunit alpha	8.58
• Succinate--CoA ligase [ADP-forming] subunit beta	2.59
• Transketolase 1	7.3
• Triosephosphate isomerase	16.43
Transcription and translation	
• Elongation factor G	42.15
• Elongation factor P	4.84
• Elongation factor Ts	2.28
• Probable transcriptional regulatory protein pmpR	3.06
• Proline-tRNA ligase	23.01
• Transcription termination/antitermination protein NusG	12.39
• Translation initiation factor IF-2	4.4
• 30S ribosomal protein S3	10.36
• 30S ribosomal protein S4	6.3
• 30S ribosomal protein S8	2.043
• 30S ribosomal protein S13	3.68
• 50S ribosomal protein L1	5.62
• 50S ribosomal protein L2	4.48

• 50S ribosomal protein L5	4.39
• Aspartate-tRNA ligase	4.81
• Cys regulon transcriptional activator	13.97
• Glutamine-tRNA ligase	12.86
• Ribonuclease E	6.74
• RNA polymerase sigma factor RpoD	3.2
DNA replication and repair	
• DNA gyrase subunit A	20.76
• DNA-binding protein HU-beta	4.16
• Histone-like DNA-binding protein	6.99
Stress response	
• 10 kDa chaperonin or GroES protein	8.69
• Chaperone protein ClpB	8.28
• Glutathione S-transferase	2.86
• GST-like protein yfcG	6.66
• Heat-shock protein Hsp20	2.38
• Methyl-accepting chemotaxis protein 4	8.62
• Organic hydroperoxide resistance protein	8.28
• Chemotaxis protein CheA	4.43
• Protein phosphatase CheZ	1.73
Redox	
• Alkyl hydroperoxide reductase subunit C	2.0
• ATP synthase subunit beta	7.13
• Electron transfer flavoprotein small subunit	3.22
• Electron transfer flavoprotein subunit beta	2.99
• NADH-quinone oxidoreductase chain 1	5.06
Transport	
• Ferric hydroxamate uptake	12.5
• Glutathione-binding protein gsiB	7.53
• Iron ABC transporter substrate-binding protein	6.42

• Leucine-, isoleucine-, valine-, threonine and alanine-binding protein	2.44
• Nickel uptake substrate-specific transmembrane region	4.55
• Potassium-transporting ATPase ATP-binding subunit	2.71
• Potassium-transporting ATPase potassium- binding subunit	2.4
• Protein TolB	3.72
• Thiol reductant ABC exporter subunit CydC	30.76
• Transporter	5.34
Others	
• Alpha-2-macroglobulin family N-terminal region	8.69
• Carboxy-terminal processing protease CtpB	3.34
• Lipoprotein	4.43

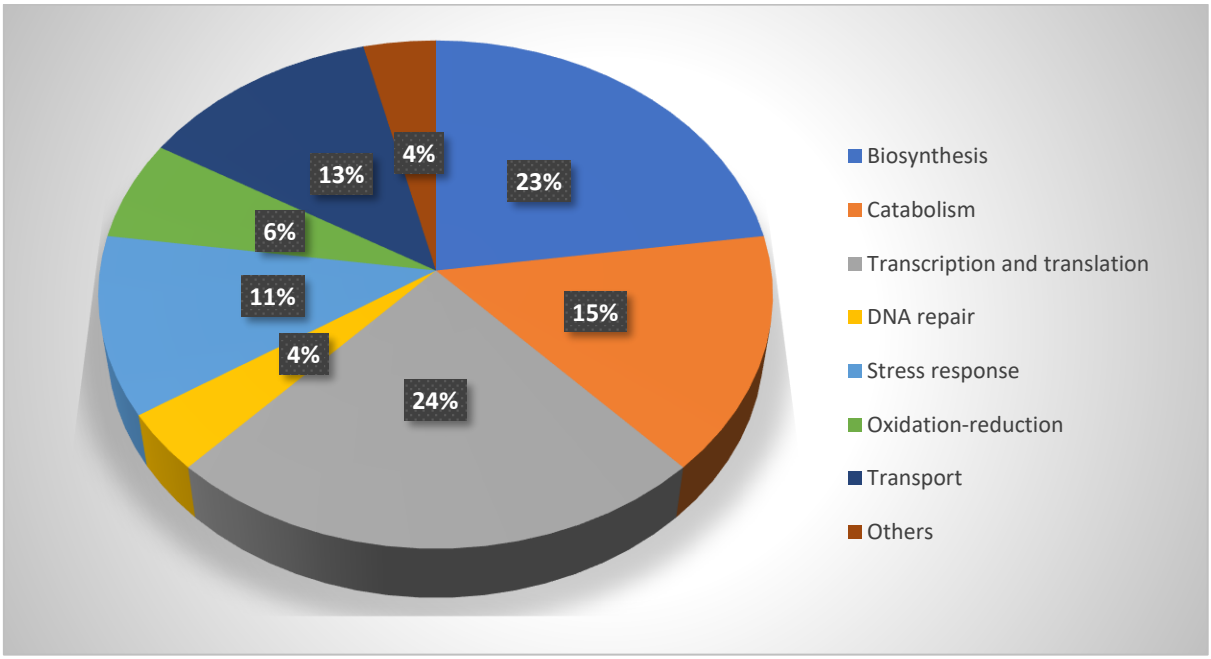

Fig. 5.7 Up-regulated proteins from *A. xylosoxidans* strain SJ11 were classified based on their involvement in various biological processes.

5.3 Cell motility assay

P. vermicola strain SJ2A demonstrated a drastic reduction in cell motility in presence of lead. This is clearly evident from the significant decrease in growth ring on PYE soft agar plate amended with 0.5 mM lead nitrate and a complete absence of the growth ring in presence of 1 mM lead nitrate (Fig. 5.8). However, the cell motility remained unaffected in case of *A. xylosoxidans* strain SJ11. The proteomic analysis of *P. vermicola* strain SJ2A had shown induction of BolA and BolA-like protein when the cells were exposed to lead. These proteins are negative modulators of flagellar biosynthesis which explains the inhibition of bacterial motility in presence of lead. Yung et al. (2014) had also reported slight reduction in motility of *Caulobacter crescentus* in presence of cadmium. Interestingly, this is the first study demonstrating effect of lead on bacterial cell motility.

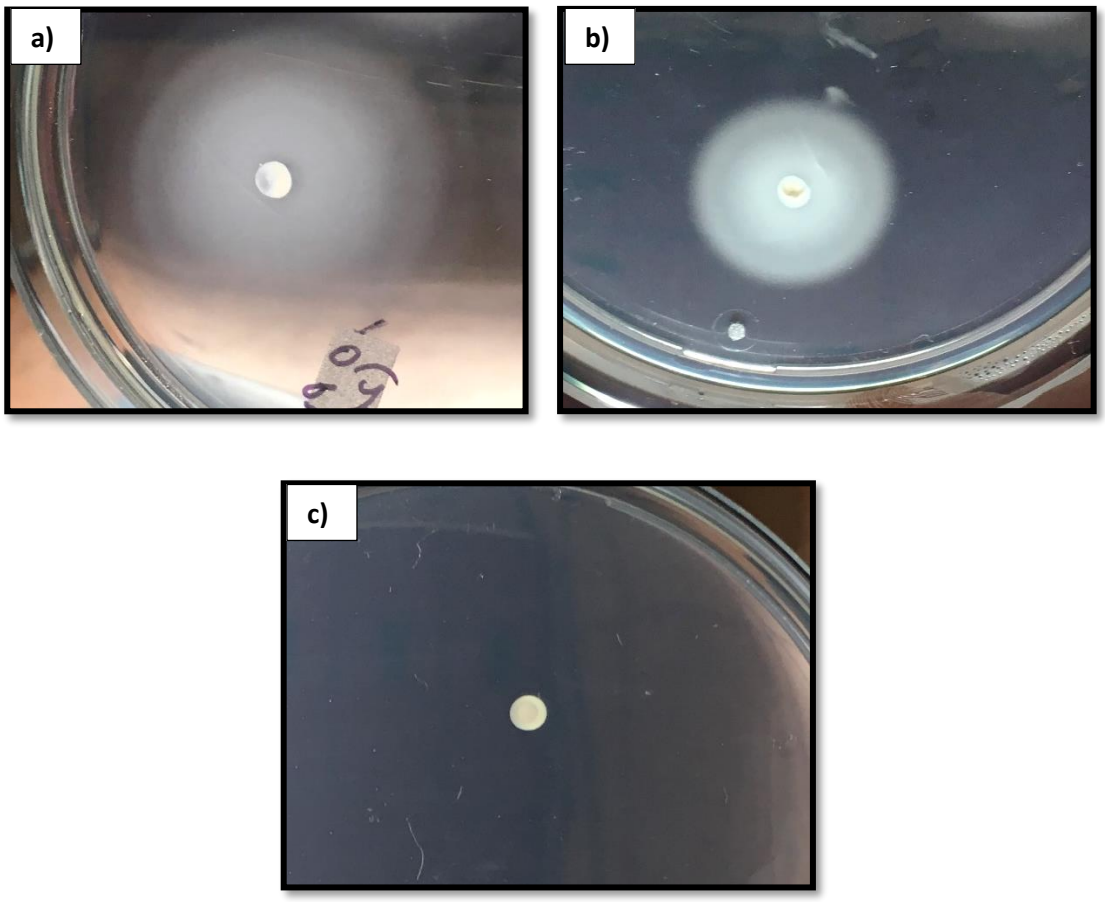

Fig. 5.8 Cell motility assay for *P. vermicola* strain SJ2A.

a) Cells inoculated in PYE agar without lead nitrate

b) Cells inoculated in PYE agar supplemented with 0.5 mM lead nitrate

c) Cells inoculated in PYE agar supplemented with 1 mM lead nitrate

Summary

The lead resistant bacterial isolates demonstrated a significant up-regulation and induction of certain proteins in response to lead. In *P. vermicola* strain SJ2A, 721 proteins were identified in the lead exposed cells, of which 120 were induced while 79 were found to be overexpressed. These proteins include chaperones, chaperonins, metal binding proteins, stress proteins, lipoproteins, siderophore receptor, peptidoglycan-binding protein, oxidoreductase, cadmium-exporting ATPase, zinc/cadmium/mercury/lead-transporting ATPase, copper-sensing histidine kinase, cell division proteins, bacterioferritin, glutathione-dependent thiol reductase and efflux transporters from RND family.

While in *A. xylosoxidans* strain SJ11, 688 proteins were identified in cells exposed to lead, of which 38 were found to be induced and 79 were overexpressed proteins. These lead responsive proteins include chaperones, GroES protein, elongation factors, glutathione S-transferase, ferric hydroxamate uptake protein, glutathione-binding protein gsiB, MerR family transcriptional regulator, general stress protein CsbD, Cd(II)/Pb(II)-responsive transcriptional regulator, cobalt-zinc-cadmium resistance protein CzcC, copper-transporting P-type ATPase and bacterial extracellular solute-binding proteins.

6.1 PCR mediated detection of *smtAB*

The *smt* locus comprises of two divergently transcribed genes, *smtA* and *smtB* which encode a small class II metallothionein and a repressor molecule respectively, thereby mediating resistance to zinc and cadmium ions (Turner et al., 1995; Naz et al., 2005; Blindauer, 2011). This was the first prokaryotic metallothionein discovered in cyanobacterial strains, *Synechococcus* sp. strain PCC 7942 (Huckle et al., 1993) and *Synechococcus* sp. strain PCC 6301 (Olafson et al., 1988; Robinson et al., 1990). MT genes have also been detected in strains of *Streptomyces* sp., *Salmonella choleraesuis* and *Proteus penneri* (Rifaat et al., 2009; Naik et al., 2012d). The internal fragment of known *smtAB* which usually results in an amplicon of 507 bps was not observed in any of our lead resistant bacterial isolates.

6.2 Amplification and sequencing of *bmtA*

The *bmtA* gene is known to encode a bacterial metallothionein which is a low molecular weight, cysteine and histidine rich protein involved in metal binding thus mitigating the effect of toxic metals (Blindauer et al., 2002; Blindauer, 2008, 2011). PCR amplification of *bmtA* using plasmid DNA as a template resulted in an amplicon of approximately 240 bp in the three lead resistant isolates, SJ2A, SJ3A and SJ20 (Fig. 6.1). The *bmtA* gene sequence has been deposited in Genbank with accession number KU565493.2 (https://www.ncbi.nlm.nih.gov/nuccore/KU565493.2). The presence of bacterial metallothionein like proteins have earlier been reported in bacteria for instance, the pseudothionein, CdBP1 in *P. putida* as well as the copper binding metallothionein, MymT in *Mycobacterium tuberculosis* (Higham et al., 1986; Gold et al., 2008).

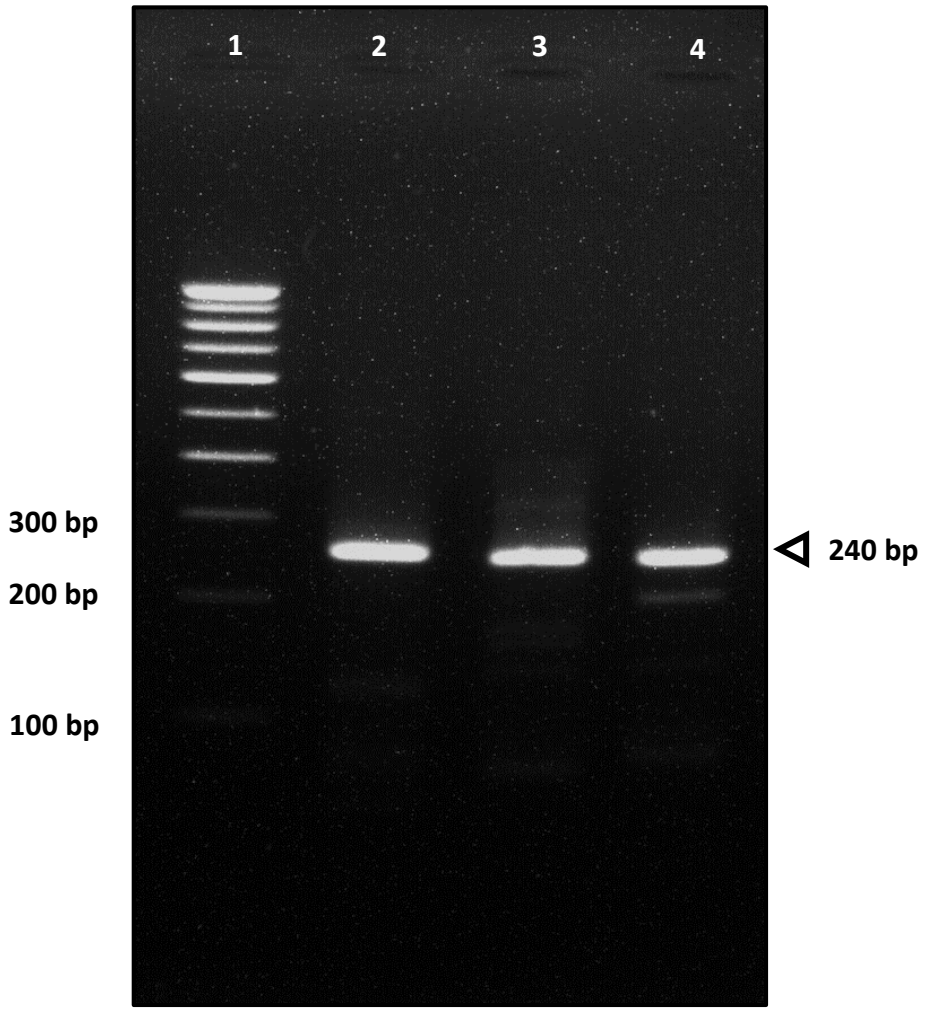

Fig. 6.1 PCR amplification of *bmtA* gene using bacterial plasmid DNA.

Lane 1: 100 bp standard DNA marker

Lane 2: *bmtA* amplicon from isolate SJ2A

Lane 3: *bmtA* amplicon from isolate SJ20

Lane 4: *bmtA* amplicon from isolate SJ3A

The *bmtA* gene sequence when translated using ExPASy (https://web.expasy.org/translate/) gave the following peptide:

M N S E T C A C P K C T C Q P G A D A V E R D G Q H Y C C A A C A S G H P Q G E P C R D A D C P C G G T T R P Q V A E D R Q

BLASTx analysis indicated that BmtA from *P. vermicola* strain SJ2A showed 100% homology to the metallothionein (MT) from *Pseudomonas* sp. (Accession number WP_003100805.1). Phylogenetic analysis of BmtA from *P. vermicola* strain SJ2A along with various other bacterial genera and SmtA from cyanobacteria was performed to understand the relatedness between Smts and Bmts (Fig. 6.2). They showed a distinct separate grouping in the phenogram clearly indicating significant differences between the two.

Multiple sequence alignment (MSA) carried out for Bmts and Smts revealed that 8 cysteine, 1 histidine and 2 alanine residues were conserved throughout the cyanobacterial as well as bacterial metallothioneins (Fig. 6.3). Metallothioneins are well known for the presence of cysteine and histidine residues which are usually involved in binding with the metal ions like Zn and Cu for sequestration (Blindauer, 2011). However, conservation of alanine residues is another interesting aspect and its role in metal binding can be studied further.

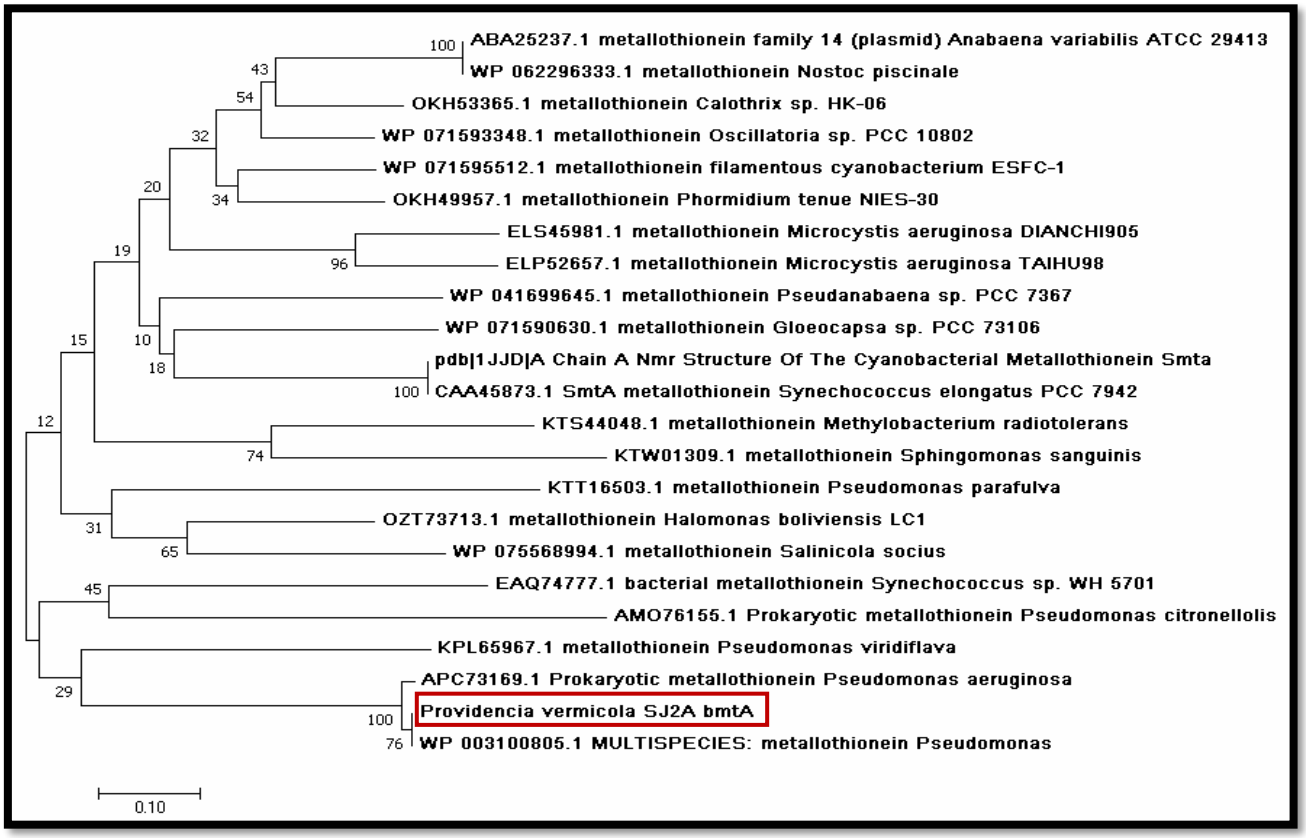

Fig. 6.2 Evolutionary relationship of Bmts and Smts from bacteria and cyanobacteria using neighbour-joining method. The BmtA from *P. vermicola* strain SJ2A has been marked. The bootstrap values are based upon 10000 replicates. The scale bar, 0.1 indicates 10 amino acid residues substitutions per 100 positions.

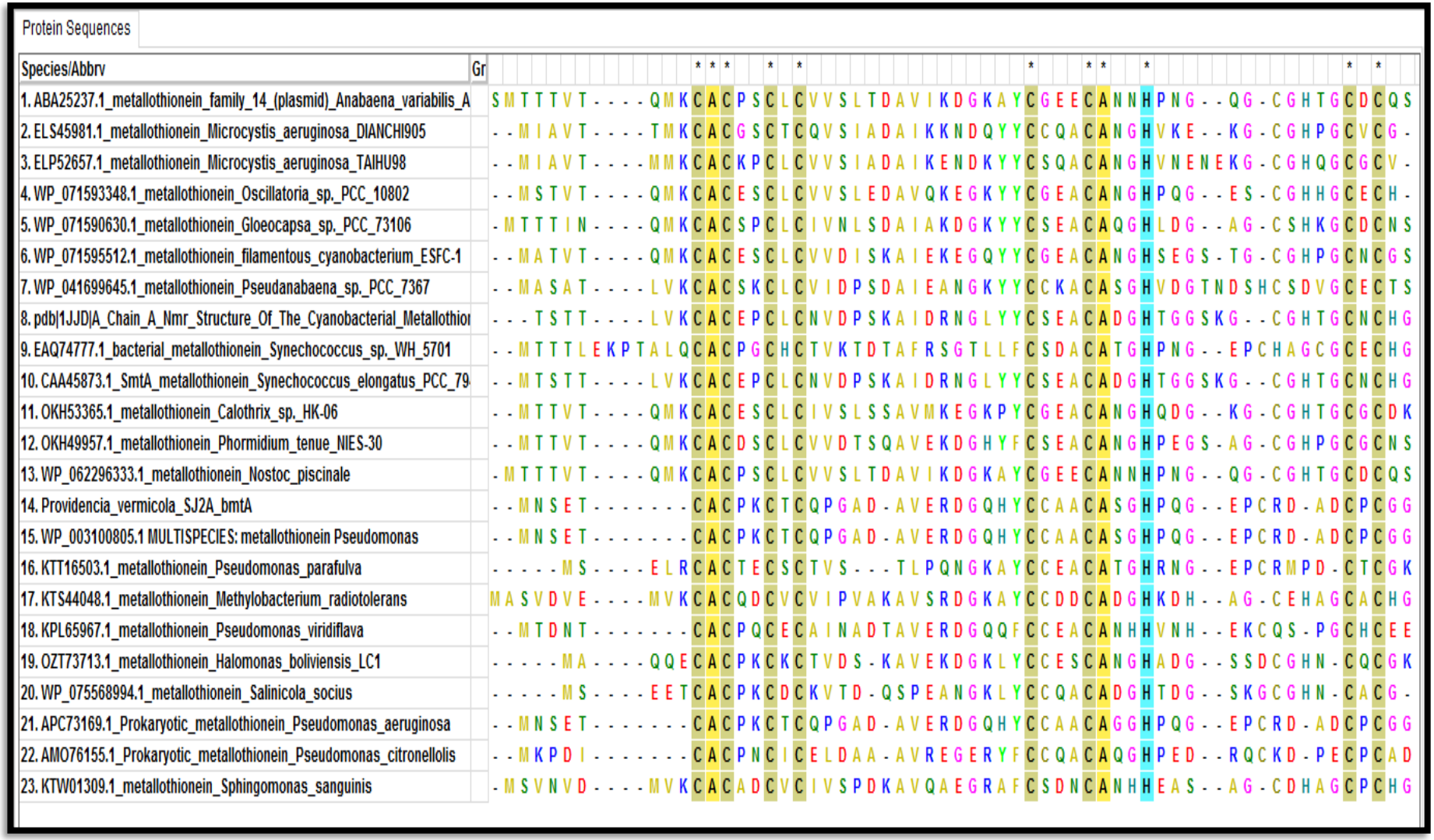

Fig. 6.3 Multiple sequence alignment of cyanobacterial and bacterial metallothioneins.

6.3 Homology Modelling of BmtA

Since BmtA from *P. vermicola* strain SJ2A showed complete homology with MT from *Pseudomonas* sp. (Accession number WP_003100805.1) containing 79 amino acid residues, this MT was used to carry out further modelling and docking studies. The constructed protein model (Fig. 6.4) clearly depicts the alpha helices, beta strands and coils along with disulphide regions which are usually involved in ligand binding. I-TASSER server also predicted the secondary structure of proteins with a high confidence score demonstrating 25 α-helices and 4 β-strands (Fig. 6.5). Hydropathy plot (Fig. 6.6) for this protein suggests that it has a single hydrophobic transmembrane segment lying in between two hydrophilic segments of the protein (Kyte and Doolittle, 1982).

The protein model was assessed by various local and global assessment tools at SAVES and the Swiss model server. The Z-score, QMEAN6 score and Dfire energy for the predicted model were evaluated to be -0.988, 0.602 and -70.97 kJ mol^{-1} (Zhou and Zhou, 2002). Qmean is a complex scoring function for estimation of both global quality of the whole model and the local, that is, per residue analysis of diverse regions within the model (Benkert et al., 2009) (Fig. 6.7). On the other hand, Gromos is an all-purpose computer simulation package for molecular dynamics which is applied in order to analyse the conformations obtained from experimentation or computer simulation (Dawar et al., 2013). Moreover, when the model was assessed by PROCHECK, which determines the stereochemical quality of the structure by analysing residue by residue geometry as well as the overall structural geometry, indicated 46.0% core regions in BmtA. The Ramachandran plot for BmtA illustrates the PROCHECK results (Fig. 6.8). ERRAT evaluates the statistics of non-bonded interactions between different types of atoms and the overall quality factor was determined as 69.01 for BmtA. Furthermore, VERIFY3D showed that 100% of the amino acid residues had an average 3D-1D score of ≥ 0.2. Thus, SAVES approved the three-dimensional model of BmtA for further studies.

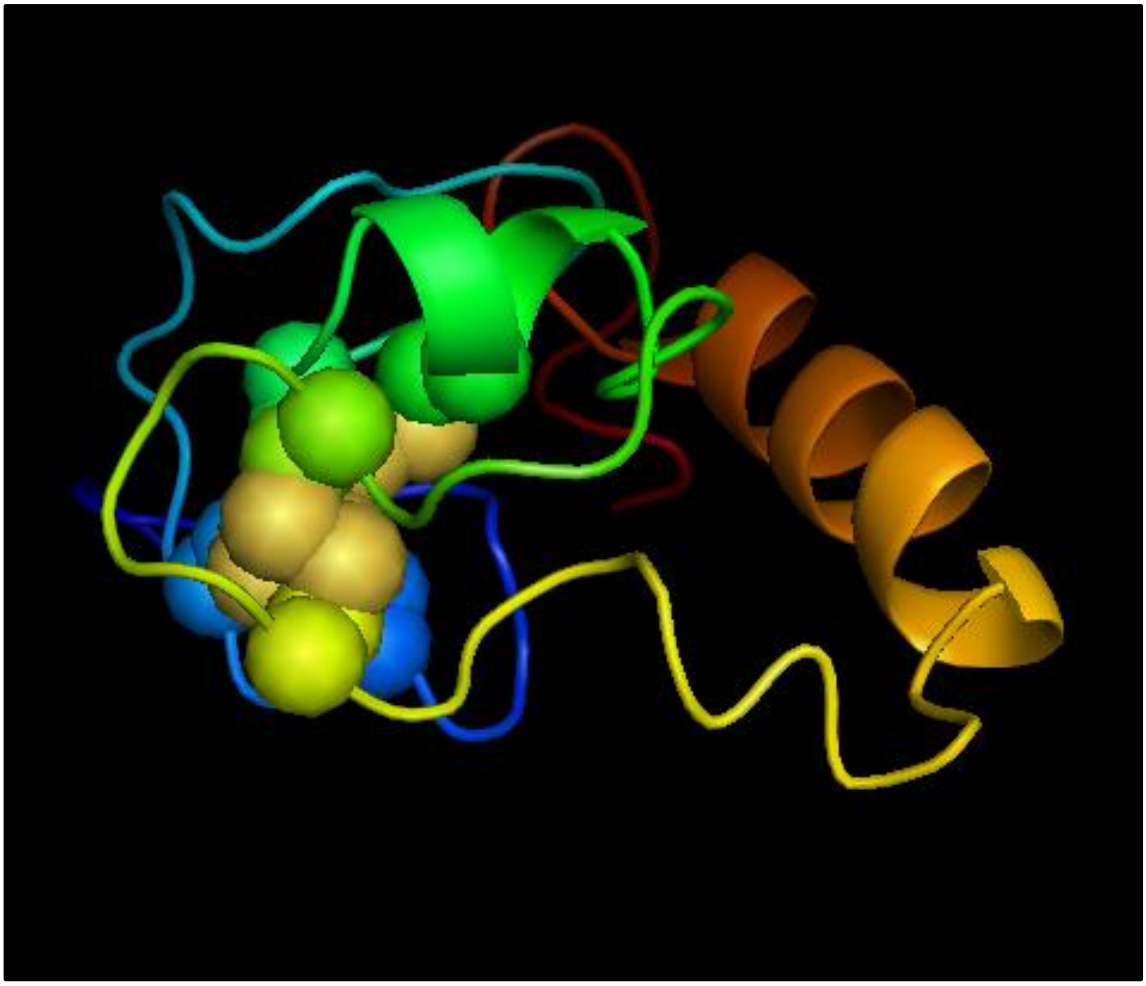

Fig. 6.4 Protein model of BmtA constructed using I-TASSER suite.

The protein model shows the helices, strands as well as the coils while the spheres represent the disulphide regions.

```
                    20                  40                  60
                    |                   |                   |
Sequence    MNSETCACPKCTCQPGADAVERDGQHYCCAACASGHPQGEPCRDADCPCGGTTRPQVAEDRQLDDALKETFPASDPISP
Prediction  CCCCCCCCCCCSSSSCHHHHHHCCHHHHHHHHHHCCCCCCCCCCCCCCCCCCCCCCCCCCHHHHHHHHHHCCCCCCCCCC
Conf.Score  976410699875541837877514667889986359899988888885544268777317788888860067778889 7
            H:Helix; S:Strand; C:Coil
```

Fig. 6.5 Predicted secondary structure of BmtA constructed using I-TASSER server.

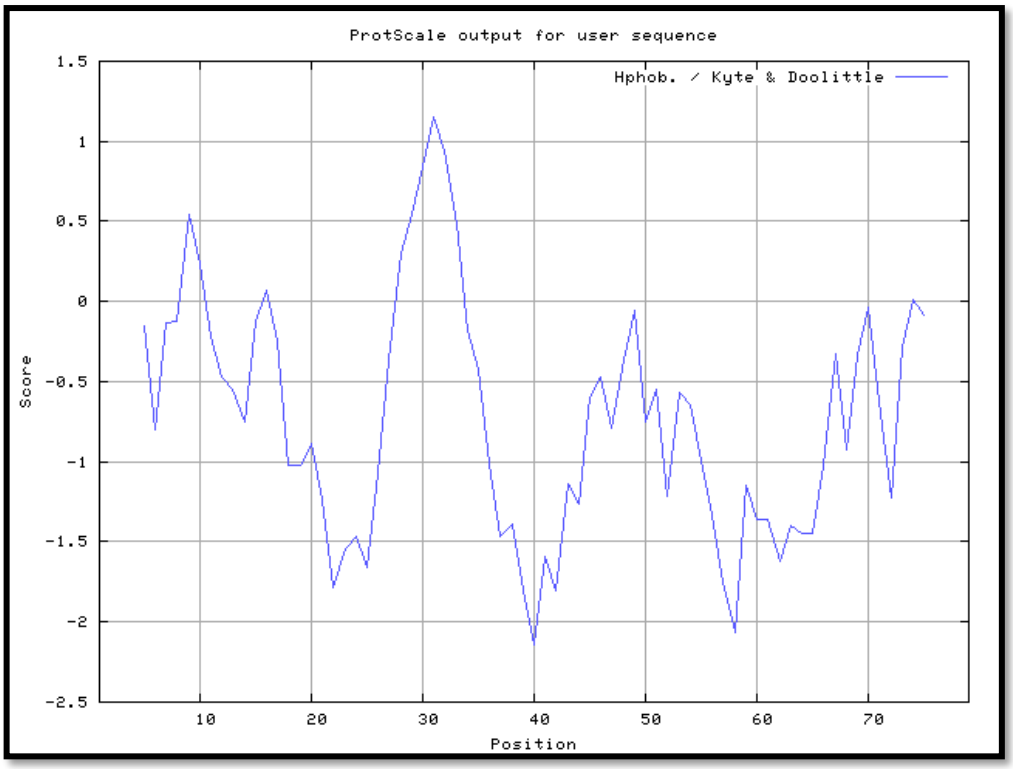

Fig. 6.6 Hydropathy plot for BmtA.

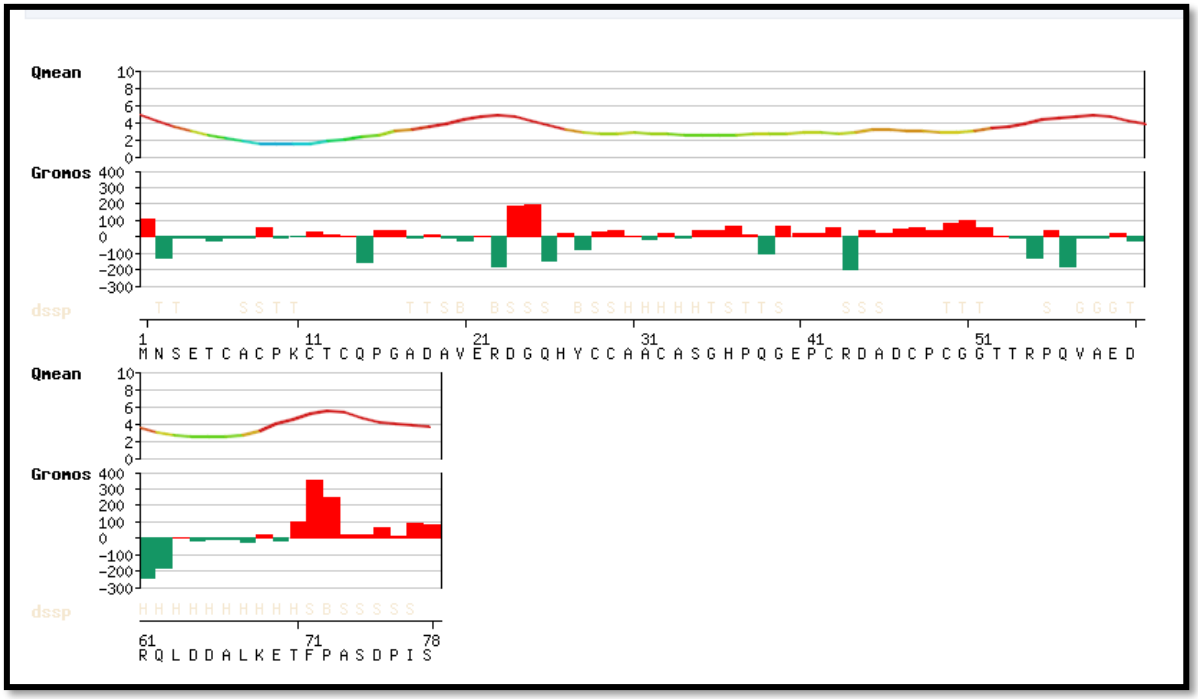

Fig. 6.7 Evaluation for Qmean and Gromos force fields of BmtA.

Negative energy values (in green) represent a favourable energy environment whereas positive values (in red) depict unfavourable energy environment for a given amino acid.

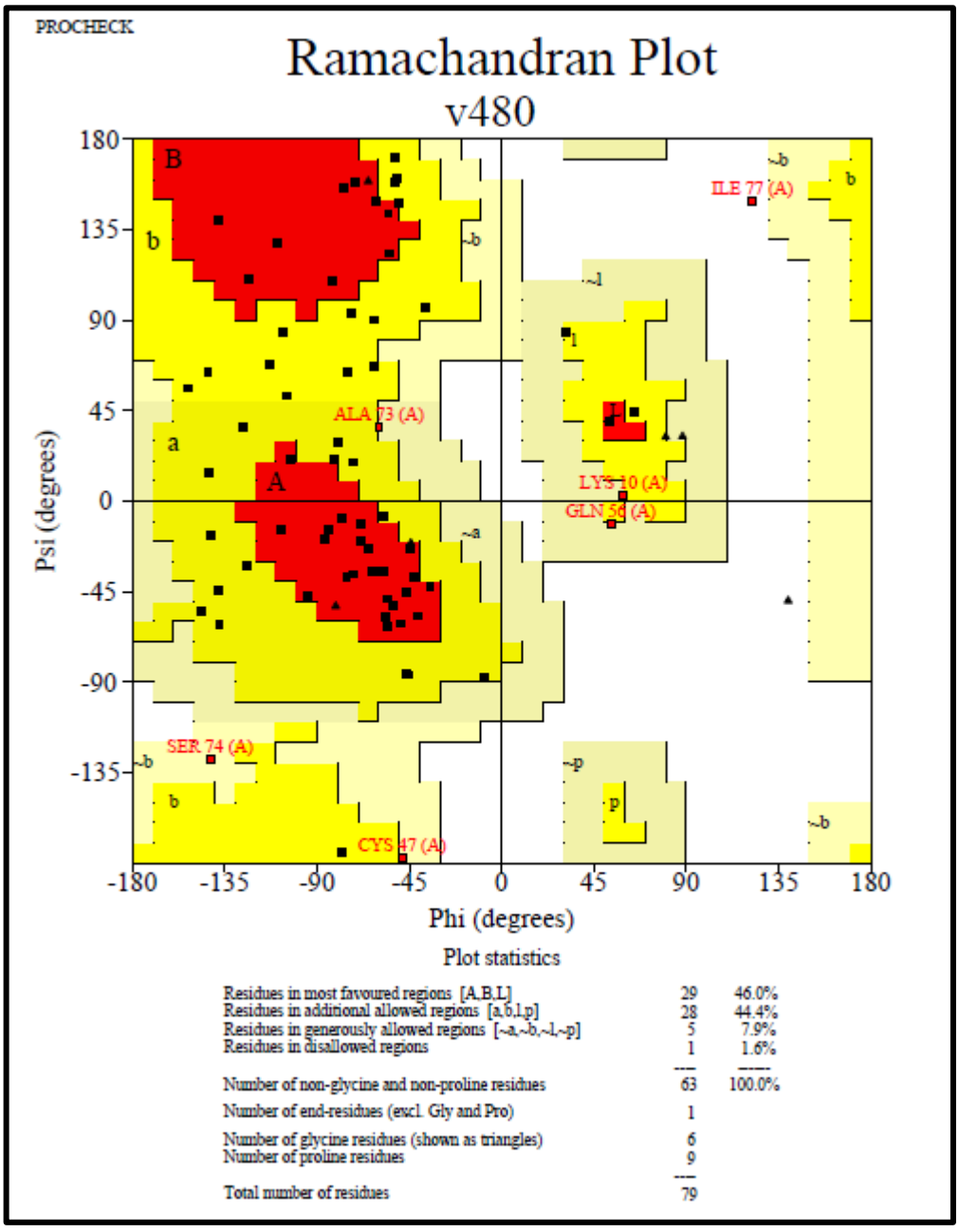

Fig. 6.8 Ramachandran plot depicting PROCHECK results for BmtA.

6.4 *In silico* docking studies of BmtA and metal ions

Docking studies were performed *in silico* to develop a better understanding of the interaction of BmtA metallothionein with various metal ions (Fig. 6.9, 6.10, 6.11, 6.12, 6.13, 6.14, 6.15). Docking results clearly show that BmtA could interact very well with lead. Interestingly, three cysteine residues displayed major involvement in this interaction (Fig. 6.9). Table 6.1 enlists the amino acid residues od BmtA along with their respective positions that docked with various metal ions. Blindauer et al. (2001) had confirmed that the α-helices and 4 β-strands of SmtA form a zinc finger which facilitates zinc uptake by cyanobacteria. Various mammalian MT peptides were docked with zinc, mercury and cadmium that enabled molecular dynamics simulation studies. Molecular modelling along with techniques viz. NMR, XANES and XAFS has enabled determination of 3D structures of a range of MTs (Fowle and Stillman, 1997; Chan et al., 2002). Therefore, docking studies help in developing new insights with respect to protein-protein or protein-ligand interactions.

Table 6.1 Docking interactions of amino acid residues of BmtA with various metal ions.

S.N.	Metal Ions	Amino acid residues	Position
1.	**Pb**	CYS	6
		CYS	13
		GLN	14
		PRO	15
		CYS	28
		ASP	44
		ALA	45
2.	**Zn**	GLY	35
		ASP	60
3.	**Cu**	PRO	9
		GLN	56
		GLU	59
		LEU	63
4.	**Cd**	PRO	9
		GLN	56
		GLU	59
		LEU	63
5.	**Co**	PRO	9
		GLN	56
		GLU	59
		LEU	63
6.	**Ni**	MET	1
		GLU	4
		ALA	17
		HIS	26
7.	**Ca**	PRO	9
		GLN	56
		GLU	59
		LEU	63

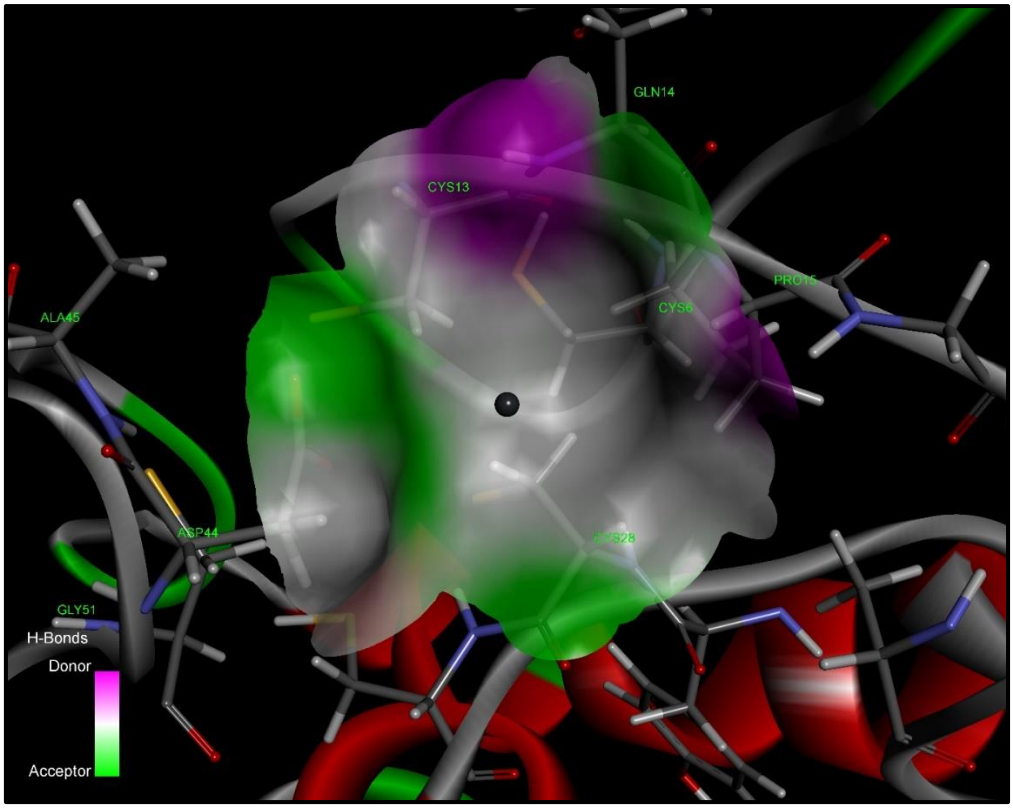

Fig. 6.9 Docking of BmtA with lead (Pb) ion.

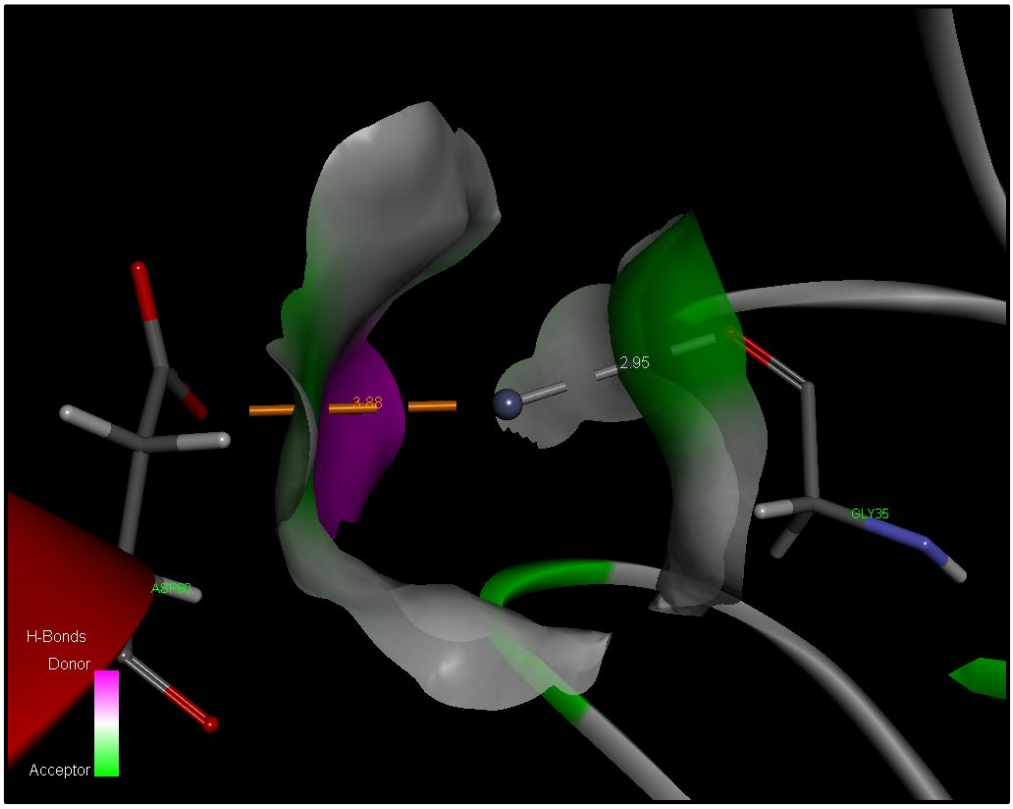

Fig. 6.10 Docking of BmtA with zinc (Zn) ion.

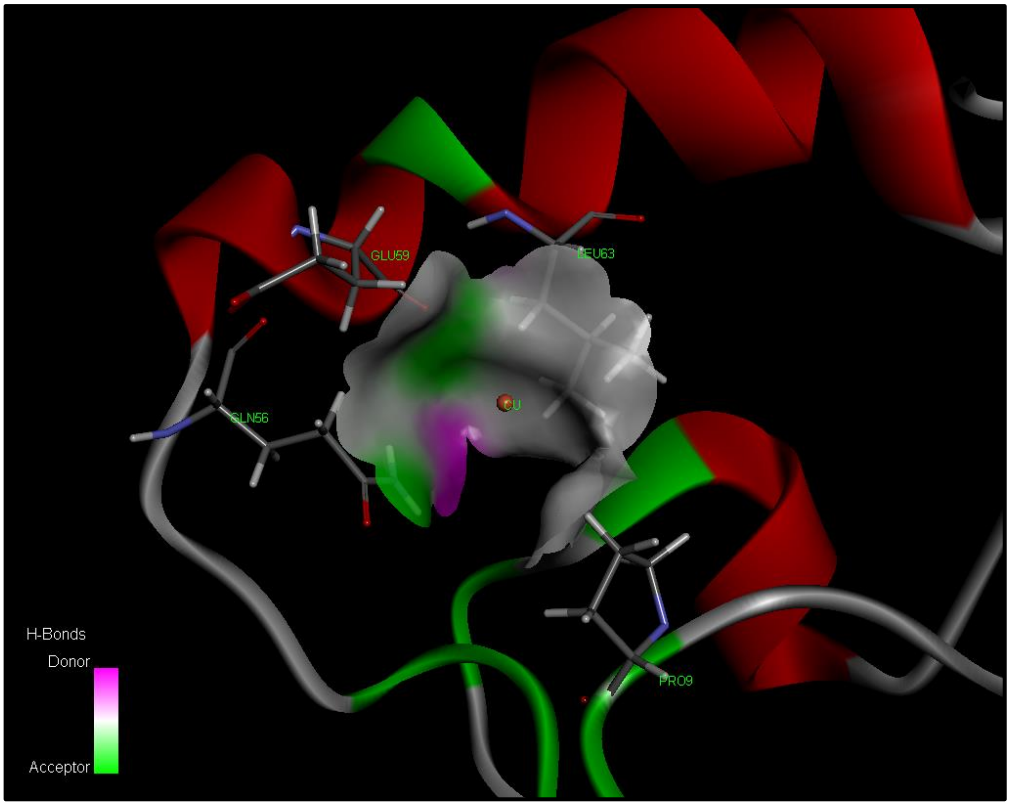

Fig. 6.11 Docking of BmtA with copper (Cu) ion.

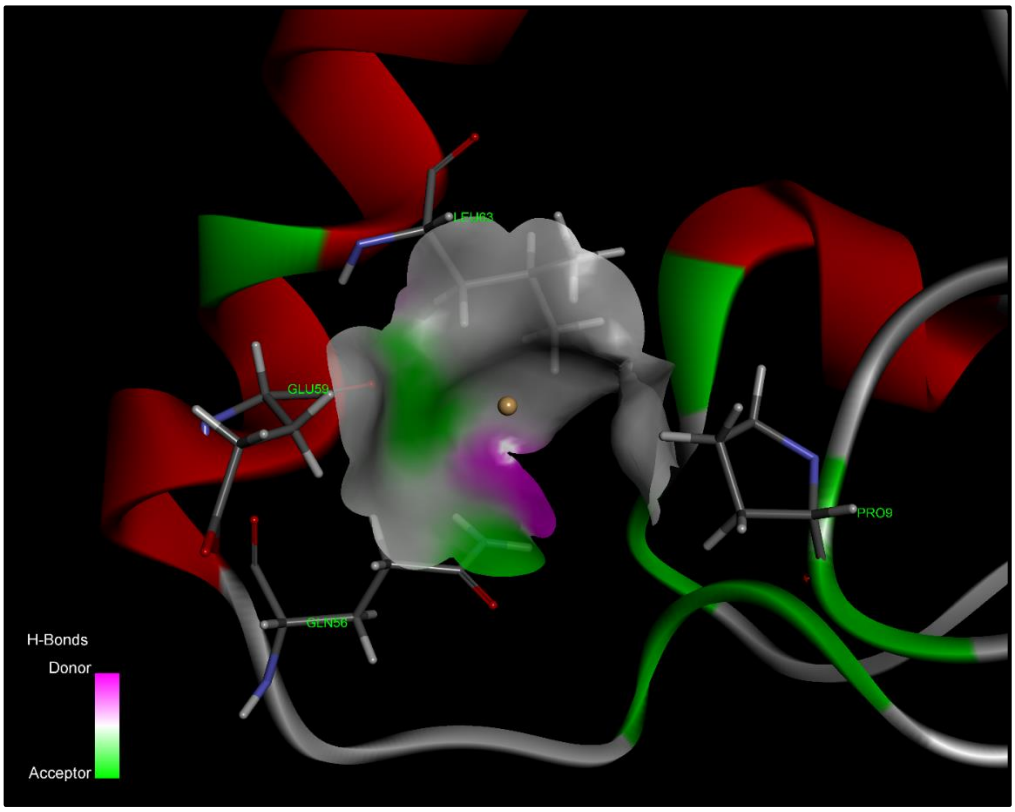

Fig. 6.12 Docking of BmtA with cadmium (Cd) ion.

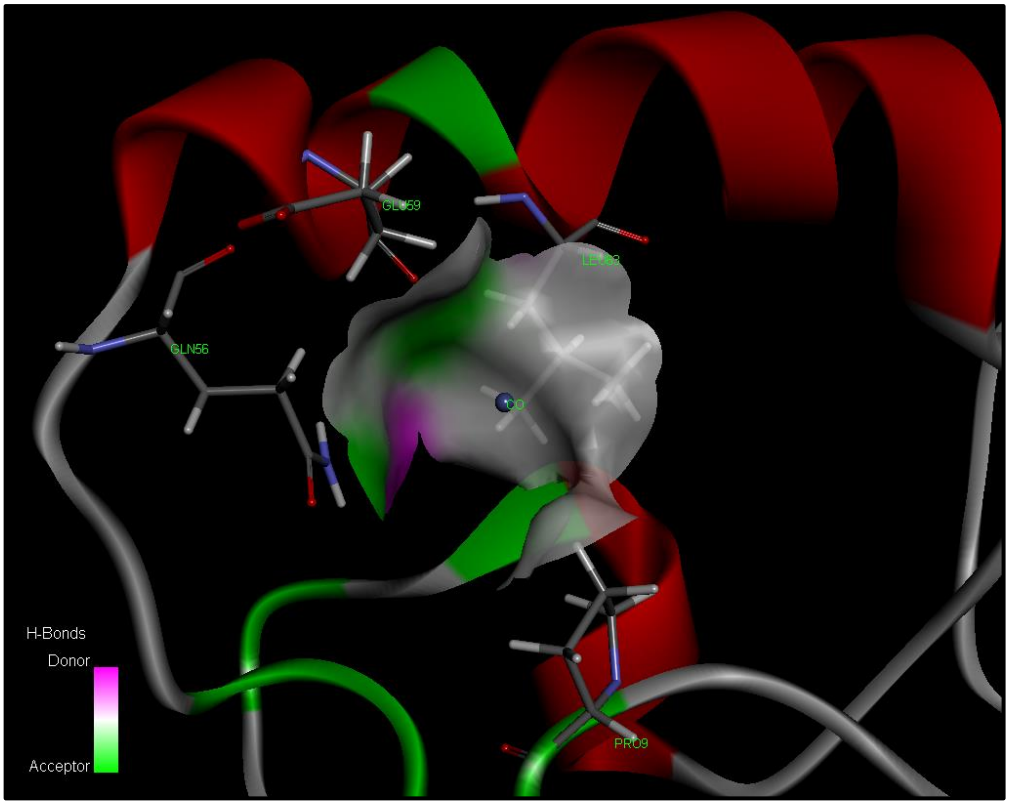

Fig. 6.13 Docking of BmtA with cobalt (Co) ion.

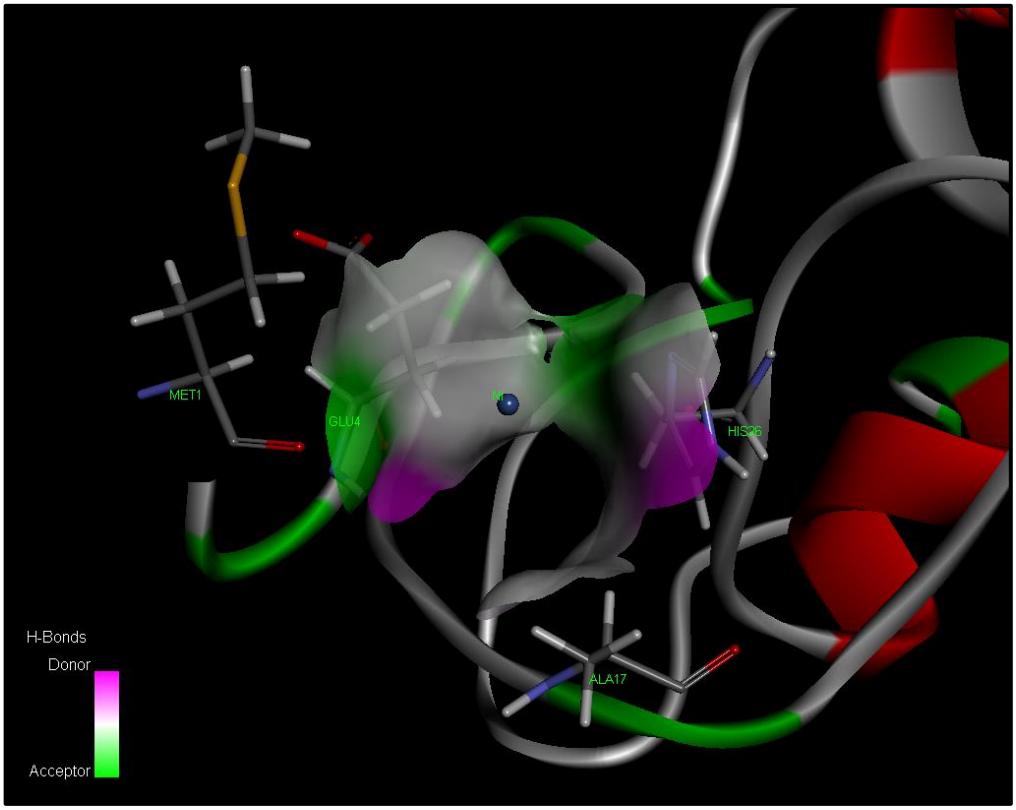

Fig. 6.14 Docking of BmtA with nickel (Ni) ion.

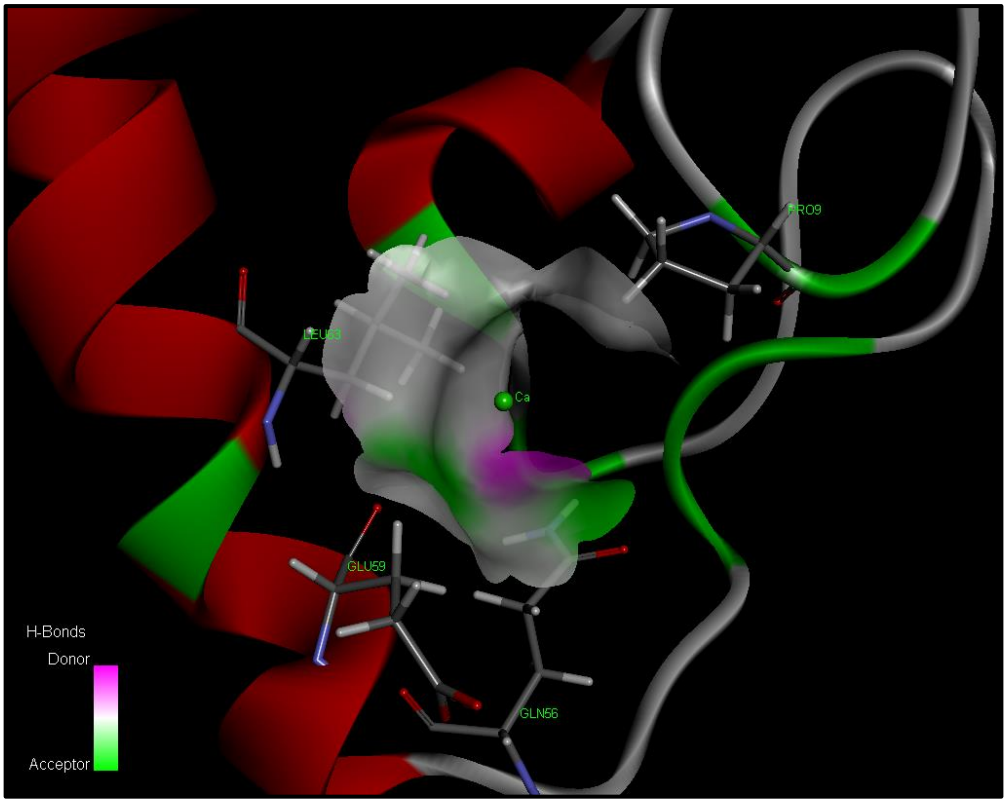

Fig. 6.15 Docking of BmtA with calcium (Ca) ion.

Summary

We have tried to explore bacterial *smtAB* and *bmtA* genes in the lead resistant bacterial isolates. Although *smtAB* was not detected but approximately, 240 bp amplicon was generated using *bmtA* specific primers and plasmid DNA from *P. vermicola* strains. The sequence of *bmtA* was subsequently submitted to Genbank. Additionally, the Blastx search interestingly revealed that the *bmtA* amplicon showed 100% homology to the metallothionein (MT) protein from *Pseudomonas* sp. Multiple sequence alignment (MSA) was performed using the MT amino acid sequences from cyanobacteria as well as other bacterial strains. It was evident from the MSA that 8 cysteine residues along with 1 histidine and 2 alanine residues were conserved throughout the cyanobacterial and bacterial metallothioneins. Additionally, docking studies also revealed strong interactions of BmtA with various metal ions particularly, lead. Pb was found to interact specifically with the cysteine residues (positions 6, 13 and 28) of the metallothionein, BmtA.

The present study was carried out in order to explore novel lead resistance mechanisms in selected bacterial strains. The important findings of the research are as follows:

- Lead resistant bacterial strains with a MTC ranging from 3 to 4 mM lead were isolated from the waste site of a battery manufacturing industry in Goa.
- These isolates demonstrated alterations in their colony characteristics viz. pigmentation, zone of clearance and precipitation ring on exposure to lead nitrate.
- The bacterial isolates SJ2A, SJ3A and SJ20 possessed plasmids.
- The isolates, SJ2A and SJ11 were identified as *Providencia vermicola* and *Achromobacter xylosoxidans* respectively, based on biochemical tests and 16S rDNA sequencing.
- *Providencia vermicola* strain SJ2A demonstrated periplasmic sequestration of lead as the mechanism governing resistance.
    - It carried the *pbrR* gene on plasmid as well as chromosomal genome.
    - Scanning electron micrographs of bacterial cells exposed to lead revealed a unique alteration in the cell morphology from rods to long inter-connected filaments.
    - Electron dispersive X-ray spectroscopy did not indicate adsorption of lead.
    - Transmission electron micrographs of the bacterial cells exposed to lead evidently demonstrated sequestration of lead in the periplasmic space.
    - FTIR analysis revealed involvement of phospholipids, LPS and peptidoglycan in interaction with lead.
    - The bacterium internalised 155.12 mg Pb^{2+}/g biomass as determined by atomic absorption spectroscopy.
    - The sequestered lead was subsequently identified as lead sulfite by X-ray diffraction analysis.

- *Achromobacter xylosoxidans* strain SJ11 exhibited precipitation of lead in the form of pyromorphite.
    - PCR mediated detection of *pbrR* indicated that chromosomal genome was solely responsible for conferring lead resistance.
    - Scanning electron micrographs showed aggregation of bacterial cells as well as presence of a precipitate on lead exposure.
    - Energy dispersive X- ray spectroscopic analysis revealed presence of lead (48.5 % by weight) along with phosphorus and chlorine in the precipitate.
    - FTIR indicated phosphate groups being the dominant groups involved in interaction with lead.
    - Atomic absorption spectroscopic analysis clearly demonstrated that 465.8 mg Pb^{2+}/g was precipitated by the bacterial cells.
    - The extracellular precipitate was identified as pyromorphite, $Pb_5(PO_4)_3Cl$ by X-ray diffraction analysis.
    - There was a remarkable increase (i.e. 160%) in phosphatase activity in presence of 0.5 mM lead.
- The lead resistant bacterial isolates demonstrated a significant up-regulation and induction of certain proteins in response to lead.
    - In *P. vermicola* strain SJ2A, 721 proteins were identified in the lead exposed cells, of which 120 were found to be induced while 79 were overexpressed. These include proteins viz. chaperones, chaperonins, metal binding proteins, stress proteins, lipoproteins, siderophore receptor, peptidoglycan- binding protein, oxidoreductase, cadmium-exporting ATPase, zinc/cadmium/mercury/lead-transporting ATPase, copper-sensing histidine

kinase, cell division proteins, bacterioferritin, glutathione-dependent thiol reductase and efflux transporters from RND family.

- In case of *A. xylosoxidans* strain SJ11, 688 proteins were identified in cells exposed to lead, of which 38 were induced and 79 were overexpressed proteins. These lead responsive proteins included chaperones, GroES protein, elongation factors, glutathione S-transferase, ferric hydroxamate uptake protein, glutathione-binding protein gsiB, MerR family transcriptional regulator, general stress protein CsbD, Cd(II)/Pb(II)-responsive transcriptional regulator, cobalt-zinc-cadmium resistance protein CzcC, copper-transporting P-type ATPase and bacterial extracellular solute-binding proteins.

- The amplicon of bacterial metallothionein gene (*bmtA*) with a size of 240 bp was generated using plasmid DNA of *P. vermicola* strains SJ2A, SJ3A and SJ20 as template. It showed 100% homology to the metallothionein (MT) protein from *Pseudomonas* sp.
- It was evident from the multiple sequence alignment that 8 cysteine residues along with 1 histidine and 2 alanine residues were conserved throughout the cyanobacterial and bacterial metallothioneins.
- Docking studies also revealed strong interactions of BmtA with various metal ions particularly, lead which was found to interact specifically with the cysteine residues (positions 6, 13 and 28) of the bacterial metallothionein.

Appendix-A

Media

A.1 Nutrient Broth

	(per litre)
Peptone	10.0 g
Beef extract	10.0 g
Sodium chloride	5.0 g
pH	7.3±0.1

A.2 M9 minimal medium

Per litre: To 750 ml of sterile water (cooled to 50^{o}C or less), add:

M9 salts (5X)	200 ml

(Dissolved 64.0 g $Na_2HPO_4.7H_2O$; 15.0 g KH_2PO_4; 2.5 g NaCl; 5.0 g NH_4Cl in deionized water to make the final volume as 1 L)

$MgSO_4$ (1 M)	2.0 ml
$CaCl_2$ (1 M)	0.1 ml
20% solution of the appropriate carbon source	20.0 ml

A.3 Defined minimal medium

	(per litre)
Sodium citrate	0.5 g
Magnesium sulphate	0.1 g
Ammonium sulphate	1.0 g

Glucose	1.0 g
Sodium tripolyphosphate	0.1 g
pH	6.0

A.4 Mueller Hinton Agar

	(per litre)
Meat infusion	2.0 g
Casein acid hydrolysate	17.5 g
Starch	1.5 g
Agar agar	17.0 g
pH	7.3±0.1

A.5 PYE Agar

	(per litre)
Peptone	2.0 g
Yeast extract	1.0 g
Agar agar	2.5 g

Appendix-B

Other Chemicals

B.1 Lead nitrate

Prepare a stock solution of 100 mM lead nitrate:

Lead nitrate	3.3121 g
Deionized water	100 mL

Filter the solution through a 0.22 micron membrane and store.

B.2 KOH (3%)

KOH	3.0 g
Distilled water	100 mL

B.3 Phosphate buffered saline (PBS)

137 mM NaCl

2.7 mM KCl

10 mM Na_2HPO_4

2 mM KH_2PO_4

Adjust the pH to 7.4

Appendix-C

Agarose Gel Electrophoresis

C.1 0.8%, 1% and 1.5% agarose

Weigh 0.8 g, 1.0 g or 1.5 g and dissolve in 100 mL of 1X TAE buffer to prepare 0.8%, 1% and 1.5% agarose respectively. Melt the solution in microwave oven until clear, transparent solution is obtained. Add ethidium bromide to a final concentration of 0.5 µg/mL and cast the gel.

C.2 Ethidium Bromide

Add 1.0 g of ethidium bromide to 100 mL of deionized water. Stir on magnetic stirrer for several hours to ensure that the dye has dissolved. Transfer the solution to amber coloured bottle and store at room temperature.

C.3 Gel Loading Buffer

0.05% (w/v) Bromophenol blue

40% (w/v) Sucrose

0.1M Ethylenediaminetetraaceticacid (EDTA) (pH 8.0)

0.5% (w/v) Sodium dodecyl sulphate

C.4 50X Tris Acetate EDTA

Tris base	24.2 g
Glacial acetic acid	5.71 mL
0.5M EDTA	10 mL
Deionized water	100 mL

C.5 10X Tris EDTA (TE) Buffer (pH 8.0)

Tris Chloride	100 mM
EDTA	10 mM

Sterilize for 20 min at 15 psi.

Appendix-D

Sodium Dodecyl Sulphate-Polyacrylamide gel electrophoresis (SDS-PAGE)

D.1 Stock solutions for SDS-PAGE

D.1.1 Acrylamide-*bis*-acrylamide solution (monomer solution)

Acrylamide	29.0 g
N,N' methylene *bis* acrylamide	1.0 g
Deionized water	100 mL

Dissolve acrylamide and N,N'-methylene *bis*-acrylamide in 80 mL of warm deionized water. Adjust pH of the solution to 7.0. Make the final volume to 100mL using deionized water. Store in amber coloured bottle at room temperature.

D.1.2 Resolving gel buffer (Tris 1.5 M, pH 8.8)

Tris (base)	18.171 g
Deionized water	100 ml

Dissolve tris base in 60 mL of deionized water. Adjust the pH of solution to 8.8 with 6 N HC1 and make the final volume to 100mL with deionized water. Store the solution at 4°C.

D.1.3 Stacking gel buffer (Tris 1.0 M, pH 6.8)

Tris (base)	12.114 g
Deionized water	100 mL

Dissolve tris base in 60 mL of deionized water. Adjust the pH of solution to 6.8 with 6 N HC1 and make the final volume to 100mL with deionized water. Store the solution at 4°C.

D.1.4 10% ammonium per sulphate (APS)

Ammonium per sulphate	0.1 g
Deionized water	1 mL

D.1.5 10% Sodium dodecyl sulphate

Sodium dodecyl sulphate	10 g
Deionized water	100 mL

D.1.6 6N Hydrochloric acid

Concentrated HCl	51 mL
Deionized water	100 mL

D.1.7 1% Bromophenol blue

Bromophenol blue	0.1 g
Deionized water	10 mL

D.1.8 5X Tris-glycine electrophoresis buffer (pH 8.3)

25 mM Tris base	3.02 g
250 mM Glycine	18.8 g
10% (w/v) SDS	10 mL
Deionized water	200 mL

Preparation of 1X tank buffer: Make 100 mL of 5X Tris-glycine electrophoresis buffer to 500 mL using de-ionized water.

D.1.9 2X Sample Solubilizing buffer

1 M Tris HC1 (pH 6.8)	1 ml
Glycerol	2 mL
1% (w/v) Bromophenol blue	2 mL
10% (w/v) SDS	4 ml
200 mM β-mercaptoethanol	284 µL
Deionized water	716 µL

D.1.10 Preparation of resolving and stacking gel

Components	12% Resolving gel (10 mL)	5% Stacking gel (3 mL)
Monomer	3.98	0.597
1.5 M Tris (pH 8.8)	2.486	-
1.0 M Tris (pH 6.8)	-	0.373
10% (w/v) SDS	0.1	0.03
10% (w/v) APS	0.05	0.015
TEMED	0.005	0.0015
Deionized water	3.381	1.984

D.2 Visualisation of SDS-PAGE Gels

D.2.1 Coomassie Brilliant Blue Staining Solution

Coomassie Brilliant Blue R-250	0.05 g
Methanol	50 mL
Glacial acetic acid	10 mL

Make the volume to 100 mL using deionized water.

D.2.2 Destaining Solution

Methanol	30 mL
Glacial acetic acid	10 mL

Make the volume to 100 mL using deionized water.

Appendix-E

Polymerase Chain Reaction

E.1 Primer sets

27F	5’ GAGAGTTTGATCCTGGCTCAG 3’
1495R	5’ CTACGGCTACCTTGTTACGA 3’
pbrR1	5’ GCTCTAGACTAGTCGCTTGGATGGGCGGTG 3’
pbrR2	5’ CGGAATTCGGCAACCCCTTGTGTGTATTCATCTCG 3’
smt1	5’ GATCGACGTTGCAGAGACAG 3’
smt2	5’ GATCGAGGGCGTTTTGATAA 3’
P3	5’ GGTGGATCCCCATGAACAGCGAAACCT 3’
P4	5’ GGTGAATTCTCAGGGCGAGATCGGGTCGC 3’

E.2 PCR reaction mixture

Component	Concentration	Quantity
Template DNA	50 ng/µL	4 µL
Master mix	2X	25 µL
Forward primer	20 mM	2 µL
Reverse primer	20 mM	2 µL
Deionized water	-	17 µL
Total volume		50 µL

Standard curves

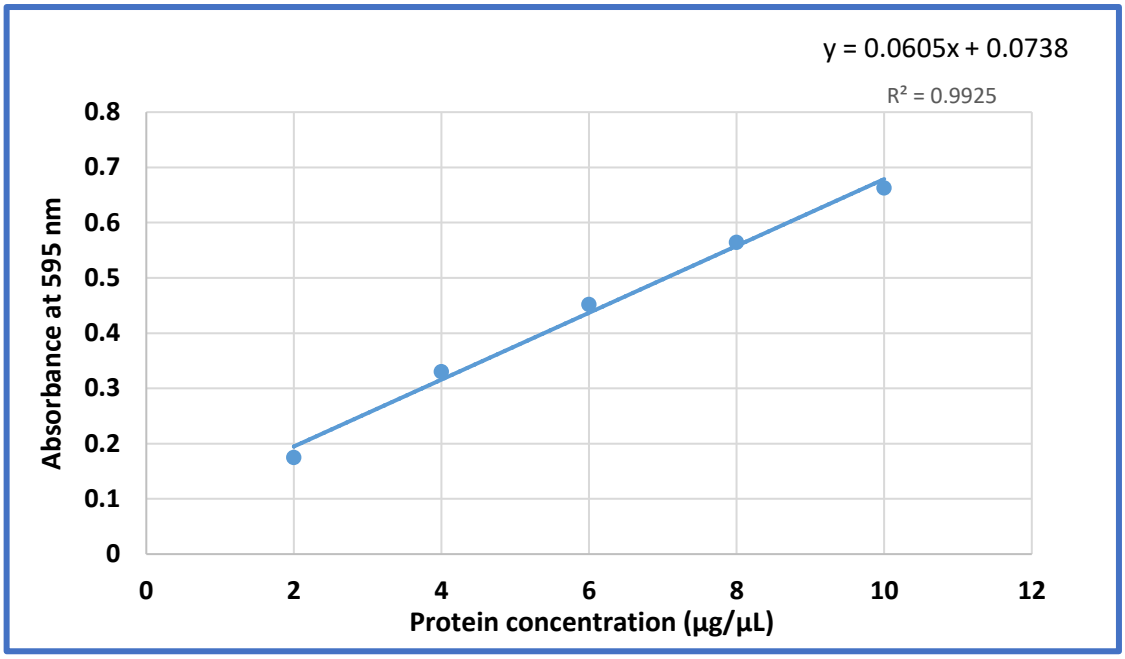

Fig. A. Standard curve for estimation of protein by Bradford assay.

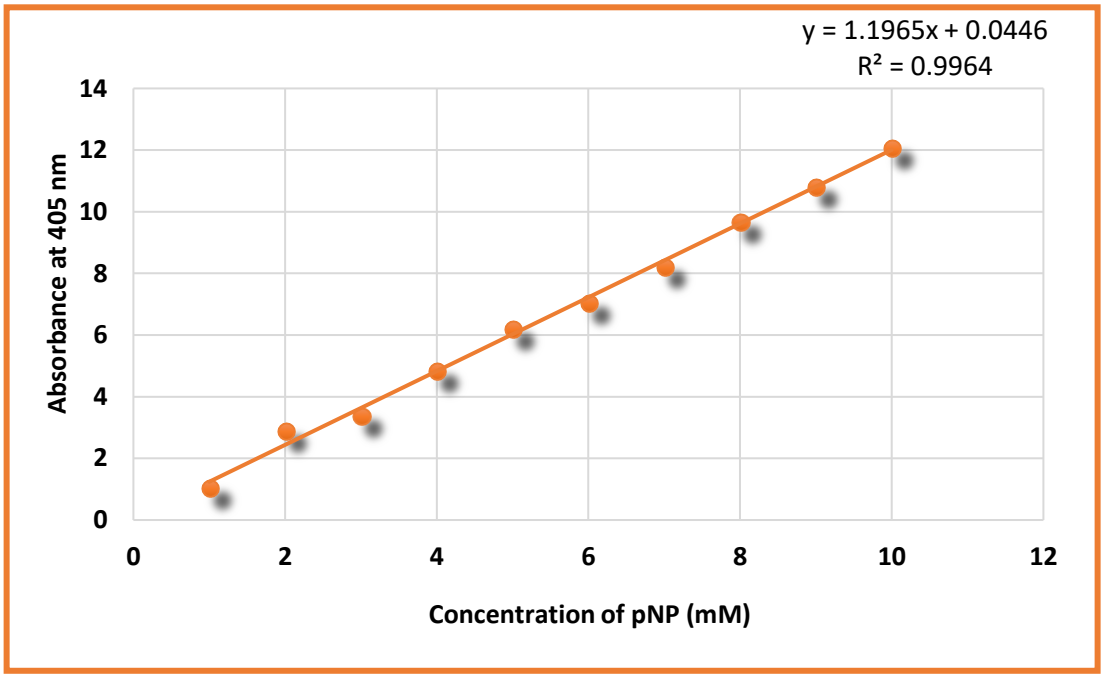

Fig. B. Standard curve for estimation of phosphatase activity.

Achard-Joris M, Moreau JL, Lucas M, Baudrimont M, Dudons NM, Gonzalez P, Boudou A, Bourdineaud JP. 2007. Role of metallothioneins in superoxide radical generation during copper redox cycling: Defining the fundamental function of metallothioneins. Biochimie 89:1474-1488.

Aickin RM, Dean ACR, Cheetham AK, Skarnulis AJ. 1979. Electron microscope studies on the uptake of lead by a *Citrobacter* species. Microbios Lett 9:7-15.

Aickin RM, Dean ACR. 1979. Lead accumulation by *Pseudomonas fluorescens* and by a *Citrobacter* sp. Microbios Lett 9: 55-66.

Aiking H, Govers H, Riet JV. 1985. Detoxification of mercury, cadmium, and lead in *Klebsiella aerogenes* NCTC 418 growing in continuous culture. App Environ Microbiol 50:1262-1267.

Altschul SF, Gish W, Miller W, Myers EW, Lipman DJ. 1990. Basic Local Alignment Search Tool. J Mol Biol 215:403-410.

Amoozegar MA, Ghazanfari N, Didari M. 2012. Lead and cadmium bioremoval by *Halomonas* sp., an exopolysaccharide producing halophilic bacterium. Prog Biol Sci 2:1-11.

Anton A, Weltrowski A, Haney CJ, Franke S, Grass G, Rensing C, Nies DH. 2004. Characteristics of zinc transport by two bacterial cation diffusion facilitators from *Ralstonia metallidurans* CH34 and *Escherichia coli*. J Bacteriol 186:7499-7507.

Atanesyan L, Gunther V, Celniker SE, Georgiev O, Schaffner W. 2011. Characterization of MtnE, the fifth metallothionein member in *Drosophila*. J Biol Inorg Chem 16:1047-1056.

Bai JH, Zhang ZM. 2009. Microbial synthesis of semiconductor lead sulphide nanoparticles using immobilized *Rhodobacter sphaeroides*. Materials Letters, 63: 764-766.

Baker MD, Wolanin PM, Stock JB. 2006. Signal transduction in bacterial chemotaxis. Bioessays 28(1):9-22.

Bauer AW, Kirby WMM, Sherris JC, Turck M. 1966. Antibiotic susceptibility testing by a standardized single disc method. Am J Clin Pathol 45:493-496.

Benkert P, Tosatto SCE, Schomburg D. 2008. QMEAN: a comprehensive scoring function for model quality assessment. Proteins Struct Funct Bioinformatics 71(1):261- 277.

Benkert P, Schwede T, Tosatto SC. 2009. QMEANclust: estimation of protein model quality by combining a composite scoring function with structural density information. BMC Struct Biol 9(1):35.

Beveridge TJ, Fyfe WS. 1985. Metal fixation by bacterial cell walls. Can J Earth Sci 22(12):1893-8.

Binet MR, Poole RK. 2000. Cd (II), Pb (II) and Zn (II) ions regulate expression of the metal-transporting P-type ATPase ZntA in *Escherichia coli*. FEBS Lett 473(1):67-70.

Blindauer CA, Harrison MD, Parkinson JA, Robinson AK, Cavet JS, Robinson NJ, Sadler PJ. 2001. A metallothionein containing a zinc finger within a four-metal cluster protects a bacterium from zinc toxicity. Proc Natl Acad Sci U S A 98(17):9593-8.

Blindauer CA, Harrison MD, Robinson AK, Parkinson JA, Bowness PW, Sadler PJ, Robinson NJ. 2002. Multiple bacteria encode metallothioneins and SmtA-like fingers. Mol Microbiol 45(5):1421-1432.

Blindauer CA. 2008. Metallothioneins with unusual residues: Histidines as modulators of zinc affinity and reactivity. J Inorg Biochem 102:507-521.

Blindauer CA. 2011. Bacterial metallothioneins: past, present, and questions for the future. J Biol Inorg Chem 16:1011-1024.

Borremans B, Hobman JL, Provoost A, Brown NL, van der Lelie D. 2001. Cloning and functional analysis of the *pbr* lead resistance determinant of *Ralstonia metallidurans* CH34. J Bacteriol 183(19):5651-8.

Bradford MM. 1976. A rapid and sensitive method for the quantitation of microgram quantities of protein utilizing the principle of protein-dye binding. Anal Biochem 72(12):248-54.

Braud A, Geoffroy V, Hoegy F, Mislin GL, Schalk IJ. 2010. Presence of the siderophores pyoverdine and pyochelin in the extracellular medium reduces toxic metal accumulation in *Pseudomonas aeruginosa* and increases bacterial metal tolerance. Environ Microbiol Rep 2(3):419-25.

Brown NL, Stoyanov JV, Kidd SP, Hobman JL. 2003. The MerR family of transcriptional regulators. FEMS Microbiol Rev 27:145-163.

Bruins MR, Kapil S, Oehme FW. 2000. Microbial resistance to metals in the environment. Ecotoxicol Environ Saf 45:198-207.

Busenlehner LS, Pennella MA, Giedroc DP. 2003. The SmtB/ArsR family of metalloregulatory transcriptional repressors: structural insights into prokaryotic metal resistance. FEMS Microbiol Rev 27(2-3):131-43.

Cabuk A, Akar T, Tunali S, Tabak Ö. 2006. Biosorption characteristics of *Bacillus* sp. ATS-2 immobilized in silica gel for removal of Pb (II). J Hazard Mater 136(2):317-23.

Cajaraville MP, Bebianno MJ, Blasco J, Porte C, Sarasquete C and Viarengo A. 2000. The use of biomarkers to assess the impact of pollution in coastal environments of the Iberian Peninsula: a practical approach. Sci Total Environ 247(2-3):295-311.

Cavet JS, Graham AI, Meng W, Robinson NJ. 2003. A cadmium-lead-sensing ArsR-Smtb repressor with novel sensory sites complementary metal discrimination by NmtR and CmtR in a common cytosol. J Biol Chem 278(45):44560-6.

Chan J, Huang Z, Merrifield ME, Salgado MT, Stillman MJ. 2002. Studies of metal binding reactions in metallothioneins by spectroscopic, molecular biology, and molecular modeling techniques. Coord Chem Rev 233:319-39.

Chen PR, He C. 2008. Selective recognition of metal ions by metalloregulatory proteins. Curr Opin Chem Biol 12(2):214-21.

Chen PR, Wasinger EC, Zhao J, van der Lelie D, Chen LX, He C. 2007. Spectroscopic insights into lead (II) coordination by the selective lead (II)-binding protein PbrR691. J Am Chem Soc 129(41):12350-1.

Chen Z, Pan X, Chen H, Guan X, Lin Z. 2016. Biomineralization of Pb(II) into Pb-hydroxyapatite induced by *Bacillus cereus* 12-2 isolated from lead-zinc mine tailings. J Hazard Mater 301: 531-537.

Choudhary S, Sar P. 2009. Characterization of a metal resistant *Pseudomonas* sp. isolated from uranium mine for its potential in heavy metal (Ni^{2+}, Co^{2+}, Cu^{2+} and Cd^{2+}) sequestration. Bioresour Technol 100:2482-2492.

Cleveland LM, Minter ML, Cobb KA, Scott AA, German VF. 2008. Lead hazards for pregnant women and children: Part 1: immigrants and the poor shoulder most of the burden of lead exposure in this country. Part 1 of a two-part article details how exposure happens, whom it affects, and the harm it can do. Am J Nurs 108:40-49; quiz 50.

Cobbett C, Goldsbrough P. 2002. Phytochelatins and metallothioneins: roles in heavy metal detoxification and homeostasis. Annu Rev Plant Biol 53(1):159-82.

Colovos C, Yeates TO. 1993. Verification of protein structures: patterns of non-bonded atomic interactions. Protein Sci 2:1511-1519.

Coombs JM, Barkay T. 2005. New findings on evolution of metal homeostasis genes: evidence from comparative genome analysis of bacteria and archaea. Appl Environ Microbiol 71(11):7083-91.

Cory-Slechta DA. 1996. Legacy of lead exposure: consequences for the central nervous system. Otolaryngol Head Neck Surg 114:224-226.

Das S, Dash HR, Chakraborty J. 2016. Genetic basis and importance of metal resistant genes in bacteria for bioremediation of contaminated environments with toxic metal pollutants. Appl Microbiol Biotechnol 100(7):2967-84.

Dawar C, Jain S, Kumar S. 2013. Insight into the 3D structure of ADP-glucose pyrophosphorylase from rice (*Oryza sativa* L.). J Mol Model 19(8):3351-67.

Deshmukh AB, Bai S, Aarthy T, Kazi RS, Banarjee R, Rathore R, Vijayakumar MV, Thulasiram HV, Bhat MK, Kulkarni MJ. 2017. Methylglyoxal attenuates insulin signaling and downregulates the enzymes involved in cholesterol biosynthesis. Mol Biosyst doi: 10.1039/c7mb00305f.

Dressaire C, Moreira RN, Barahona S, de Matos AP, Arraiano CM. 2015. BolA is a transcriptional switch that turns off motility and turns on biofilm development. MBio 6(1):e02352-14.

Dunn MA, Blalock TL, Cousins RJ. 1987. Metallothionein. Proc Soc Exp Biol Med 185:107-119.

Eisenberg D, Luthy R. 1997. VERIFY3D: assessment of protein models with three-dimensional profiles. Methods Enzymol 277:396-404.

Enshaei M, Khanafari A, Sepahey. 2010. Metallothionein induction in two species of *Pseudomonas* exposed to cadmium and copper contamination. Iranian J Environ Health Sci Eng 7(4):287-298.

Flora G, Gupta D, Tiwari A. 2012. Toxicity of lead: a review with recent updates. Interdiscip Toxicology 5(2):47-58.

Flora SJ, Flora G, Saxena G. 2007. Mishra, M. Arsenic and lead induced free radical generation and their reversibility following chelation. Cell Mol Biol 53:26-47.

Fowle DA, Stillman MJ. 1997. Comparison of the structures of the metal-thiolate binding site in Zn (II)-, Cd (II)-, and Hg (II)-metallothioneins using molecular modeling techniques. J Biomol Struct Dyn 14(4):393-406.

Gabr RM, Hassan SH, Shoreit AA. 2008. Biosorption of lead and nickel by living and non-living cells of *Pseudomonas aeruginosa* ASU 6a. Int Biodeterior Biodegradation 62(2):195-203.

Gadd GM. 1990. Heavy metal accumulation by bacteria and other microorganisms. Cell Mol Life Sci 46(8): 834-840.

Gadd GM. 2010. Metals, minerals and microbes: geomicrobiology and bioremediation. Microbiol 156:609-643.

Gillet LC, Navarro P, Tate S, Röst H, Selevsek N, Reiter L, Bonner R, Aebersold R. 2012. Targeted data extraction of the MS/MS spectra generated by data-independent acquisition: a new concept for consistent and accurate proteome analysis. Mol Cell Proteomics 11(6):O111-016717.

Gillis BS, Arbieva Z, Gavin IM. 2012. Analysis of lead toxicity in human cells. BMC Genomics 13(1):344.

Gold B, Deng H, Bryk R, Varqas D, Eliezer D, Roberts J, Jiang X and Nathan C. 2008. Identification of a copper-binding metallothionein in pathogenic mycobacteria. Nat Chem Biol 4(10):609-616.

Govarthanan M, Lee KJ, Cho M, Kim JS, Kamala-Kannan S, Oh BT. 2013. Significance of autochthonous *Bacillus* sp. KK1 on biomineralization of lead in mine tailings. Chemosphere 90:2267-2272.

Gummersheimer BS, Giblin T. 2003. Identification of lead resistant bacteria from a heavily contaminated site. Bios 1:48-54.

Guo H, Luo S, Chen L, Xiao X, Xi Q, Wei W, Zeng G, Liu C, Wan Y, Chen J, He Y. 2010. Bioremediation of heavy metals by growing hyperaccumulator endophytic bacterium *Bacillus* sp. L14. Bioresour Technol 101:8599-8605.

Gupta S, Goyal R, Prakash NT. 2014. Biosequestration of lead using *Bacillus* strains isolated from seleniferous soils and sediments of Punjab. Environ Sci Pollut Res 21:10186-10193.

Hamer DH. 1986. Metallothionein. Ann Rev Biochem 55(1):913-51.

Haney CJ, Grass G, Franke S, Rensing C. 2005. New developments in the understanding of the cation diffusion facilitator family. J Ind Microbiol Biotechnol 32(6):215-26.

Holt JG, Krieg NR, Sneath PH, Staley JT, Williams ST. 1994. Bergey's manual of determinative microbiology. Williams and Wilkins, Maryland.

Hernberg S. 1973. Prevention of occupational poisoning from inorganic lead. Working Environmental Health 10:53-61.

Higham DP, Sadler PJ, Scawen MD. 1986. Cadmium-binding proteins in *Pseudomonas putida*: pseudothioneins. Environ Health Persp 65:5-11

Hložková K, Šuman J, Strnad H, Ruml T, Paces V, Kotrba P. 2013. Characterization of *pbt* genes conferring increased Pb^{2+} and Cd^{2+} tolerance upon *Achromobacter xylosoxidans* A8. Res Microbiol 164(10):1009-18.

Huckle JW, Morby AP, Turner JS, Robinson NJ. 1993. Isolation of a prokaryotic metallothionein locus and analysis of transcriptional control by trace metal ions. Mol Microbiol 7(2):177-87.

Hynninen A, Touzé T, Pitkänen L, Mengin-Lecreulx D, Virta M. 2009. An efflux transporter PbrA and a phosphatase PbrB cooperate in a lead-resistance mechanism in bacteria. Mol Microbiol 74(2):384-94.

Hynninen A. 2010. Zinc, cadmium and lead resistance mechanisms in bacteria and their contribution to biosensing. Academic Dissertation in Microbiology, Department of Food and Environmental Sciences, Faculty of Agriculture and Forestry, University of Helsinki.

Islam E, Sar P. 2016. Diversity, metal resistance and uranium sequestration abilities of bacteria from uranium ore deposit in deep earth stratum. Ecotoxicol Environ Saf 127:12-21.

Janssen PJ, Van Houdt R, Moors H, Monsieurs P, Morin N, Michaux A, Benotmane MA, Leys N, Vallaeys T, Lapidus A, Monchy S. 2010. The complete genome sequence of *Cupriavidus metallidurans* strain CH34, a master survivalist in harsh and anthropogenic environments. PLoS One 5(5):e10433.

Jaroslawiecka A, Piotrowska-Seget Z. 2014. Lead resistance in micro-organisms. Microbiology 160:12-25.

Järup L. 2003. Hazards of heavy metal contamination. Br Med Bull 68(1):167-82.

Ji G, Silver S. 1995. Bacterial resistance mechanisms for heavy metals of environmental concern. J Ind Microbiol 14(2):61-75.

Jiang W, Saxena A, Song B, Ward BB, Beveridge TJ, Myneni SCB. 2004. Elucidation of functional groups on gram-positive and gram-negative bacterial surfaces using infrared spectroscopy. Langmuir 20:11433-11442.

Justice SS, Hunstad DA, Cegelski L, Hultgren SJ. 2008. Morphological plasticity as a bacterial survival strategy. Nat Rev Microbiol 6:162-167.

Kagi JHR. 1991. Overview of Metallothionein. Methods Enzymol 205:613-626.

Kamala-Kannan S, Krishnamoorthy R. 2006. Isolation of mercury resistant bacteria and influence of abiotic factors on bioavailability of mercury – a case study in Pulicat Lake north of Chennai, south east India. Sci Total Environ 367:341-353.

Kang CH, Oh SJ, Shin Y, Han SH, Nam IH, So JS. 2015. Bioremediation of lead by ureolytic bacteria isolated from soil at abandoned metal mines in South Korea. Ecol Eng 74:402-407.

Klaassen CD, Liu J, Choudhuri S. 1999. Metallothionein: an intracellular protein to protect against cadmium toxicity. Annu Rev Pharmacol Toxicol 39(1):267-94.

Kumar S, Stecher G, Tamura K. 2016. MEGA7: Molecular Evolutionary Genetics Analysis version 7.0 for bigger datasets. Mol Biol Evol 33:1870-1874.

Kyte J, Doolittle RF. 1982. A simple method for displaying the hydropathic character of a protein. J Mol Biol 157(1):105-32.

Laemmli UK. 1970. Cleavage of structural proteins during the assembly of the head of bacteriophage T4. Nature 227:680-685.

Landrigan PJ. 1990. Current issues in the epidemiology and toxicology of occupational exposure to lead. Environ Health Perspect 89:61.

Landrigan PJ. 1991. Current issues in the epidemiology and toxicology of occupational exposure to lead. Toxicol Ind Health 7(5-6):9-14.

Lanphear BP, Hornung R, Khoury J, Yolton K, Baghurst P, Bellinger DC, Canfield RL, Dietrich KN, Bornschein R, Greene T, Rothenberg SJ. 2005. Low-level environmental lead exposure and children's intellectual function: an international pooled analysis. Environ Health Perspect 113(7):894.

Laskowski RA, MacArthur MW, Moss DS, Thornton JM. 1993. PROCHECK: a program to check the stereochemical quality of protein structures. J Appl Crystallogr 26: 283-291.

Levinson HS, Mahler I, Blackwelder P, Hood T. 1996. Lead resistance and sensitivity in *Staphylococcus aureus*. FEMS Microbiol Lett 145(3):421-425.

Levinson HS, Mahler I. 1998. Phosphatase activity and lead resistance in *Citrobacter freundii* and *Staphylococcus aureus*. FEMS Microbiol Lett 161(1):135-138.

Lupo A, Coyne S, Berendonk TU. 2012. Origin and evolution of antibiotic resistance: the common mechanisms of emergence and spread in water bodies. Front Microbiol 3.

Macaskie LE, Bonthrone KM, Yong P, Goddard DT. 2000. Enzymically mediated bioprecipitation of uranium by a *Citrobacter* sp.: a concerted role for exocellular lipopolysaccharide and associated phosphatase in biomineral formation. Microbiology 146(8):1855-67.

Martinez JL, Sánchez MB, Martínez-Solano L, Hernandez A, Garmendia L, Fajardo A, Alvarez-Ortega C. 2009. Functional role of bacterial multidrug efflux pumps in microbial natural ecosystems. FEMS Microbiol Rev 33(2):430-49.

Mergeay M, Nies D, Schlegel HG, Gerits J, Charles P, Van Gijsegem F. 1985. *Alcaligenes eutrophus* CH34 is a facultative chemolithotroph with plasmid-bound resistance to heavy metals. J Bacteriol 162(1):328-34.

Mire CE, Tourjee JA, O'Brien WF, Ramanujachary KV, Hecht GB. 2004. Lead precipitation by *Vibrio harveyi*: Evidence for novel quorum-sensing interactions. Appl Environ Microbiol 70(2): 855-864.

Monchy S, Benotmane MA, Janssen P, Vallaeys T, Taghavi S, van der Lelie D, Mergeay M. 2007. Plasmids pMOL28 and pMOL30 of *Cupriavidus metallidurans* are specialized in the maximal viable response to heavy metals. J Bacteriol 189(20):7417-25.

Murthy S, Bali G, Sarangi SK. 2011. Effect of lead on metallothionein concentration in lead-resistant bacteria *Bacillus cereus* isolated from industrial effluent. Afr J Biotechnol 10(71):15966-15972.

Naik MM, Dubey SK. 2011. Lead-enhanced siderophore production and alteration in cell morphology in a Pb-resistant *Pseudomonas aeruginosa* strain 4EA. Curr Microbiol 62:409-414.

Naik MM, Dubey SK. 2013. Lead resistant bacteria: Lead resistance mechanisms, their applications in lead bioremediation and biomonitoring. Ecotoxicol Environ Saf 98:1-7.

Naik MM, Khanolkar DS, Dubey SK. 2012a. Lead resistant *Providencia alcalifaciens* strain 2EA bioprecipitates Pb^{2+} as lead phosphate. Lett Appl Microbiol 56:99-104.

Naik MM, Pandey A, Dubey SK. 2012b. *Pseudomonas aeruginosa* strain WI- 1 from Mandovi estuary possesses metallothionein to alleviate lead toxicity and promote plant growth. Ecotoxicol Environ Saf 79: 129-133.

Naik MM, Pandey A, Dubey SK. 2012c. Biological characterization of lead enhanced exopolysaccharide produced by a lead resistant *Enterobacter cloaceae* strain P2B. Biodegradation 23:775-783.

Naik MM, Shamim K, Dubey SK. 2012d. Bacterial characterization of lead- resistant bacteria to explore role of bacterial metallothionein in lead resistance. Curr Sci 103(4): 426- 429.

Naumann D. 2000. Infrared spectroscopy in microbiology. **In**: Meyers RA (ed.) Encyclopedia of Analytical Chemistry, John Wiley and Sons Ltd. Chichester, UK, pp 102-131.

Navas-Acien A, Guallar E, Silbergeld EK, Rothenberg SJ. 2007. Lead exposure and cardiovascular disease-a systematic review. Environ Health Perspect 115:472-482.

Naz N, Young HK, Ahmed N, Gadd GM. 2005. Cadmium accumulation and DNA homology with metal resistance genes in sulfate-reducing bacteria. Appl Environ Microbiol 71(8):4610-8.

Needleman H. 2004. Lead poisoning. Annu Rev Med 55:209-222.

Nies DH, Silver S. 1995. Ion efflux systems involved in bacterial metal resistances. J Ind Microbiol Biotechnol 14(2):186-199.

Nies DH. 1999. Microbial heavy-metal resistance. Appl Microbiol Biotechnol 51:730-750.

Nies DH. 2003. Efflux-mediated heavy metal resistance in prokaryotes. FEMS Microbiol Rev 27:313-339.

Olafson RW, Mccubbin WD, Kay CM. 1988. Primary-and secondary-structural analysis of a unique prokaryotic metallothionein from a *Synechococcus* sp. cyanobacterium. Biochem J 251(3):691-9.

Pan X, Chen Z, Li L, Rao W, Xu Z, Guan X. 2017. Microbial strategy for lead remediation: a review study. World J Microbiol Biotechnol, 33(35). DOI 10.1007/s11274-017-2211-z

Park JH, Bolan N, Megharaj M, Naidu R, Chung JW. 2011a. Bacterial-assisted immobilization of lead in soils: implications for bioremediation. Pedologist 162-174.

Park JH, Bolan N, Megharaj M, Naidu R. 2011b. Concomitant rock phosphate dissolution and lead immobilization by phosphate solubilizing bacteria (*Enterobacter* sp.). J Environ Manage 92:1115-1120.

Patel KS, Shrivas K, Hoffmann P, Jakubowski N. 2006. A survey of lead pollution in Chhattisgarh State, central India. Enviro Geochem Health 28(1):11-7.

Patrick L. 2006. Lead toxicity, a review of the literature. Part I: exposure, evaluation, and treatment. Altern Med Rev 11(1):2-3.

Pérez JA, García-Ribera R, Quesada T, Aguilera M, Ramos-Cormenzana A, Monteoliva-Sánchez M. 2008. Biosorption of heavy metals by the exopolysaccharide produced by *Paenibacillus jamilae*. World J Microbiol Biotechnol 24(11):2699.

Powers EM. 1995. Efficacy of the Ryu non-staining KOH technique for rapidly determining gram reactions of food-borne and waterborne bacteria and yeasts. Appl Environ Microbiol 61(10):3756-8.

Rensing C, Sun Y, Mitra B, Rosen BP. 1998. Pb(II)- translocating P- type ATPases. J Biol Chem 273(49):32614-32617.

Rifaat HM, Mahrous KF, Khalil WK. 2009. Effect of heavy metals upon metallothioneins in some *Streptomyces* species isolated from Egyptian soil. J Appl Sci Environ Sanit 4(3):187-206.

Riva MA, Lafranconi A, D'orso MI, Cesana G. 2012. Lead poisoning: historical aspects of a paradigmatic "occupational and environmental disease". Saf Health Work 3(1):11-6.

Roane TM. 1999. Lead resistance in two bacterial isolates from heavy metal- contaminated soils. Microb Ecol 37:218-224.

Robinson NJ, Gupta A, Fordham-Skelton AP, Croy RR, Whitton BA, Huckle JW. 1990. Prokaryotic metallothionein gene characterization and expression: chromosome crawling by ligation-mediated PCR. Proc R Soc London B 242(1305):241-7.

Rouch DA, Lee BT, Morby AP. 1995. Understanding cellular responses to toxic agents: a model for mechanism-choice in bacterial metal resistance. J Ind Microbiol 14(2):132 41.

Rousseau MC, Straif K, Siemiatycki J. 2005. IARC carcinogen update. Environ Health Perspect 113(9): A580- A581.

Saha R, Saha N, Donofrio RS, Bestervelt LL. 2012. Microbial siderophores: a mini review. J Basic Microbiol 53(4):303-17.

Salehizadeh H, Shojaosadati SA. 2003. Removal of metal ions from aqueous solution by polysaccharide produced from *Bacillus firmus*. Water Res 37(17):4231-5.

Sambrook J, Fritsch EF, Maniatis T. 1989. Molecular Cloning: A Laboratory Manual. Cold Spring Harbor Laboratory Press, New York.

Sand M, Rodrigues M, González JM, Crécy-Lagard V, Santos H, Müller V, Averhoff B. 2015. Mannitol-1-phosphate dehydrogenases/phosphatases: a family of novel bifunctional enzymes for bacterial adaptation to osmotic stress. Environ Microbiol 17(3):711-9.

Sanders T, Liu Y, Buchner V, Tchounwou PB. 2009. Neurotoxic effects and biomarkers of lead exposure: A Review. Res Environ Health 24:15-45.

Schneidman-Duhovny D, Inbar Y, Nussinov R, Wolfson HJ. 2005. PatchDock and SymmDock: servers for rigid and symmetric docking. Nucleic acids Research 33(suppl_2):W363-7.

Shamim K, Naik MM, Pandey A, Dubey SK. 2013. Isolation and identification of *Aeromonas caviae* strain KS-1 as TBTC- and lead-resistant estuarine bacteria. Environ Monit Assess 185:5243-5249.

Sharma J, Shamim K, Dubey SK, Meena RM. 2017. Metallothionein assisted periplasmic lead sequestration as lead sulfite by *Providencia vermicola* strain SJ2A. Sci Total Environ 579:359-365.

Sharma S, Sundaram CS, Luthra PM, Singh Y, Sirdeshmukh R, Gade WN. 2006. Role of proteins in resistance mechanism of *Pseudomonas fluorescens* against heavy metal induced stress with proteomics approach. J Biotechnol 126(3):374-82.

Silver S, Misra TK. 1988. Plasmid-mediated heavy metal resistances. Annu Rev Microbiol 42(1):717-43.

Silver S, Phung LT. 1996. Bacterial heavy metal resistance- New Surprises. Annu Rev Microbiol 50:753-789.

Silver S, Phung LT. 2005. A bacterial view of the periodic table: genes and proteins for toxic inorganic ions. J Ind Microbiol Biotechnol 32:587-605.

Silver S, Walderhaug M. 1992. Gene regulation of plasmid and chromosome determined inorganic ion transport in bacteria. Microbiol Rev 56(1):195-228.

Silver S. 1996. Bacterial resistances to toxic metal ions-a review. Gene 179:9-19.

Silversmith RE, Levin MD, Schilling E, Bourret RB. 2008. Kinetic characterization of catalysis by the chemotaxis phosphatase CheZ modulation of activity by the phosphorylated CheY substrate. J Biol Chem 283(2):756-65.

Silversmith RE. 2010. Auxiliary phosphatases in two-component signal transduction. Curr Opin Microbiol 13(2):177-83.

Sparks DL. 2005. Toxic metals in the environment: the role of surfaces. Elements 1: 193-196.

Taghavi S, Lesaulnier C, Monchy S, Wattiez R, Mergeay M, van der Lelie D. 2009. Lead (II) resistance in *Cupriavidus metallidurans* CH34: interplay between plasmid and chromosomally-located functions. Antonie Van Leeuwenhoek 96(2):171.

Templeton AS, Trainor TP, Spormann AM, Newville M, Sutton SR, Dohnalkova A, Gorby Y, Brown GE. 2003. Sorption versus biomineralization of Pb(II) within *Burkholderia cepacia* biofilms. Environ Sci Technol 37:300-307.

Tong S, Schirnding YE, Prapamontol T. 2000. Environmental lead exposure: a public health problem of global dimensions. Bull World Health Organ 78(9):1068-77.

Trevors JT, Oddie KM, Belliveau BH. 1985. Metal resistance in bacteria. FEMS Microbiol Lett 32(1):39-54.

Turner JS, Robinson NJ, Gupta A. 1995. Construction of Zn^{2+}/Cd^{2+}-tolerant cynaobacteria with a modified metallothionein divergon: Further analysis of the function and regulation of *smt*. J Ind Microbiol Biotechnol 14(3):259-64.

van Gunsteren WF, Billeter SR. 1996. Biomolecular simulations: the GROMOS96 manual and user guide. ETHZ, Zurich.

Volesky B, Holan ZR. 1995.Biosorption of heavy metals. Biotechnol Prog (3):235-50.

Wani AA, Usmani JA. 2015. Lead toxicity: a review. Interdiscip Toxicol 8(2):55.

Wei W, Liu X, Sun P, Wang X, Zhu H, Hong M, Mao ZW, Zhao J. 2014. Simple whole-cell biodetection and bioremediation of heavy metals based on an engineered lead-specific operon. Environ Sci Technology 48(6):3363-71.

Yang J, Yan R, Roy A, Xu D, Poisson J, Zhang Y. 2015. The I-TASSER Suite: protein structure and function prediction. Nature methods 12(1):7-8.

Yung MC, Ma J, Salemi MR, Phinney BS, Bowman GR, Jiao Y. 2014. Shotgun proteomic analysis unveils survival and detoxification strategies by *Caulobacter crescentus* during exposure to uranium, chromium, and cadmium. J Proteome Res 13(4):1833-47.

Zanardini E, Andreoni V, Borin S, Cappitelli F, Daffonchio D, Talotta P, Sorlini C, Ranalli G, Bruni S, Cariati F. 1997. Lead-resistant microorganisms from red stains of marble of the Certosa of Pavia, Italy and use of nucleic acid-based techniques for their detection. Int Biodeterior Biodegradation 40(2-4):171-82.

Zhang YF, He LY, Chen ZJ, Zhang WH, Wang QY, Qian M, Sheng XF. 2011. Characterization of lead-resistant and ACC deaminase-producing endophytic bacteria and their potential in promoting lead accumulation of rape. J Hazard Mater 186(2):1720-5.

Zhao R, Collins EJ, Bourret RB, Silversmith RE. 2002. Structure and catalytic mechanism of the *E. coli* chemotaxis phosphatase CheZ. Nat Struct Mol Biol 9(8):570-5.

Zhou H, Zhou Y. 2002. Distance-scaled, finite ideal-gas reference state improves structure-derived potentials of mean force for structure selection and stability prediction. Protein Sci 11(11):2714-26.

PUBLICATIONS

- **Sharma J**, Shamim K, Dubey SK, Meena RM. 2017. Metallothionein assisted periplasmic lead sequestration as lead sulfite by *Providencia vermicola* strain SJ2A. Sci Total Environ 579: 359-365. (IF: 4.9)
- **Sharma J**, Shamim K, Dubey SK. 2018. Phosphatase mediated bioprecipitation of lead as pyromorphite by *Achromobacter xylosoxidans*. J Environ Manage 217: 754-761. (IF: 4.01)
- **Sharma J**, Dubey SK. 2018. Differential expression of bacterial proteins in response to lead. (Under preparation)
- **Sharma J**, Mutnale M, Dubey SK. 2018. *In silico* docking studies of bacterial metallothionein BmtA with various metal ions. (Under preparation)

Other Publications

- Shamim K, **Sharma J**, Dubey SK. 2017. Rapid and efficient method to extract metagenomic DNA from estuarine sediments. 3 Biotech 7(3):182. (IF: 1.36)
- Shamim K, **Sharma J**, Mutnale M, Dubey SK, Mujawar S. 2018. Characterisation of a metagenomic serine metalloprotease and molecular docking studies. Process Biochem (In Press, https://doi.org/10.1016/j.procbio.2018.05.020) (IF: 2.497)

RESEARCH PAPERS PRESENTED IN NATIONAL AND INTERNATIONAL CONFERENCES

- "*Providencia vermicola* exhibits metallothionein mediated periplasmic sequestration of lead" - presented at 58th International Annual Conference of Association of Microbiologists of India (AMI-2017) held at Lucknow, Uttar Pradesh. (Poster)
- "Proteomic approach to study the differential expression of bacterial proteins in response to lead" - presented at 56th International Annual Conference of Association of Microbiologists of India (AMI-2015) held at Jawaharlal Nehru University, New Delhi. (Poster)
- "What enables bacteria to resist the heavy metal lead" - presented at 55th Annual National Conference of Association of Microbiologists of India (AMI-2014) held at TNAU, Coimbatore, Tamil Nadu. (Poster)
- "Isolation and characterization of lead resistant bacteria from estuarine and terrestrial ecosystems of Goa" - presented at 54th International Annual Conference of Association of Microbiologists of India (AMI-2013) held at MDU, Rohtak, Haryana. (Poster)

WORKSHOPS AND SYMPOSIA ATTENDED

- Attended a Science Academies' Lecture workshop on "Role of three-dimensional structures in biological function" held by Department of Biotechnology, Goa University in December 2017.
- Attended a UGC-sponsored short-term course in research methodology for science students, held by HRDC, Goa University in December 2016.
- Attended the 83rd Annual session and Symposium on "Space for Human Welfare" organized by Goa University in December 2013.
- Attended a workshop on "Phylogenetics" organized by the Department of Botany, Goa University in August 2013.